

TOWARD THE DEVELOPMENT OF AN EFFECTIVE  
UPWARD-ACTING ICEBREAKING BOW: THE  
PRELIMINARY DESIGN AND TESTING OF THE S-BOW

CENTRE FOR NEWFOUNDLAND STUDIES

**TOTAL OF 10 PAGES ONLY  
MAY BE XEROXED**

(Without Author's Permission)

ROBERT BRUCE PATERSON







TOWARD THE DEVELOPMENT OF AN EFFECTIVE  
UPWARD-ACTING ICEBREAKING BOW:

The Preliminary Design and Testing of the S-Bow

BY

Robert Bruce Paterson ©

A thesis submitted to the School of Graduate  
Studies in partial fulfillment of  
the requirements for the degree of  
Master of Engineering

Faculty of Engineering and Applied Science  
Memorial University of Newfoundland

June 1989

St. John's

Newfoundland



National Library  
of Canada

Bibliothèque nationale  
du Canada

Canadian Theses Service    Service des thèses canadiennes

Ottawa, Canada  
K1A 0N4

The author has granted an irrevocable non-exclusive licence allowing the National Library of Canada to reproduce, loan, distribute or sell copies of his/her thesis by any means and in any form or format, making this thesis available to interested persons.

The author retains ownership of the copyright in his/her thesis. Neither the thesis nor substantial extracts from it may be printed or otherwise reproduced without his/her permission.

L'auteur a accordé une licence irrévocable et non exclusive permettant à la Bibliothèque nationale du Canada de reproduire, prêter, distribuer ou vendre des copies de sa thèse de quelque manière et sous quelque forme que ce soit pour mettre des exemplaires de cette thèse à la disposition des personnes intéressées.

L'auteur conserve la propriété du droit d'auteur qui protège sa thèse. Ni la thèse ni des extraits substantiels de celle-ci ne doivent être imprimés ou autrement reproduits sans son autorisation.

ISBN 0-315-65313-2

DEDICATION

In Memory of

ERNEST GEORGE TOUZEAU

1905 - 1984

B.A.Sc (Forestry Engineering), Class of 1928  
University of British Columbia

## ABSTRACT

An upward-acting icebreaking bow offers certain features, referred to as operational advantages, that may improve the utility, reliability, or some aspect of the performance of ice-transitting shipping. Since the cessation of testing of icebreaking plow designs in the mid-1970's, there have been important developments in icebreaking technology that may make an upward-acting icebreaking bow feasible.

A new concept for an upward-acting icebreaking bow, designated the S-Bow, incorporates a shearing fracture action as a method of reducing ice resistance. This study was directed toward generating a bow form to demonstrate the concept. An experimental program was conducted in level uniform ice, but the range of conditions that an icebreaking vessel would encounter was considered in the development of the bow form.

Alternative bow configurations were tested in a small-scale experimental program. The S-Bow form selected for 1:30 scale resistance tests resulted from this design program. The resistance trials were conducted in the ice tank of the

NRCC Institute for Marine Dynamics using the M.V. "ARCTIC" as a test case.

The trials were evaluated from videotaped observations, resistance measurements, and a numerical analysis of the breaking mechanisms. A clearly defined fracture sequence and an adequate flow of broken ice could be observed, but the measured average resistance levels ranged from 2.0 to 5.0 times the ice resistance of the "ARCTIC" with its present bow form. The analyses indicated a large component of the recorded resistance could be attributed to design problems but it was also established that a significant inherent resistance resulted from the lifting and movement of broken ice.

A set of revisions are proposed to rectify the design problems. The indicated performance envelope was assessed against the potential influence of the operational advantages of an upward-acting bow. The development of the open water capability of the S-Bow and reduction of the magnitudes of ice resistance are required to demonstrate its feasibility.

## ACKNOWLEDGEMENTS

I would like to thank my supervisor, Dr. D.B. Muggerridge, for his encouragement, direction, and financial support of this research program.

I wish to thank Dr. S.J. Jones, Head of the Ice Group, Mr. D. Spencer, Project Officer, and the members of the Ice Group of the National Research Council of Canada's (NRCC) Institute for Marine Dynamics (IMD) for their advice and effort throughout the program, and particularly during the resistance trials. I would like to express my appreciation to Mr. T. Randell, as well as the staff of the Model shop, Technical Services, Memorial University, and the staff of the Model Preparation Shop of IMD, for their efforts in constructing the model. I would also like to acknowledge the co-operation of Melville Shipping Ltd. and Dr. F.M. Williams for allowing access to model test results for the M.V. "ARCTIC".

The assistance of the Laboratory Technicians at Memorial University was much appreciated. I would also like to acknowledge the assistance of: Mr. W.H. Lau and Mr. D. Sen, graduate students; Ms. S.G. Decker, a work-term student; and Mr. J. Almlund, an exchange student from Denmark.

Financial support was provided by the Natural Sciences and Engineering Research Council of Canada (NSERC), Grant No. A4885. Certain phases of the research were conducted as NRCC Internal Research Project I5306. The author would also like to thank the Board of Directors of the Centre for Cold Ocean Research Engineering (C-CORE) for their personal financial support through their Fellowship program, 1985-1986.

I would also like to thank Mrs. M. Brown for her assistance in preparing this manuscript, and would like to acknowledge the co-operation of the OEIC and IMD library staff.

## TABLE OF CONTENTS

	<u>Page</u>
ABSTRACT	i
ACKNOWLEDGMENTS	iii
LIST OF TABLES	vii
LIST OF FIGURES	viii
NOMENCLATURE	x
1.0 INTRODUCTION.....	1
1.1 The New Upward-Acting Icebreaking Concept	1
1.2 Operational Advantages	4
1.3 The Operational Profile	6
1.4 Scope of Research	8
2.0 DESCRIPTION OF THE UPWARD-BREAKING BOW.....	10
2.1 General Arrangement	10
2.2 The S-Bow Breaking Action in Level, Uniform Ice	11
3.0 DEVELOPMENT OF THE UPWARD-ACTING BOW FORM.....	14
3.1 Form Development Methodology	14
3.2 Small Scale Towing Trials	17
3.3 Evaluation Criteria for the Small-Scale Evaluation Program	18
3.4 The Evolution of the S-Bow Configuration	22
4.0 RESISTANCE TRIALS WITH THE S-BOW IN LEVEL ICE....	25
4.1 Test Facilities	25
4.2 Model Description	26
4.3 Outline of Test Program	29
4.4 Analysis of IMD Resistance Trials	31
4.5 Summary of the Analyses of the S-Bow Level Ice Resistance	45
5.0 RECOMMENDATIONS: CONDITIONS FOR FURTHER RESEARCH..	46
5.1 Refinement of the S-Bow Form	46
5.2 Investigation of the Upward-acting Icebreaking Concept based on the S-Bow	49
REFERENCES.....	56
TABLES.....	68

## TABLE OF CONTENTS (Continued)

	<u>Page</u>
FIGURES.....	73
APPENDICES:	
A. Background to Development.....	88
B. Specifications of the M.V. "ARCTIC": Model M326B/M326BMS	93
C. Ice Characterization Tests for the Small-Scale Ice Tank	101
D. Design of the Small-Scale Model Mounting.....	112
E. Small-Scale Ice Test Program Data.....	117
F. Specifications of the M.V. "ARCTIC" fitted with the S-Bow: Model M326BP	124
G. Summary of the IMD Resistance Trials.....	129
H. Numerical Analysis of the S-Bow Resistance.....	138
I. Performance Analysis: Two Operational Profile Case Studies	158

## LIST OF TABLES

<u>Table</u>	<u>Page</u>
1. Details of Alternative S-Bow Designs.....	68
2. Summary of Small-Scale Tests by Bow Type.....	69
3. Schedule for IMD Resistance Tests.....	70
4. Summary of Resistance Data.....	71
5. Summary of the Numerical Analysis.....	72
 <b>APPENDICES</b>	
<u>Table</u>	<u>Page</u>
B.1 Hydrostatic Particulars of the M.V. "ARCTIC" and Model M326BMS	...97
B.2 Form Coefficients for M.V. "ARCTIC": Melville Bow..	99
C.1 UR/D/S Ice Mix Calculations.....	106
C.2 UR/D/S Ice Grain Sizes.....	106
E.1 Small-Scale Ice Tank Trial Data.....	120-123
F.1 Hydrostatic Particulars of Model M26BP.....	127
F.2 Form Coefficients for M.V. "ARCTIC": S-Bow.....	128
G.1.1- G.1.5 Average Model Resistance Data, Tests 1- 5	....130-134
G.2 Model Motion Data for Typical Trials.....	136
H.2.1 Radial Cracking Resistance Models.....	143
H.2.2 Radial Cracking Resistance from Ralston.....	143
I.1 Route Description.....	161
I.2 Performance Data for Case Study.....	162
I.3 Energy Consumption Rates.....	164

## LIST OF FIGURES

<u>Figure</u>	<u>Page</u>
1. Route Spectrum.....	73
2. S-Bow Lines.....	74
3. The S-Bow Model Segment.....	75
4. Schematic Diagram of S-Bow Components.....	76
5. The S-Bow Breaking Sequence in Level Ice.....	77-78
6. The S-Bow in Pre-Sawn Ice.....	78
7. Small-Scale Ice Towing Tank.....	79
8. Small-Scale Model Mounting.....	80
9. FF1 - The Pontoon-type Forefoot.....	81
10. FF2 Forefoot with the FB2 Forecastle.....	81
11. The over-hanging Forecastle used in FB1.....	82
12. FB5 - showing shorter Forefoot integrated with Forecastle	82
13. 1:30 Scale Model Construction	83
14. Deflection and Deformation of Ice Sheet around Bow	84
15. Radial Cracking during Quarter Point Trial.....	84
16. Broken Channel produced by the S-Bow.....	85
17. Time History of Resistance Data: S-Bow and Melville Bow	86
18. Model Resistance Data - IMD Tests.....	87

## LIST OF FIGURES (Continued)

## APPENDICES

<u>Figure</u>	<u>Page</u>
B.1 Body Plan- Melville Bow.....	100
C.1 Flexural Strength vs. Tempering Time.....	107
C.2 Flexural Strength from Modulus Tests.....	108
C.3 Modulus Ratio vs. Tempering Time.....	109
C.4 Thin Section Photographs.....	110-111
I.1 Resistance Data for Narrow Beam Case Study.....	166

## NOMENCLATURE

$A_{ij}$ ,  $A_{1j}$  = added mass;  $i, j$  components  
 $a$  = roll, pitch period coefficient  
 $A_{wp}$  = area of waterplane  
 $AP$  = aft perpendicular  
 $B$  = beam (width)  
 $B_{ij}$  = damping coefficient  
 $BL$  = baseline  
 $BM$  = metacentric radius from centre of buoyancy  
 $C_b$  = block coefficients  
 $C_M$  = midships coefficients  
 $C_p$  = prismatic coefficient  
 $C_w$  = waterplane coefficients  
 $CA_{ij}$  = added mass coefficients  
 $CAM$  = computer automated machining  
 $CASPPR$  = Canadian Arctic pollution prevention regulations;  
           also CASPP  
 $Ch$  = Cauchy number  
 $D$  = moulded hull depth  
 $DWT$  = deadweight tonnes  
 $d, d_i$  = inner or least diameter  
 $E$  = (elastic) modulus  
 $ECR_1$  = energy consumption ratio  
 $EG/AD/S$  = artificial ice dopants; ethylene glycol,  
           detergent, sugar  
 $F$  = test rating: fair  
 $F_e$  = external force  
 $F_i$  = force in  $i$  direction  
 $FA$  = failed test  
 $FBx$  = forebody, model  $x$   
 $FFx$  = forefoot, model  $x$   
 $FG$  = test rating: fair to good  
 $Fn$  = Froude number  
 $fwd$  = forward  
 $G$  = test rating: good  
 $g$  = gravitational acceleration constant = 9.81 m/s<sup>2</sup>  
 $GE$  = test rating: good to excellent  
 $GM$  = metacentric height  
 $H_i$  = ice thickness, location  $i$  in small tank  
 $HC$  = heavy ice cover  
 $h$  = ice thickness  
 $I_L$  = moment of area (longitudinal)  
 $IMD$  = Institute for Marine Dynamics  
 $J_i$  = moment of inertia,  $i$  component  
 $k$  = radius of gyration factor  
 $k_i$  = spring constant,  $i$  mode

## NOMENCLATURE (Continued)

$K_{Ic}$  = stress intensity factor, tension mode, fracture toughness  
 KB = height of centre of buoyancy from keel (moulded)  
 KG = vertical centre of gravity from keel (moulded)  
 L = length (of cantilever, tip to root)  
 $L_{BP}, L_{PP}$  = length between perpendiculars  
 $l_c$  = critical length  
 $L_n$  = length from AP to midships  
 $l_s$  = length to shoulder from midships  
 $L_{sh}$  = " " " from AP  
 $L_{wl}, LWL$  = length on waterline  
 LCF = longitudinal centre of flotation  
 LCG = " " of gravity  
 LVDT = linear voltage displacement transducer  
 $M, M_i$  = moment, about i axis  
 M326BMS = designation for 1:30 scale M.V. "ARCTIC" fitted with the Melville Bow  
 M326BP = designation for 1:30 scale M.V. "ARCTIC" fitted with the S-Bow  
 MCT(x)m = moment to change trim "x" metres  
 MP = medium pack ice  
 $N_j$  = specific weight of ice dopant component j  
 OA = overall  
 OP = open pack  
 $OW, OW_s$  = open water; s includes seakeeping factor  
 P = ice test rating: poor  
 $P_v$  = vertical component of ice loading  
 PF = ice test rating: poor to fair  
 QP = quarter point location in ice sheet  
 r = radius of ice loading  
 $R, R_i$  = total ice resistance  
 $R_1, R_2$  = radii of gyration, longitudinal, transverse  
 $R1, R2$  = resistance record from LVDT's 1 and 2  
 RATE = numerical test rating  
 RPM = revolutions per minute  
 S = drive setting  
 S = total distance travelled [Appendix J]  
 $SF_j$  = ratio of route distances, ice condition:total length  
 SMP = milling machine control program  
 SSx = stem splitter model x  
 t = time  
 t = trim [Appendices B and F]  
 $T_r$  = roll period  
 U = velocity (feet/sec.)  
 UR/D/S = model ice dopants; urea/detergent/sugar

## NOMENCLATURE (Continued)

$V$  = volume  
 $V_p, v_m$  = velocity; full-scale and model scale respectively  
 $X, x$  = segment distance (ice piece)  
 $X'$  = broken ice piece size  
 $W_i$  = weight of ice dopant component  $i$   
 $z_i$  = vertical displacement,  $i$  component

Subscripts

$AP$  = from aft perpendicular  
 $c$  = in compression or crushing  
 $f$  = in flexure  
 $fw$  = fresh water  
 $FP$  = from/at forward perpendicular  
 $I, i$  = component due to ice  
 $i, j$  = general component counter, orthogonal system  
 $M$  = from/at midships  
 $m$  = model scale  
 $P, p$  = prototype (full scale)  
 $s, sh$  = at shoulders  
 $sw$  = sea water  
 $t$  = in tension  
 $x, y, z,$  = components in  $x, y, z$  direction, RHS orthogonal system  
 $3$  = component in heave ( $y$ ) direction  
 $5$  = component about pitch axis ( $z$ )

Greek Symbols

$\alpha$  = stem or slope angle, from horizontal  
 $\alpha'$  = complement of slope angle  
 $\beta$  = waterline entrance angle  
 $\gamma$  = local forefoot frame angle  
 $\psi$  = local forepeak angle, in  $x-y$  plane  
 $\phi$  = pitch angle  
 $\epsilon$  = resolution factor  
 $\eta_{1j}$  = displacement (distance)  
 $\lambda$  = wavelength  
 $k$  = scale factor  
 $\omega$  = angular frequency  
 $\mu$  = Coulomb friction coefficient  
 $\rho_j$  = density of material  $j$   
 $\sigma$  = normal stress  
 $\tau$  = shear stress  
 $\zeta$  = local forepeak angle, in  $x-z$  plane

## CHAPTER ONE

## INTRODUCTION

Over the past two decades, the ice covered regions of the world have grown in both strategic and economic importance. Shipping activity in these regions has increased in volume and diversity. Operations in ice-covered waters require specialized equipment and navigation procedures, which result in higher capital investment and operating costs when compared with open water operations. Shipping designed for ice navigation must find an optimum between the conflicting requirements for ice transit and open water operation. Naval architects have recognized the role of balancing performance requirements in icebreaking design, but researchers have tended to concentrate on the reduction of ice resistance. The importance of optimizing the performance range of a vessel, and the factors involved in optimization, are an essential aspect of this study.

## 1.1 THE NEW UPWARD-ACTING ICEBREAKING CONCEPT

An upward-acting icebreaking bow offers certain advantages over conventional, downward-acting icebreaking designs. These advantages, designated "operational" advantages, may not affect ice resistance directly, but would affect the utility or overall efficiency of a vessel. As the roles of icebreaking vessels become more diverse, these advantages can be expected to receive a higher priority.

Previous upward-acting icebreakers have taken a plow configuration (German and Dadachanji,1975; German,1971; Shvaimstein,1971; Alexander,1970; Davies,1969); their development is presented in Appendix A. The problems reported with the icebreaking plow included: blockage of broken or pack ice; poor open water performance; and higher level ice resistance. No reliable model-scale performance data are available in open literature.

Since the suspension of the development of the icebreaking plow in the mid-1970's, there have been significant developments in icebreaking technology and ice engineering. Among the most prominent developments are the various "pontoon" type bow forms (Enkvist and Mustamaki,1986; Schwarz,1986; Tronin, 1986; Freitas and Wilckens,1980). This bow form reduces ice resistance by the use of a low stem angle and a rectangular section, which exploits the weakness of ice in shear and bending; the Thyssen/Waas bow features side runners to assist in shearing. The major limitation of this type of bow is its relatively poor open water performance and seakeeping properties (Enkvist and Mustamaki,1986; Discussion as noted, Schwarz,1986; Freitas and Nishizaki,1985; Freitas and Wilckens,1980).

The new concept for an upward-acting icebreaking bow, referred to as the S-Bow, combines the superior shearing

action of the pontoon-type form with the upward action of the ice plow. There is a resistance penalty associated with any upward-acting bow because the entire weight of the broken ice must be lifted by the bow. Field data indicates that the (macroscopic) mechanical properties of ice are unchanged by the direction of action (Mellor,1983), but a downward acting bow must only submerge the buoyant component of that ice. Resistance is affected directly by the weight component and by the added friction created by the increased normal load. The elimination of hydraulic or hydrodynamically -induced resistance provides some compensation for the resistance penalty, but the absence of waterflow also increases the risk of ice blockage. The intent of the new concept was to compensate for the higher ice resistance due to the movement of broken ice by an improved fracture action.

Icebreaking resistance is generally treated as a process consisting of ice fracture and broken ice components, but the relative contribution of each individual component to the total resistance is not clearly understood (Carter,1985; Glen,1984; Pozniak et al.,1981; Milano,1975; Enkvist,1972). An experimental program was required to evaluate the performance of the bow.

The objective of this study was to produce a configuration with an ice resistance competitive with downward-acting

forms, as defined by the candidate vessel's operational profile, in order to exploit the operational advantages associated with the upward-acting bow.

## 1.2 OPERATIONAL ADVANTAGES

The operational advantages associated with upward-acting icebreaking are derived from three features.

- a) Bow Geometry - has a potential effect on performance by: offering greater control over the submerged hull form, with regard to open water performance (Appendix A), or the employment of unorthodox hull forms to reduce ice resistance (Schonecht et al., 1977; German and Dadachanji, 1975; Kallipke, 1972); and the use of auxiliary icebreaking technology or low friction coatings uniquely suited to an upward-acting bow form. Other features of the geometry include: ease of maintenance because much of the ice contact region is above the waterline; and a more full hull form giving a greater DWT:L ratio.
  
- b) Management of Broken Ice - which deposits the ice around the hull above the waterline offers a range of advantages:
  - i) increased utility and the reduction of risk of ice damage to vessels or structures operating as a platform in an ice field while engaged in activities requiring a

"moonpool", the towing of an appendage, or engaged in sub-ice surveillance. A limited model study (Kitami et al., 1983) and field reports indicate ice contact is a problem (Arctic News Record, 1984; Offshore Engineer, 1983).

- ii) an indirect improvement in safety by providing a superior platform for ice detection sonar by a reduction of ice interference with the array (Elkholm, 1986). Damage statistics (Koehler, 1986; Glen et al., 1982) indicate that the majority of incidents are caused by situations that exceed reasonable design criteria, such as "growler" impact or extreme ice pressures. Hazard avoidance is the ideal strategy in these cases.
  - iii) a direct improvement in safety and reliability, by reducing ice contact with the propulsion and steering systems. Significant ice contact is reported in all types of ice-going vessels (Peirce, 1986; Laskow et al., 1986; Peirce et al., 1985; Kramek and Gulik, 1981; Macdonald, 1969). Damage events are rare, but critical systems such as the propellers are at risk.
  - iv) a reduction in ice milling or nozzle masking, resulting in higher propulsive efficiency.
- c) Production of an Ice-Free Channel - has historically been the basis for interest in upward-acting icebreakers, but

the condition of the ice channel is a function of the integrity of the ice sheet and the amount of ice pressure (Shvaistein,1971). A clear channel immediately aft of the icebreaker may be of value when reversing to ram (Gray and Maybourn,1981), or when towing.

Treated individually or cumulatively, the operational advantages are an essential aspect of the upward-acting ice-breaking concept. They would not receive consideration in a standard performance evaluation based on resistance tests. Neglect of the operational advantages of the bow seriously underestimates the potential of the concept. It is difficult to quantify the significance of a particular advantage or what qualifies as "sufficient" performance to be competitive with conventional designs. The evaluation would vary with each operational profile.

This study attempted to give priority to the operational advantages in several ways. Their exploitation was considered a design criterion, and experimental evidence of the mechanisms from which the operational advantages are derived was sought. The concept was analyzed in terms of case studies, which could incorporate some aspects of the operational advantages.

### 1.3 THE OPERATIONAL PROFILE: FACTORS AFFECTING THE TECHNICAL EVALUATION OF NEW TECHNOLOGY

The operational profile of a vessel can be defined in terms of the environmental conditions characteristic of its route, and the vessel's function (Schwarz,1986; German and Dadachanji,1975; Macdonald,1969). Definition of the environmental conditions should include the variation in ice conditions, the ratio of ice to open water, and the route hydrography, in addition to identifying extreme ice conditions. The route environmental conditions can be classified according to a spectrum, where one extreme represents a route profile consisting entirely of heavy ice conditions along the entire route for the entire season, while the other extreme is entirely in open water. A schematic is shown in Figure 1. The performance of the vessel should be considered over the entire range of route conditions, rather than over a specific segment. The ability of remote sensing technology to assist in routing should be considered, as it will tend to skew the route conditions to the lighter end of the spectrum. The availability of icebreaking, navigational, and repair services is also a factor.

The performance of an icebreaking vessel will be a function of its capability to transit various ice conditions; its hazard avoidance capability; and its open water perform-

ance. The capability of a vessel will be a function of its size, form, propulsive thrust, and its navigational facilities. Greater specialization in one operating mode is usually achieved at the expense of other modes. The problem is to produce a vessel that is neither underdesigned or overspecialized. Apart from achieving a basic capability to operate efficiently in each environmental condition, the optimum design will strike the best balance of performance appropriate for the route conditions. A comparative evaluation of alternative designs should treat performance over the full range of route environmental conditions.

The vessel's function is the other factor in the operational profile. Capital costs will be higher to adapt to the harsh operating environment. An icebreaking vessel is the sum of many sub-systems; the interaction of these systems is an important factor in achieving an optimum design (Kramek and Gulik, 1981). Some of the operational advantages will contribute to an efficient interaction of the hull and propulsion system. Unfortunately the assessment of these effects was outside the scope of this program.

#### 1.4 SCOPE OF RESEARCH: OBJECTIVES OF THE RESEARCH PROGRAM

The research program attempted to reflect the importance of the operational profile, which will be quite specific to

a route or vessel, in the determination of the research objectives and evaluation criteria. The design was treated as a problem in naval architecture, which involved a broader set of problems than those related to ice mechanics. Continuous transit of level, uniform, ice was selected as the initial design condition because it required the most extensive form development, and is the condition most widely used to assess icebreaking performance. Other ice conditions and open water performance were considered in the design of alternative bow configurations. A form that offered better prospective performance in other conditions while still maintaining the shearing fracture action was favoured, possibly at the expense of level ice resistance. Because the research was a preliminary study, some of the evaluation decisions were speculative, requiring verification by further research in other operating conditions.

The object of this research was to establish whether the proposed upward-acting shearing bow concept was feasible. A basic form had to be created for this research. Level ice resistance data was used to define a performance envelope, rather than to definitively evaluate the bow. This performance envelope was then used to investigate the potential concept. A full evaluation of the concept would require an extensive long-term research program.

## CHAPTER TWO

## DESCRIPTION OF THE UPWARD-ACTING BOW

## 2.1 GENERAL ARRANGEMENT

Figures 2 and 3 show the bow configuration, designated as the S-Bow, that was developed for the comparative resistance tests with a downward-acting bow. While the design concept originated as a combination of the ice plow and the pontoon-type bow, the S-Bow configuration owes much to the snout bow employed by many late-nineteenth century warships, and to the extreme bulbous bow featured by some recent merchant vessels (Appendix A). The S-Bow consists of the following elements, as labelled in Figure 2:

- 1) the bow underside - not treated in this study.
- 2) centreline skeg or runner.
- 3) forefoot - a snout form, featuring a parabolic section forward, a rectangular section aft.
- 4) shoulders.
- 5) forecastle - featuring:
  - 5a) the lower section featuring "tumblehome".
  - 5b) a flared forepeak of circular section

This nomenclature will be used throughout the text. The bow geometry can be defined by characteristic angles, as in Figure 4.

The driving mechanism for the breaking action of the S-Bow in unbroken level ice is the buoyancy force created as the bow is driven under the ice sheet. Bow geometry affects the hull trim induced by the ice sheet, the fracture action, and the flow of broken ice. A critical aspect of the breaking action is the maintenance of the flow of broken ice over the bow. There is no waterflow to entrain the broken ice as in downward-acting designs. The S-Bow uses inclined surfaces to ensure an adequate flow of ice, through the use of the weight of the broken ice.

## 2.2 THE S-BOW BREAKING ACTION IN LEVEL UNIFORM ICE

It is possible to describe the breaking action as a series of discrete events, based on experimental observation. The sequence is illustrated in Figures 5 and is described below.

- 1) A centreline crack is induced in the ice sheet by the bow stem runner. A lifting force is generated as the bow submerges under the ice sheet; a region of ice deformation is generated around the snout (Figure 5a).
- 2) A circumferential crack develops over the snout, to form a "tee" with the centreline crack (Figure 5b). The development of this crack corresponds with a release in the lifting load on the snout. Shearing is initiated at the shoulders.
- 3) The circumferential crack connects with radial cracks that develop from the initial shear crack created at each

shoulder (Figure 5c). This forms the "two-dimensional" failure sequence of the short, wide, cantilever formed on each side of the centreline extending back to the shoulders. The geometry of the fractured segment will depend on the relative location of the circumferential crack to the shoulders, as determined by the induced hull trim, bow form, the ice thickness, and ice quality. In tests in laboratory ice, the S-Bow on a hull with a high length:beam ratio formed crescent-shaped cantilevers, as the bow did not trim significantly prior to fracture.

- 4) As the ice moves aft over the snout and on to the shoulders, the cantilever segments begin to separate into two distinct "trains" as the ice rides up onto the spine of the snout.
- 5) Each side of the crescent slides outward and aft, conforming to the shape of the bow and inducing some secondary cracking in the crescents. This breaks the ice into smaller segments. The lateral motion is induced by the action of the stem and the weight of broken ice on the inclined bow surfaces.
- 6) As the broken ice slides laterally and aft on the shoulders (Figure 5c):
  - 6a) the outer segments of the crescent are pushed outward off the shoulders; when unsupported they will collapse on to the adjacent ice sheet.

6b) the inner piece of ice will slide further aft along the forecastle; no longer confined by the outer segments of the crescent, the ice will slide down the inclined surfaces onto the adjacent ice sheet under its own weight.

This description of the breaking action is somewhat idealized; certain problems believed to originate with the test configuration will be analyzed in succeeding sections dealing with experimental results (Section 4.4).

The behaviour of the S-Bow in broken ice was not specifically studied but it was a factor in developing the bow geometry. The snout forefoot was designed to deflect broken ice laterally and down. Earlier ice plow designs were reported to accumulate broken ice ahead of the plow until forward movement stalled (Shvaistein, 1971; Davies, 1969). A limited number of experiments with the S-Bow in pre-sawn and unconfined ice indicated a speed dependency. At low speeds, the ice pieces were observed to rotate, move laterally and submerge (Figure 6); with increasing speed the ice began to ride up on the bow, until the ice flowed as an unbroken ice sheet. A complete analysis of broken/pack ice performance would require the design of the bow underside.

## CHAPTER THREE

## DEVELOPMENT OF THE UPWARD-ACTING BOW FORM

## 3.1 FORM DEVELOPMENT METHODOLOGY

The objective of the form development phase was to develop a feasible upward-acting bow in accordance with the principles outlined in Section 1.4. Previous experience with upward-acting icebreakers (Appendix A) indicated several problems that had to be resolved in the new design. A suitable test case, the icebreaking bulk carrier M.V. "ARCTIC" was selected; specifications are given in Appendix B.

The S-Bow as described in Chapter 2 was one of several alternative configurations of the upward-acting shearing concept. An inexpensive method was required for evaluating the alternative designs. Available computational methods lacked the flexibility and accuracy needed to predict the behaviour of a new concept, and therefore it was decided to attempt a small scale experimental program using the latest (1985) developments in model ice.

A small-scale towing tank was constructed for use in a standard refrigerated "cold room" at Memorial University. The size of the cold room limited the tank length to about one metre: if the M.V. "ARCTIC" with a 23m beam was used as

the test case then a geometric scale of about 1:100 was possible. The models were towed along a monorail uni-slide track by cables and a vee-belt/pulley drive from a 0.8 kW variable-speed electric motor. The system gave a speed range equivalent to 0.5 to 3.5 knots full scale. Speed was monitored using a cam-switch system on the towing axle, which recorded revolutions on an X-Y Plotter; linear velocity was obtained from the time scale and the axle dimensions. Braking was initiated by tripping a limit switch. The towing tank is shown in Figure 7.

The model ice consisted of fresh water doped with a mix of 2% (by weight) urea (carbamide), 0.05% detergents(AD), and 0.03% sugar; the mix was referred to as UR/D/S ice. A seeded ice sheet averaging 1.5cm thick could be grown after 1.5 hours at  $-24^{\circ}\text{C}$ ; target ice properties were achieved after tempering at  $-2^{\circ}\text{C}$  for about 1.5 hours. The ice structure was columnar with an extensive "polycrystalline" granular upper layer; thin sections are shown in Appendix C.

A series of characterization tests were performed prior to the start of the model test program; they are discussed in Appendix C. These tests were intended to identify the scaling limits of UR/D/S ice and to develop a standard operating point. The tests included monitoring of growth rates, pro-

filing ice sheet thickness, measurement of flexural strength and modulus of the ice sheet using the cantilever beam method, and measurement of shear strength using the "guillotine" method (Timco, 1980). The tests are described in a M.U.N. Ocean Engineering internal report (Paterson and Lau, 1986)

It proved possible to scale down UR/D/S ice well below the limits of standard urea ice (Timco, 1980). Flexural strength was the most sensitive to tempering; strengths averaged 15 kPa but could be reduced if ice quality was monitored. Modulus ratios ( $E/\sigma_t$ ) were always satisfactory, but measurement of shear strength was unreliable. The effort to identify a standard operating point failed, because it proved impossible to isolate the ice sheet from external conditions with the equipment available. Each model trial had to be reviewed to determine the ice quality.

The models consisted of a bow segment constructed of laminated blue styrofoam, reinforced with thin plastic sheet and coated with epoxy resin. The bow segment was mounted on a frame using compressive springs sized to simulate the restoring buoyancy of the hull, as shown in Figure 8. The equations of motion for the M.V. "ARCTIC" were analyzed with the assistance of a computer simulation developed for sea-keeping, where wave-induced hull motion was treated as an

analogue for the induced icebreaking motion. Calculation of spring size is given in Appendix D. A distortion factor of two was required to accommodate the variation between the scaling limits of the model ice and the geometric scale.

### 3.2 SMALL SCALE TOWING TRIALS: OBSERVATIONS ON TECHNIQUE

Owing to model scaling limitations, a qualitative test program was adopted for the small scale trials. Therefore the scaling limits were not as important. Rather than measuring resistances, each trial was videotaped to assess the fracture pattern and the size of the broken ice pieces produced. A system of ranking the quality of trials was developed (Appendix E). Observations from model tests and field trials (Freitas and Nishizaki, 1985; Molyneux, 1982), and a semi-empirical equation from Milano (1982) provided the basis for evaluation. A series of acceptable trials were used to assess the performance of a particular bow design.

A total of 123 trials were attempted over a five month period; the growth time allowed for two trials per day, with a maximum of three trials possible. About 30% of the trials were performed in a pre-drilled sheet; a pattern of holes was drilled in the ice sheet to promote fracture to the predicted ice piece size. The trials are classified by quality and bow type in Tables 1 and 2. About 70% of the 102

successful trials were rated of fair to excellent quality; the supporting data on ice conditions and speeds from these trials are given in Appendix E.

Most of the problems encountered with the trials could be eliminated with higher quality equipment and improved procedures. The increment in quality achieved would have to be considered against the cost, in equipment and testing time, noting that this is a preliminary design method. The major non-technical limitation of small-scale testing was the subjective nature of the qualitative evaluation. It was necessary to define specific criteria and outline some design principles for the test program to follow.

### 3.3 EVALUATION CRITERIA FOR THE SMALL-SCALE DESIGN PROGRAM

The first objective of the design program was to produce a functional configuration that would demonstrate the shearing action of the concept. A series of specific design problems were identified and used to develop alternative bow configurations. These problems then effectively formed the evaluation criteria for the small-scale test program.

- 1) An adequate trim moment had to be provided by the test hull, to ensure a sufficient icebreaking buoyant force and to avoid propeller immersion problems. This is essential

to the successful operation of an upward-acting bow, but is more related to matching the hull to the ice conditions. The test case, the M.V. "ARCTIC", is a large vessel with a high length:beam ratio, such that induced trim angles would be small. The hydrostatic particulars indicate a trim of one metre would generate a lifting force of over 600 tonnes at the forward perpendicular (Appendix B). This was sufficient for the estimated ice load. A very conservative ice fracture model was used, basically a linear elastic cantilever beam with small deflection, and an assumed weight of broken ice. Trim by the bow was predicted to be about the thickness of the ice sheet. This estimate affected the bow geometry and was carried into the spring analogue for the model mounting.

- 2) The most basic configuration of the bow used an inverted "pontoon" form (labelled FF1, Figure 9), which was a short, simple form that was certain to shear the ice sheet. However its potential performance in other operating conditions was limited by its geometry. A forefoot (labelled FF2, Figure 10) resembling the "snout bow", discussed above, was proposed. It was expected to have better open water performance, and to be more effective in pack ice and ridges (where displacement of the ice is more important than ice fracture). The inverted-pontoon form

was believed to share the same ice-clearing problems as the ice plow (Appendix A) because of its two-dimensional form. The snout was intended to discriminate between ice conditions and deflect broken ice laterally. It had to be determined how the snout form affected the breaking action in level ice; the shearing action of the concept had to be maintained.

- 3) The length of the bow had to be similar to a conventional icebreaking bow, to keep construction costs comparable and to avoid a reduction in manouverability. This placed limits on the waterline angles of the snout form. The limitation was expected to be compensated by bow trim which would expose the upper part of the snout, with a reduced stem angle and finer entrance angles, to the ice sheet.
- 4) Development of a centreline crack was essential to ensuring a lateral flow of broken ice. Both stem profile and bow height are factors. Bow height had to be sufficient to keep ice from falling on the deck, yet a high bow impedes visibility and adds to construction costs. Because the inverted-pontoon bow initiates a centreline crack on a stem splitter located aft of the forefoot (Figure 9), the bow height had to be about half the beam. The snout forefoot produces the centreline crack ahead of the shoulders using

a stem splitter as with the Alex-Bow icebreaking plow (Alexander, 1970); consequently bow height is less critical, although higher in-plane forces may result.

- 5) The entire upper forebody, including the stem profile and forepeak, had to provide an adequate flow of broken ice laterally and aft. This was a critical problem with the early ice plow designs. During this test program some design principles became apparent. In the absence of water flow, ice clearance depends on maintaining a "train" of broken ice, and the use of the ice's own weight. A flared forepeak was adopted to deflect extreme ice excursions without increasing bow height. However sufficient clearance under the forepeak was required for the main flow of broken ice.
  
- 6) The importance of broken ice management relative to ice fracture had to be investigated. The configuration of the bow shoulders was of particular concern. The location of the shoulders relative to the forecastle stem was also a factor. Locating the shoulders ahead of the forecastle emphasized the shearing action but resulted in a longer bow and an increased risk of ice blockage.

An important trend was identified from these six problems. The concept was based on the assumption that recent design developments that reduced the resistance of downward-acting bow forms could be applied directly to an upward-acting form. These criteria depart from that assumption, suggesting that practical concerns related to upward-acting icebreaking forms may result in different set of design priorities, unique to this type of bow.

#### 3.4 THE EVOLUTION OF THE S-BOW CONFIGURATION

The development of the S-Bow configuration was treated in three stages: forefoot, forecastle profile, and complete forebody. The alternative configurations are shown in Figures 9-12; a summary of the test program is given in Table 3. The test program followed several trends which eventually resulted in the selection of the FB5 form for resistance trials, as the S-Bow.

The snout configuration (FF2) was adopted for the forefoot; the shearing action could be maintained along with a centreline crack. The snout produced diagonal, but relatively straight cantilever segments in these trials.

Trials with modified inverted-pontoon forms (FF1B and FF1C) indicated that a stem-splitter had to be prominent to

produce an effective centreline crack. Consequently the stem splitter was placed forward on the snout, despite the higher in-plane forces that could result. Tests with the complete forebody indicated that a fine entrance at the upper stem was required to maintain the centreline crack and ensure the lateral separation of the ice flow. The upper stem profile was extended ahead of the shoulders.

Much effort was directed toward ensuring an adequate flow of broken ice; the pre-drilled tests (Section 3.2) were used in this phase of the program. A shorter snout, more closely integrated with the forecastle was adopted (FB3). The recognition of the role of gravity in clearing ice resulted in the replacement of the original snout form (FB2) with a form that featured more inclined surfaces (FB3 - FB5). The initial snout forms (FF2 - FB3M) featured side runners, as with the Thyssen/Waas bow, and a "tunnelled" section at the shoulders. This arrangement assisted the shearing action, but could impede the lateral flow of broken ice. In the final configurations (FB4, FB5), the runners were removed, and in the FB5 version the tunnelled section was replaced by a truncated airfoil shoulder configuration. It was observed that a sharp edge on the shoulders would shear the ice adequately, without the risk of ice blockage.

Two observations are relevant to the later tests. An overhanging forecastle (FB1) was observed to create ice blockage problems, but a small overhanging forepeak was retained to deflect extreme ice excursions (FB3 - FB5) while minimizing bow height. The crushing that was observed under the forepeak was attributed to the poor fracture properties of the model ice. The other observation was that the models were observed to settle consistently with each trial, and would produce a "chevron" pattern of relatively straight cantilever segments.

## CHAPTER FOUR

## RESISTANCE TESTS WITH THE S-BOW IN LEVEL ICE

The form development program demonstrated the S-Bow concept qualitatively; the purpose of the resistance program was to provide performance data for assessment of the S-Bow. A comparative resistance program was adopted, where the S-Bow was compared with a modern conventional icebreaking bow. This was intended to minimize the effect of scaling problems on the evaluation, by providing a standard for verifying results.

## 4.1 TEST FACILITIES

The resistance tests were performed at the Institute for Marine Dynamics (IMD), St. John's, Newfoundland, from 6- 16 December 1986. A full description of the IMD facilities can be found in Jeffrey and Jones (1986). The S-Bow resistance tests were performed as internal project I5306.

The ice tank has a length of 75m and a width of 12m, large enough to permit tests at several speeds per trial and a run at the side of the ice sheet (the quarter point) as well as down the centre of the ice sheet. There is a large towing carriage capable of speeds up to 4m/s and equipped with its own microcomputer-based data collection system. Resistance

and model motion is measured using a towing post dynamometer allowing three degrees of freedom, mounted on the towing carriage frame. A videotaping system with two cameras was used to record the trials. A service carriage is used as a platform for ice testing. The tank uses EG/AD/S model ice developed by Timco (1985) A typical model ice sheet can be grown, tempered, and tested every 24 hours.

IMD has complete model preparation facilities, including a five-axis computer-aided milling (CAM) machine and a paint shop. Computer support is provided, with software for milling machine control and for data analysis.

#### 4.2 MODEL DESCRIPTION

A 1:30 scale model of the M.V. "ARCTIC", designated as M326BMS or M326B, was available at IMD. The model was constructed as three components; bow, stern, and parallel mid-body segments, modelled up to the weather deck. The stern segment was constructed of wood laminate and was fitted with a rudder, ice knife, stern tube swelling, propeller bossing and duct. The parallel mid-body extended from 2.29m to 4.81m forward of the aft perpendicular, and was constructed in fibreglass (FRG) with plywood framing. The S-Bow was to be compared with the CASPPR Class 4 bow developed by Melville Shipping Ltd. for the M.V. "ARCTIC", referred to as the

Melville Bow. The bow segment was also constructed in fibre-glass. The hydrostatics and ballasting information for the Model M326B are provided in Appendix B.

The availability of a segmented model meant that only a new bow segment with the S-Bow had to be constructed. The bow segment was created by fairing the S-Bow into the model segment of the Melville bow. This involved the digitization and transfer of the FB5 (Section 3.3) lines into the IMD computer system, which were then faired using the in-house SMP programs to a form acceptable for milling. The "beak" seen in Figure 3 was introduced for fairing. A basic plug suitable for milling was constructed by laminating sheets of blue R-30 styrofoam. This plug was milled to 2.5mm layers on the CAM system, as three segments because of limits on the cutter head motion, then assembled and hand sanded smooth at the Memorial University model shop. The plug was sent with a Melville Bow shell to the Newfoundland and Labrador Marine Institute for fibreglassing; the S-Bow plug had to be joined with the Melville Bow segment as indicated. The fibreglass shell was returned to the IMD model shop for framing, sanding, painting and fitting out. The stem splitter was constructed of hardwood. Foam insulation was sprayed inside the snout to reinforce the fibreglass shell when hardened. The construction sequence is shown in Figure 13.

It must be commented that the complex set of exchanges involved in the model construction resulted in some quality problems. The definition of the shoulders and the forepeak suffered in particular.

The hydrostatics for the M.V. "ARCTIC" fitted with the S-Bow, designated Model M326BP, are presented in Appendix F. In spite of changes in hull dimensions, the towing post gimbal could be placed in the same location as the Model M326BMS (Appendix B). The same vertical centre of gravity (VCG) and radii of gyration were also assumed. The S-Bow reduced the waterline length of the "ARCTIC" by 5.0%; the S-Bow itself was 28% shorter than the Melville Bow. The use of the Melville Bow as the underside resulted in a very hollow forefoot with a slightly reduced displacement compared with M326BMS; however the forebody block coefficient increased from 0.754 to 0.829 because of the waterline geometry. Ballasting for M326BP was similar to M326BMS, with final adjustments made using the model draught marks and pre-set "trim hooks". Moments to trim one centimetre were calculated as the trials entailed some trim variations (Appendix F).

All model segments were given the same paint treatment to obtain a target dynamic friction coefficient  $\mu$ . A special test board was constructed at IMD which measured  $\mu$  by push-

ing a sample board under an ice block loaded with a given weight (Williams et al., 1987). The average coefficients obtained for the model were: bow 0.11; mid-body 0.060 ; stern 0.099. The friction data is presented in Appendix F. The reason for the variation in  $\mu$  was that each segment was painted separately.

#### 4.3 OUTLINE OF TEST PROGRAM

Six ice sheets were used in the test program. The details of the test program for the S-Bow were based on tests conducted with the Melville Bow at various ice tanks as reported by Baker (1985). The tests were performed to correspond with the following full scale conditions: level ice thicknesses of 0.75m and 1.2m; flexural ice strength of 500 kPa, a typical value for first-year sea ice; and a speed range of 1.5 to 5.0 knots. These conditions were adopted for the S-Bow program, with another speed interval corresponding to 7.0 knots to get better data distribution. The target conditions at model scale were: ice thicknesses of 25mm and 40mm; an upward flexural strength of 17 kPa; and a speed range of 0.141 to 0.740 m/s. One 40mm ice sheet was dedicated to a resistance test for the Melville Bow to "calibrate" the EG/AD/S ice sheet; the published data had been obtained in different types of model ice.

Only resistance tests were planned for the S-Bow. Self-propulsion tests would have exceeded the resources of the program. Trim alterations were planned for the first trial to identify an optimum geometry. The final two ice sheets were tested at different ice strengths in an attempt to isolate the ice resistance components. A similar technique is described by Pozniak et al. (1981). A schedule of the trials is given in Table 3.

The ice characterization tests specified for the program were: cantilever beam tests, a modulus test, a "notch test" for fracture toughness, and an ice sheet thickness profile. As the flexural strength of EG/AD/S ice varies with load direction, three cantilever beams were tested in the upward direction, and three downward. Flexural strength and fracture toughness were measured at regular intervals at each side of the ice sheet to monitor the tempering of the sheet. An ice modulus test was conducted before and after each trial using the plate deflection method. At the end of testing, the ice thickness was measured at 2m intervals along the sides of the broken channel. Uniaxial compressive strength was also measured, using a beam system. Ice density was also measured. There was no available technique for measurement of shear or tensile strength. IMD ice measurement procedures are described in Jones et al. (1987).

Resistance and hull motion were measured from the towing post dynamometer and stored with the speed as a time history on a six channel data recording system. Sample rate was 20 Hz per channel. Two channels were devoted to model resistance, such that there was a back-up channel. Three linear voltage transducers (LVDTs) were arranged around the towing post to measure roll and pitch displacements with heave; these were stored on three channels as port, starboard, and forward displacement. Carriage speed was recorded on the remaining channel. This data was transferred from the carriage data system to the main computer system for statistical analysis.

Visual observation remained an important part of the test program. Remotely controlled videotape cameras were located above the model to view the bow region and of the side of the hull. Still photographs of each test were taken for more detailed record of the breaking action and to show the condition of the broken channel.

#### 4.4 ANALYSIS OF THE IMD RESISTANCE TRIALS

The five resistance trials of the S-Bow were analyzed in three ways: by visual observation, analysis of the resistance data, and by numerical analysis. Individual summaries of each test are provided in Appendix G.

#### 4.4.1 Experimental Observations

Perhaps the major accomplishment of the large-scale trials, with regard to the development of an upward-acting bow, was the demonstration of the breaking action of the S-Bow at the larger model scale. A regular fracture sequence and a steady flow of broken ice was clearly observed, as described in Section 2.2. This was essential to exploit the operational advantages of the upward-acting icebreaking concept. Nevertheless a number of problems were observed that were believed to originate with the design configuration and resulted in very unsteady, high resistance levels. These problems are included in a series of observations described below.

##### 4.4.1a) Overprediction of Hull Trim -

A central factor in the design problems observed during the resistance trials was the overprediction of the hull trim induced by the ice sheet. This was made most apparent by the curvature of the "crescents" of broken ice (Section 2.2); the circumferential crack created as the ice sheet fractured appeared much further ahead on the snout than observed in the small ice tank. Analysis of the M326BP motion data supported the visual observations (Appendix G). At the design trim (Test 1), the induced trim was less than 50% of the prediction.

The overprediction resulted from the tendency to be conservative with the initial design, recognizing that the worst case would have been a failure to fracture the ice. A long hull was selected as the test case, and a very conservative ice loading model was used to predict hull motion. It was demonstrated that bow submergence should not be a problem in level ice, but the penalty of the conservative design approach was a series of interactions which increased ice resistance.

4.4.1b) Complex Fracture Pattern -

The reduced snout submergence meant that the formation of a circumferential crack was more prominent in the initial fracture of the ice sheet. This more complex fracture pattern can be related to higher resistances. Photographs indicated a large region of deflected ice around the snout, a function of the snout geometry presented by the reduced trim (Figure 14).

4.4.1c) Contact of Broken Ice under the Forepeak -

The extreme curvature of the fractured crescents acted to trap previously broken ice in the "hollow" of the crescent. This ice would then be driven aft over the fore-castle to crush under the flared forepeak, unless the tip of the crescent fractured to allow lateral movement. The

effect is seen in Figure 5. Crushing was more prevalent at higher speed and with greater ice thickness. The trim overprediction, the forecastle geometry, and the broken ice dimensions combined to create the problem.

The potential for crushing was identified during the small-scale trials but was attributed to the scaling problem. The overhanging forepeak was only expected to contact extreme ice excursions. (A very large ice piece rotated above the upper deck, but was deflected away by the forepeak during Test 5.)

#### 4.4.1d) Shoulder Contact -

The reduced bow trim may have caused the ice sheet to contact a lower level on the shoulder, where the edges were not well executed on the model. As with the forepeak, little ice contact was expected in this region. No crushing was observed at the shoulders but flexing of the ice sheet near the bow may have resulted from in-plane loading. The shearing action of the shoulders appeared to improve with a moderate trim by the bow (Tests 3 and 5), but probably resulted in greater crushing under the forepeak.

4.4.1e) Bow Behaviour during Quarter Point and Pre-Sawn Trials -

During trials on the quarter point of the ice sheet, the ice tended to send a radial crack out to the previously broken central channel, as in Figure 15. At lower speeds the ice would displace laterally rather than move over the bow; at higher speeds, with closely spaced wooden props to confine the ice (Tests 4 and 5), the ice would ride over the bow. This phenomena was also seen in a pre-sawn channel in 25mm ice (Test 2). It can be inferred that the S-Bow will behave "selectively" between ice floes and an unbroken ice sheet. This selective behaviour corrects a significant problem encountered by the ice plow (Davies, 1969; see Appendix A).

4.4.1f) Deposition of Broken Ice -

The deposition of broken ice is the basis for several advantages (Section 1.2). The movement of broken ice around the hull was demonstrated, but broken ice was observed between the hull and the ice sheet (Figure 5). Occasionally the model was observed to sway without any significant failure event; "wedging" of this broken ice may have been responsible. This problem was found to be a significant resistance source in other tests (Baker, 1985). The wedged pieces were generally deposited vertically by

rotating over the shoulders. The inner broken ice segments moved further aft along the forecastle to be deposited horizontally on the ice sheet, such that their weight would be distributed over the sheet. The height of the shoulders appeared to assist in the distribution of the broken ice along the ice edge.

#### 4.4.1g) Condition of the Broken Channel -

The production of an ice-free channel was affected by the wedged ice pieces, which would fall into the channel. A relatively clear channel was still produced immediately aft of the model, but the broken channel edges would eventually deflect causing the broken ice to slide into the channel.

#### 4.4.1h) Ice Modelling Limitations -

Limitations of current ice modelling technology, particularly with regard to fracture properties, may have had a role in some of the phenomena described above. The ice piece size was generally larger than predicted, possibly a result of the elimination of hydraulic effects (Frederking and Hausler, 1980; Enkvist, 1972). There was also a trend toward greater ice deformation and larger ice pieces with the later 40mm trials (Tests 3 and 5). Extensive ice sheet deformation modified the failure sequence

and induced heavy rolling incidents. Variation in the model trim was a probable contributing factor, but fracture toughness scaling also had to be considered.

The problem of scaling fracture toughness is well documented (Timco,1985; Parsons et al.,1985; Enkvist, 1983). The data shows the final 40mm sheets were "tougher" than the first sheet. The problem is less apparent in the 25mm sheet, but the unbroken length of the fractured crescents could extend to the half beam of the model. Maintenance of consistent properties was complicated by the requirement to scale flexural strength upward. Tempering conditions were modified in later tests to better control the tempering rate of flexural strength, but other ice properties may have been negatively affected.

The amount of deflection around the snout may also have indicated fracture toughness problems (Figure 14). If the ice sheet should have been more rigid and brittle, the more bow trim might have been induced and the breaking action modified. Whether this would have favourably affected resistance is unclear, but it would more closely represent the design conditions.

.

The readiness of the ice sheet to radially crack during the quarter point trials (Section 4.4.1e) was also observed when cuts were made parallel to the end of the central track prior to the final test. Radial cracks seemed to "find" the prepared cuts. A review of studies of downward-acting bow forms that rely on a stem crack indicates a discrepancy in the amount of radial cracking observed between the model tank and the field (Milano, 1982; Naegle, 1980; Milano, 1975; Enkvist, 1972; Macdonald, 1969). This problem may also result from fracture toughness scaling, but the observations would indicate a confinement problem. The laboratory ice sheet may be too "pure" relative to field conditions, where flaws will be present. The implication is that an evaluation of a bow form relying on a stem crack may be biased because the laboratory ice sheet represents an extreme case, rather than a typical field condition.

The effect of these modelling problems could not be assessed adequately from the limited number of trials performed. But they are of some consequence to the refinement of the S-Bow form, and the evaluation of the concept.

#### 4.4.2 Resistance Results

The resistance data were recorded as a time history which was statistically analyzed and plotted. The S-Bow output plot was very unsteady with extreme peak resistances, when compared with the Melville Bow. A sample output is given in Figure 17. The resistance data were analyzed over the complete time history, and were also averaged over selected time segments to eliminate the worst resistance episodes. The resistance time history and the selective analysis were consistent with the assumption that the high resistance episodes could be attributed to the test configuration rather than the basic concept. This technique was thought to better indicate the potential of the concept.

Average resistance lines for each bow at the design trim for the two ice thicknesses are plotted in Figure 18. The data for the quarter point trials and the selective analysis are shown with the untreated data. The data are summarized in Table 4. The average resistance of the S-Bow measured in 25mm ice is about 2.5 to 3.0 times that of the Melville Bow at a given speed. In contrast, the S-Bow in 40mm ice has a resistance four to five times higher than the Melville Bow based on untreated data; the selective data reduced the ratio to the lower (2.5- 3.0) range.

The S-Bow resistance is approximately linear with speed in both ice thicknesses, but the increased slope of the 40mm line indicates the effect of additional resistance-causing factors. This observation complements the rationale for the selective resistance analysis. For example, the frequency of crushing under the forepeak was observed to increase with velocity, such that resistance would radically increase. As indicated by the observations on radial cracking in Section 4.4.1, there is a reduction in resistance recorded during quarter point trials.

Average resistance versus speed is plotted for each trial in Appendix G. The results show that resistance was minimized when at the design (zero) trim. When trimmed by the stern, the resistance probably increased because the fracturing action was less efficient. The effect of trimming by the bow was probably negated by additional crushing under the forepeak, inspite of better exposure of the shoulder edges.

The attempt to investigate the resistance components by varying the ice properties (Tests 4 and 5) was inconclusive. The analyses are presented in Appendix G. It may be that the effect was masked by other mechanisms. This would be consistent with the hypothesis regarding design problems.

Very high resistance levels were recorded at zero speed, at the start and end of each test. The towing post calibration was verified and a review of the videotapes showed little correlation between the amount of ice coverage on the bow and the resistance level recorded. No crushing was visible. The deformation of the ice over the snout was identified as the probable source of resistance.

#### 4.4.3 Numerical Analysis of the S-Bow Breaking Action in Level Ice

A cursory view of the S-Bow resistance data might suggest that a CASPPR Class 2 or 3 bow had been tested in Class 4 conditions, and that a general scaling up of the S-Bow dimensions might be required. However experimental observations, as reported in Section 4.4.1, identified specific design problems with the test configuration. It had to be established whether design refinements could significantly reduce the ice resistance of the S-Bow, or whether the high resistance levels were inherent in the basic concept. The resistance lines provide a performance envelope for analyzing the utility of the design but were not directly applicable to an analysis of specific design problems. Consequently a numerical analysis of the breaking action of the S-Bow was used to investigate the observations reported in Section 4.4.1.

The breaking action of the S-Bow in level ice was analyzed using a format similar to that outlined by Frederking and Timco (1985) for an inclined plane. Ice resistance was treated as series of mechanisms or events, as identified from the trial videotapes. Each event has an individual load history, that in a particular combination at a given time will oppose motion. The average resistance will be the average of instantaneous resistances over a specified time; a cumulative addition of the individual peak resistances would give very conservative results. Velocity dependence will be reflected by the frequency of events and a higher probability of occurrence for certain events; it may also be reflected in the rheological assumptions of a particular model of an event. None of the models had a significant inertial (velocity dependent) component similar to common semi-empirical analyses (Enkvist, 1972); this would reflect the absence of waterflow and the dominance of gravity effects. Most of the models also treated ice as a homogeneous material, and assumed a simple Coulomb friction model.

The analysis consisted of isolating an individual event and assessing its magnitude relative to other events. A resistance "envelope" was developed for each event by applying a number of simple mathematical models. Convergence of results suggested that the effect of a certain event could

be assessed regardless of the rheology assumed by individual models. The analysis was based on the S-Bow model tests; no attempt was made to address possible discrepancies between the laboratory and the field. The following icebreaking mechanisms were treated:

- 1) ice fracture resistance- radial cracking component
- 2) ice fracture resistance- circumferential cracking
- 3) flexural failure at the shoulders
- 4) ice ride-up over the forefoot- rotational, sliding and edge load effects (non-simultaneous)
- 5) ice ride-up over lower forecastle- sliding
- 6) additional factors - snow friction on downward-acting bow

The following design problems identified in Section 4.4.1 were analyzed:

- 1) the deflected region around the snout
- 2) crushing at the shoulders
- 3) ice loading/crushing under the flared forepeak- limit stress; limit force; crescent tip failure
- 4) ice contact/wedging at the parallel mid-body

The effect of trim was analyzed in the treatment of a range of stem angles, and indirectly in the treatment of some of the problems listed above.

The S-Bow was treated as a combination of simple geometric shapes, with varied form angles (Figure 4) to account for the actual form; fracture geometry was also varied according to experimental observation. The forecastle ice loadings were calculated over a fixed distance (station spacing or unit length) to account for the variation in slope and in ice coverage.

The details of the numerical analysis are given in Table 5. The individual analyses are described in Appendix H.

The analysis confirmed that the design problems observed during the trials were capable of producing high resistance levels. Excessive resistances calculated in some of the crushing analyses were interpreted as an indication of the gravity of that failure mode acting over a small contact area. The direct effect of the trim overprediction on resistance was indicated by an increase in resistance with stem/slope angle. The ice fracture components appear to be sensitive to the orientation of fracture cracks and the stem inclination, but less sensitive to the type of forefoot geometry. Of significance to the upward-acting concept was the resistance due to ice-ride-up; the resistance magnitudes approximated the ice fracture component on both the forefoot and forecastle.

#### 4.5 SUMMARY OF THE S-BOW LEVEL ICE RESISTANCE ANALYSES

The S-Bow resistance tests in level ice were assessed using three complimentary analyses: a review of videotaped recordings; resistance measurements; and a numerical analysis of individual mechanisms. The aggregate conclusions from these analyses gave an insight into the physics of the concept and the character of the resistance penalty. There were two main conclusions regarding the performance of the S-Bow in level ice.

- 1.) The hypothesis that the high range of resistances was due to design problems was supported. The implication is that design refinements, if successful, could significantly reduce resistance levels.
- 2.) It was also indicated that the resistance due to ice movement over the bow was a significant component of the total level ice resistance, and that it predominates over the effect of the elimination of hydrodynamically-induced resistance. For a similar fracture action, the level ice resistance of an upward-acting bow will always exceed that of a downward-acting bow, by a factor of two or greater.

## CHAPTER FIVE

## RECOMMENDATIONS: CONDITIONS FOR FURTHER RESEARCH

The final stage of the research program sought to address two issues. The first was whether the design problems identified during the model trials were rectifiable. The second concern was to identify potential applications of the S-Bow; this involved assessing the significance of the resistance penalty identified during the model trials against the operational advantages of the S-Bow.

## 5.1 REFINEMENT OF THE S-BOW FORM BASED ON LEVEL ICE TESTS

The design problems were reviewed and possible design refinements are proposed below. The intent is to demonstrate that the design problems are not intractable.

- 5.1.a) The entrapment and crushing of broken ice under the flared forepeak was identified as a major source of resistance. The overhang and convex sections of the forepeak, adopted to reduce bow height, should be replaced with a wall-sided forepeak of adequate height.
- 5.1.b) A complementary problem was the geometry of the cantilever "crescents", which acted to trap the broken ice. Lengthening the forebody to move the shoulders

forward should improve the ice fracture pattern, but the resistance associated with sliding of the broken ice would increase. Minimizing length while eliminating the crushing problem is the ideal. A more acceptable refinement may be the use of a second set of edges or small runners ahead on the snout to ensure the "secondary" fracture of the crescents.

5.1.c) The numerical analysis indicated that even very localized crushing into the bow shoulders could cause very high resistances. It was evident that the shearing efficiency of the shoulders could be improved. Better definition of the shearing edge is recommended, but with regard to the open water performance penalty that may occur.

5.1.d) The entrapment of ice floes between the hull and the ice sheet edge largely originated with the decision to adopt an existing parent hull to a new bow type, but may be minimized by optimizing the forebody slope angles. Ice deposited horizontally on the ice sheet will be less prone to fall back into the broken channel. Excessively steep slope angles on the forecastle should be avoided in areas of high ice contact, while retaining effective use of broken ice weight in the clearing process.

5.1.e) Overprediction of hull trim resulted in a large region of ice deflection around the snout during the IMD trials. For similar hull forms (characterized by a high L/B ratio) and ice conditions, it was demonstrated that excessive hull trim should not be a problem. The snout should be re-designed for a reduced trim. The stem angle should be minimized in the ice belt region, and relocation of the stem skeg further aft on the snout should be investigated. For shorter hull forms, where hull trim may be significant, a more refined model for hull motion and ice loading should be sought.

It should be observed that the basic arrangement of the S-Bow is unchanged by these recommendations. The recommendations consist of refinements rather than major revisions. This is probably the most important outcome of the design process used to develop the S-Bow form.

The refinements listed above are based only on level ice tests, and therefore are increments on the design spiral. A variety of other factors, such as other operating conditions and structural design must be incorporated before a definitive design can be developed and fully evaluated.

## 5.2 INVESTIGATION OF THE UPWARD-ACTING ICEBREAKING CONCEPT BASED ON THE S-BOW: CONDITIONS FOR DEVELOPMENT

### 5.2.1 Overview: Conditions for Analysis

A definitive evaluation of the S-Bow concept was not possible given the limited test data and the uncertainty of the effect of the design refinements, but an assessment of the significance of the inherent level ice resistance penalty was necessary to make recommendations consistent with the principles described in the introduction. The intent was to identify potential applications or an operational profile as discussed in Section 1.3. Thus a direction for any further research might be identified.

The S-Bow level ice performance was based on the lower end of the model resistance data, 2.5-3.0 times the resistance of the Melville Bow, recognizing that there were a number of factors that could vary this estimate.

### 5.2.2 Analysis of the Performance Envelope

The level ice resistance penalty of the S-Bow was analyzed comparatively using case studies, which allowed the incorporation of some of the operational advantages into the evaluation. The magnitudes of the level ice resistance also had to be considered, as a condition for the comparative analysis. It may not be necessary for a

vessel to excel in a given operating environment, but it must achieve a certain minimum performance as a condition for operation in that environment.

The operational profile was assessed in terms of the route spectrum (Figure 1). In this context, the object of icebreaking design is to achieve an optimum balance of performance for specified route, treating the entire range of conditions over the route.

The results of the level ice resistance trials indicated that the S-Bow should never be considered for a purely "heavy" icebreaking role, as defined by the spectrum. The S-Bow requires a compensating feature to be competitive. A case study indicated an unorthodox hull form featuring narrow beam would not offer a sufficient improvement in performance in a heavy icebreaking role (Appendix I).

The light-medium range of the route spectrum was studied, where a significant proportion of a route will be in open water (Brune, 1986; Dick, 1983). This route description is typical for seasonal shipping; an open water penalty is incurred to obtain an icebreaking capability that is only required for access to local areas for a short

winter season. The impact of an open water performance penalty will be magnified when seeking off-season employment on another purely open water route.

The geometry and action of the S-Bow allows some latitude with the hull form below the waterline (Section 1.2). It may be possible to fair the S-Bow into a bulbous bow (Appendix A.2) and compensate for a higher ice resistance with an improved open water performance, provided a minimum icebreaking performance can be maintained.

The feasibility of this proposal was investigated using a case study based on the M.V. "ARCTIC" operating between Montreal and two northern lead-zinc mines over the summer season. The performance estimates were based on scaled model resistance data and therefore the icebreaking components involve a significant scale effect. A simple averaging method was used to estimate the improvement in open water performance required by the S-Bow to be competitive. The resistances were also compared with the propulsion system capability, recognizing the scaling limitations. The details of the analysis are presented in Appendix I. A study of a high speed application was not performed because of the uncertainty regarding hull trim characteristics (Section 5.1.d).

The comparative analysis indicated that a reasonable improvement in open water performance could compensate for a significant ice resistance penalty on a light-medium route. This conclusion applies generally, but in the case of the S-Bow the geometry may allow the open water performance to more closely approach a low speed open water hull form, if a bulb can successfully be designed to suppress the bow breaking wave (Harvald,1983; Eckert ar. ' Sharma,1973). This may produce a more versatile vessel, with regard to economic off-season employment or operation on varying routes, and with an icebreaking capability that would include the operational advantages associated with the upward-acting concept.

However this prospect is predicated on maintaining a minimum standard of icebreaking capability. The magnitudes of the S-Bow level ice resistances, admittedly based on model data, were such that a significantly larger propulsion system would be required to provide adequate thrust to maintain a prescribed transit speed. Any compensating improvement in open water performance would be negated by the added cost of the propulsion equipment. The magnitudes of the level ice resistance of the S-Bow must be reduced for the application to be feasible.

It is possible to conclude that the development of an efficient open water form and the reduction of the level ice resistance penalty are two parallel requirements for successful development of the S-Bow, because of the emphasis given these two operating conditions in current design practice. The capability of the bow in other ice conditions requires investigation but will vary in importance with the route or application under consideration; other ice conditions do not tend to get the same general emphasis as level icebreaking in assessing a bow form.

#### 5.2.3 Conclusions: Conditions for Further Research

The greatest potential application for an upward-acting icebreaking bow lies in the light-medium range of the route profile spectrum, particularly for multi-role vessels. The following two conditions must be met for this application to be feasible:

- 5.2.3.1) there must be a sufficient advantage in open water performance when compared with competing ice-breaking hull forms; based on the incorporation of the bow into an effective bulbous bow (for low  $F_n$  applications) to achieve an increment in performance similar to that created by an open water bulb.

5.2.3.2) the level ice resistance must be reduced to a magnitude where a prescribed performance can be maintained with a comparable propulsion system; where comparable is defined by the specifications of the candidate vessel. The correction of design problems would significantly reduce level ice resistance but the large resistance component associated with the movement of broken ice over the bow will not be eliminated by form design alone. A more rational approach would treat the bow form as a component of an upward-acting icebreaking system that incorporates auxiliary icebreaking devices (Mellor, 1984; German and Dadachanji, 1975).

The application to a light-medium route would be a departure from previous design programs. The earlier ice plow was generally developed for "heavy" icebreaking duties, without regard to open water performance. This proposed application is a role similar to that of the inclined-stem design found on some Great Lakes bulk carriers (Appendix A), extended into heavier ice conditions. An essential aspect of this proposal would be the recognition that improvement of the range of performance of icebreaking vessels is a valid direction for research.

## 5.3 SUMMARY AND CONCLUSIONS FROM RESEARCH

- 5.3.1) An upward-acting icebreaking concept potentially offers several operational advantages over conventional icebreaking bow forms.
- 5.3.2) The shearing action of the Thyssen\Waas bow offered a means for reducing the inherent resistance penalty associated with breaking ice upward.
- 5.3.3) A bow configuration incorporating a shearing action was evolved in small scale model trials in level ice using selection criteria that reflected the range of operating conditions encountered in icebreaking operations.
- 5.3.4) The bow configuration, designated the S-Bow, was tested in 1:30 scale level ice conditions at the Institute for Marine Dynamics, using the M.V. ARCTIC as the parent hull.
- 5.3.5) The IMD trials were analyzed using videotaped observations, the recorded model ice resistance, and a numerical analysis of the fracture sequence. A regular fracture sequence was observed but recorded ice resistance ran from two to five times the published resistance of the M.V. ARCTIC as fitted.

- 5.3.6) Observations and the numerical analysis indicated that the worst resistance events could be attributed to design problems, particularly in predicting the amount of trim by the bow. Recommendations were prepared to rectify the design problems.
- 5.3.7) A significant inherent resistance penalty that is associated with the lifting of broken ice was not compensated by the shearing action of the bow.
- 5.3.8) The inherent resistance penalty should preclude any further development for heavy and/or dedicated icebreaking duties.
- 5.3.9) A case study involving the M.V. ARCTIC indicated that, for an operational profile with a large open water component, a significant ice resistance penalty may be compensated by modest advantage in open water performance.
- 5.3.10) Further development of the S-Bow would seem most favourably directed toward light icebreaking and/or multi-role operations, where the operational advantages of the concept would be most significant.
- 5.3.11) Successful development will largely depend on achieving two objectives:
- a) reduction of the ice resistance penalty to a level

where no added propulsion plant is required to maintain a specified ice transit capability. This may require some integration with auxiliary icebreaking systems.

- b) development of the forefoot into an efficient bulbous bow such that open water is sufficient to compensate for the inherent ice resistance penalty.

5.3.12) Performance in other ice regimes may preclude the application of the S-Bow for specific routes or functions, depending on the importance of that ice regime to the operation. Further research into the performance of the S-Bow in other ice conditions is required.

## REFERENCES

- ALEXANDER, S.E., "Nautical Ice-breaking Structures", U.S. Patent Office, U.S. Patent No.3,521,591, June 21 1970, (Filed August 6 1968). 3p.
- ALLYN, N., "Ice Pile-Up Around Offshore Structures in the Beaufort Sea", Proceedings of Workshop on Sea Ice Ridging and Pile-Up, Associate Committee on Geotechnical Research, National Research Council Of Canada (NRCC), Ottawa, January 1982, Technical Memorandum No.134, pp.181-204.
- BAKER, D.N., THOMPSON, E.W, "M.V. ARCTIC, Design and Conversion to Arctic Class OBO", Marine Engineering Digest, Canadian Institute of Marine Engineering (C.I.Mar.E.), Ottawa, 1985/86, Vol.5 No.3, pp.8-15.
- BAKER, D.N., "Redesign of the M.V.'ARCTIC'-Additional Model Tests Performed at HSVA and WARC", Transport Development Centre (TDC), May 1985, TDC Report No.TP5812E. 70p.
- BARRY, J.P., "Ships of the Great Lakes", Howell-North Books, Berkeley CA., 1973, pp.60-61.
- BERCHA, F.G., GHONHEIM, G.A.M., "Evaluation of Pile-Up Formation and Structure Interaction Forces", Proceedings of Workshop on Sea Ice Ridging and Pile-Up, Associate Committee on Geotechnical Research, NRCC, January 1982, Technical Memorandum No. 134, pp.204-229.
- BERCHA, F.G., "The Development and Application of Multi-modal Ice Failure Theory", (Pre-print), International Union of Theoretical And Applied Mechanics (IUTAM) Symposium on the Physics and Mechanics of Ice, Copenhagen, August, 1979. (page no. N/A).
- BHATTACHARYA, R., "Dynamics of Marine Vehicles", J. Wiley and Sons Ltd., Toronto, 1978, pp.220, 311-312.
- BRENCKMAN, M., "Canada's Arctic Marine Transportation Research Program", Proceedings of International Polar Transportation Conference (IPTC'86), D.F. Dickens Associates, Vancouver, 1986, Vol.1, pp.1-18.
- BRUNE, E., "The ICEBIRD- A New Generation of Polar Resupply Vessel", Proceedings of IPTC'86, D.F. Dickens Associates, Vancouver, 1986, Vol.2, pp.512-522.

BUSTARD, E.E., "The Importance of Size in an Arctic Ship" Spring Meeting/STAR Symposium on Icebreaking Technology (IceTech'75), Montreal; Society of Naval Architects and Marine Engineers (SNAME), New York NY, 1975. 15p.

BUSTARD, E.E., "Merchant Ships for the Canadian Arctic", Marine Engineers Review, Marine Media Management, London, November 1973, pp.23-27.

CARTER, D., "Ice Forces on Fixed Structures and Ship Hulls", TDC, Montreal, TDC Report No.TP7457E, February 1986. 54p.

CARTER, J.E., COLBOURNE, D.B., "Small Waterplane Area Twin Hulled (SWATH) Vessel Ice Tests", German & Milne Inc., Ottawa, TDC Report No.TP6681E, July 1985. 80p.

COBURN, J.L., EHRLICH, N.A., "Advanced Icebreaking Concepts", Naval Engineers Journal, American Society of Naval Engineers (ASNE) Inc., New York NY, August 1973, Vol.85, No.4, pp.11-24.

COMSTOCK, E., (editor), "Principles of Naval Architecture", Society of Naval Architects and Marine Engineers (SNAME), New York NY, 1965, 3rd Edition. 830p.

DAVIES, J.F., "Summary Report of Investigation into the Circumstances Surrounding the Loss of the Dumb Steel Barges L.A. LEARMONTH and JOHNNY NORBERG etc.", Department of Transport, Ottawa, Report No.CA1 DTB12869A14, 1969. 11p.

DICK, R., "M.V. ARCTIC Northern Routing Environment- Final Report", Melville-Marine Consultancy, Calgary, March 1983. 80p.

DYKINS, J.E., "Ice Engineering- Material Properties of Saline Ice for a Limited Range of Conditions", Naval Facilities Engineering Command, Port Hueneme CA, NCEL Report No.R-720, April 1971, pp.50-53.

ECKERT, E., SHARMA, S.D., "Bugwulste für langsame, vollige Schiffe (Bow Bulbs for Slow Form Ships)", Jahrbuch der Schiffbau Technischen Gesellschaft, 1970, Vol.64, pp.129-171, Translated (to English) for Panel H-5 of the Hydrodynamics Committee, SNAME, New York NY, May 1973, Technical and Research Bulletin 1-33. 67p.

ELKHOLM, S., "Experiences from Bulk Transports in the Arctic", Proceedings of IPTC'86, D.F. Dickins Associates, Vancouver, 1986, Vol 2, pp.729-731.

ENKVIST, E., MUSTAMAKI, E., "Model and Full-Scale Tests with an Innovative Icebreaker Bow", (Pre-print) SNAME Annual Meeting, SNAME, New York NY, November 1986, Paper No. 13. (page no. N/A).

ENKVIST, E., "The New Fine-Grain Model-Ice of Wartsila Arctic Research Centre (WARC)", Wartsila Helsinki Shipyard, Helsinki, 1983. 30p.

ENKVIST, E., "On the Ice Resistance Encountered by Ships Operating in the Continuous Mode of Icebreaking", The Swedish Academy of Engineering Sciences in Finland, Report No.24, Helsinki, Finland, 1972. 75p.

ETTEMA, R., MATSUISHI, M., KITAZAWA, K., "Model Tests on Ice-rubble Size and Ship Resistance in Ice Rubble", Cold Regions Science and Technology, Elsevier Science Publishers B.V., Amsterdam, June 1986, Vol.12 No.3, pp.229-244.

FREDERKING, R.M.W., TIMCO, G.W., "Quantative Analysis of Ice Sheet Failure against an Inclined Plane", Proceedings of the Fourth International Symposium on Offshore Mechanics and Arctic Engineering (OMAE), ASME, New York, 1985, Vol. II, pp. 160-169.

FREDERKING, R.M.W, HAUSLER, E.V., "The Flexural Behaviour of Ice from In-situ Cantilever Beam Tests", Proceedings of the International Association for Hydraulic Research (IAHR) Symposium on Ice Problems, Lulea, Sweden, 1978, pp. 197-215.

FREITAS, A., NISHIZAKI, R.S., "Model Test of an Ice Class Bulk Carrier with Thyssen/Waas Bow Form", Proceedings of the Fourth International OMAE, ASME, New York, 1985, Vol II., pp.330-335.

FREITAS, A., "Thyssen/Waas Icebreaker System- Prospects for Arctic Navigation", Arctic News Record, Arctic News-Record Scanews, Bergen, Summer (September) 1984, Vol.3.2,pp.42-43.

FREITAS, A., "A Novel Icebreaking Concept", Proceedings of the International Conference on Marine Sciences and Ocean Engineering (InterMaritec'80), Hamburg, 1980, pp.484-494.

GERMAN, J.G., DADACHANJI, N., "Hull Forms for Arctic Bulk Transportation", SNAME Spring Meeting-New Horizons In Bulk Transport Systems, SNAME, New York NY, 1975,pp.60-69.

GERMAN, J.G., "Bulk Shipping and Icebreaker Support in the Arctic", Canadian Shipping & Marine Engineering, Maclean-Hunter Ltd., Toronto, January, 1971, pp.21-23.

GERMAN, W.H., "Arctic Marine Structures: Some Aspects of Systems Approach", Arctic Systems Conference, North Atlantic Treaty Organization (NATO) Scientific Affairs Division; Plenum Press, New York, 1975, pp.441-478.

GILL, R.J., Aboul-Azm, A., Terry, B.F., Russel, W.E., "A Ship Transit Model for Passage through Ice, and its Application to the Labrador Area", Proceedings of IceTech'81, SNAME, New York, 1981, pp.105-112.

GLEN, I., "The Canadian Arctic Marine Technology Program; A Review", Marine Technology, SNAME, New York NY, July 1984, Vol.1 No.3, pp.242-255.

GLEN, I., DALEY, C., EDWORTHY, J., GAREAU, G., "Studies Supporting Update of the CASPP Regulations Group I and II", Arctic Canada Ltd., Calgary, March 1982, DSS File No.19ST T8275-9-0082 (2 Volumes).

GRAY, W.O., MAYBOURN, R.O., "MANHATTAN's Arctic Venture- A Semi-Technical History", Proceedings of IceTech'81, SNAME, New York, June 1981, pp.171-201.

HARVALD, S.V., "Resistance and Propulsion of Ships", John Wiley and Sons, Toronto, 1983. 353p.

HERFORD, K., HYSING, T., "Form Design of Vessels", Marine Structures and Ships in Ice, MSIS Report No.81-03-01, Oslo, 1981. 59p.

HYSING, T., THORENSEN, T.E., JOHANSSON, P., HORJEN, I., MATHISEN, J.P., "Design Case, Part 1: Ice Transiting Vessel", Marine Structures and Ships in Ice, MSIS Report No.81-09/01, Oslo, 1981. 163p.

JANSSON, J.-E., "Ice-Breakers and Their Design", European Shipbuilding, Vol. No.5, 1956, pp.112-151.

JEFFREY, N.E., JONES, S.J., "Canada's New Institute for Marine Dynamics, Opportunity for Improved Polar Transportation", Proceedings of IPTC'86, D.F. Dickens Associates, Vancouver, Vol. 1, pp.149-167.

JOHANSSON, B.J., REVILL, C.R., "Future Icebreaker Design", Proceedings of IPTC'86, D.F. Dickens Associates, Vancouver, Vol. 1, pp.169-200.

JONES, S.J., et al., "Ice Tank Model Test Methods At IMD", IMD, NRCC, Report No.LM-AVR-20, 1987. (In process)

KALLIPKE, F., "Polar Eisfahrt mit Frachtern (Marine Transport with Commercial Vessels in Arctic Regions)", Schiff und Haven, Hamburg, 1972, No. 10, (Translation No.PB219200, National Technical Information Service). 16p.

also: discussion, KLOPPENBURG, M., SCHWARZ, J., "Neue Wege in der Eisbrechtechnik (New Ways in Icebreaking Techniques)", Jahrbuch Schiffbautechnische Gesellschaft Stg., 1975, Vol.69, pp.206-212. ( No NTIS English Translation Available).

KANERVA, M., LONNBERG, B., "Ice Breaking Cargo Ships", The Naval Architect, Royal Institute of Naval Architects (RINA), Greenwich, September 1985, pp.309-327.

KITAMI, E., KAWAMOTO, T., NOBLE, P., SEMENIUK, A., "An Experimental Investigation of Ice Impact Load on Drag Arm of an Arctic Super Trailing Suction Hopper Dredger", World Dredging Congress, Singapore, 1983, Paper J3, pp.403-416.

KOEHLER, P.E., "Safe Speed of Ships in Arctic Waters", Proceedings of IPTC'86, D.F. Dickens Associates, Vancouver, 1986, Vol.2, p.734-743.

KOSKIKIVI, J., KUJALA, P., "Long-Term Measurements of Ice Induced Loads on the Propulsion Machinery of the Product Tanker SOTKA", Technical Research Centre of Finland (VTT), Espoo, October 1985. 75p.

KRAMEK, R.E., GULICK, R.W., "Polar Class Icebreakers- Contribution to Technology", Proceedings of IceTech'81, SNAME, New York, 1981, pp.159-170.

LAINNEY, L., TINAWI, R., "The Mechanical Properties of Sea Ice- A Compilation of Available Data", Canadian Journal of Civil Engineering, NRCC, Ottawa, November 1984, Vol.11, pp.884-923.

LASKOW, V., SPENCER, P.A., BAYLY, I.M., "The M.V. ROBERT LEMEURE Ice/Propeller Interaction Project: Full Scale Data", Marine Technology, SNAME, New York, October 1986, Vol.23, No.4, pp.301-309.

LASKOW, V., "Ship/Ice Interaction Models- A Designer's Approach", Dome Petroleum Ltd., Calgary, 1982. 200p.

LEWIS, J.W., EDWARDS, R.Y., "Methods for Predicting Icebreaking and Ice Resistance Characteristics of Icebreakers", Proceedings, SNAME, New York, 1970, Vol.78, pp.213-249.

LUCE, M., SNEYD, A.R., "M.V. ARCTIC - Opening New Frontiers for Marine Transportation in the High Arctic", Proceedings of IPTC'86, D.F. Dickens Associates, Vancouver, 1986, Vol.2, pp.747-763.

LUK, C.H., "A Two-Dimensional Plasticity and Momentum Model for Ship Resistance in Level Ice", IAHR Symposium on Ice 1986, Iowa City, 1986, Vol.II, PP.101-112.

MACDONALD, E.R., "Polar Operations", U.S. Naval Institute Press, Annapolis MD, 1969. 240p.

MATHEWS, S.T., "Aspects of the Propulsion Power of Arctic Vessels, considering their Operating Environment", Proceedings of IceTech'75, SNAME, New York, 1975. 14p.

MELLOR, M., "Icebreaking by Gas Blasting", Proceedings of IAHR Symposium on Ice Problems, Hamburg, 1984, Vol.1, pp.93-102.

MELLOR, M., "Mechanical Behaviour of Sea Ice", U.S. Army Cold Regions Research and Engineering Laboratory (CRREL), Report No.82-1, Hanover NH, 1982. 136p.

MEYERS, W.G., SHERIDAN, D.J., SALVESON, N., "Manual- NSRDC Ship-Motion Sea-load Computer Program", Naval Ship Research and Development Center, Report No.3376, Bethesda MD, 1975. 129p.

MICHEL, B., "Ice Mechanics", Laval University Press, Montreal, 1978, pp.81-116.

MILANO, V.R., "A Re-analysis of Ship Resistance When in Continuous Motion through Solid Ice", Proceedings of InterMartec'80, Hamburg, 1980, pp.456-476.

MILANO, V.R., "Variation in Ship/Ice Parameters on Ship Resistance to Continuous Motion in Solid Ice", Proceedings of IceTech'75, SNAME, New York, 1975. 33p.

MOLYNEUX, W.D., "M.V. ARCTIC and Two Alternative Bow Designs- Results of Resistance, Propulsion, and Overload Experiments", NRCC Report No.LTR-SH-346, Arctic Vessel And Marine Research Institute (AVRMI), NRCC, Ottawa, May 1983. 82p. (Limited).

MOLYNEUX, W.D., "Field Trials of the MAX WALDECK", AVRMI, NRCC, Internal Report No.MTB122, Ottawa, 1982. 30p. (Limited).

MOOKHOEK, A.D., VOLKER, R.P., DeBORD, F.W., "Selected Technical Results from the MANHATTAN Arctic Marine Project", Proceedings of IceTech'81, SNAME, New York, 1981, pp.21-34.

MOTOZUNA, K., KIMURA, T., KATAGIRI, T., OKUMOTO, Y., SOINEN, H., KANNARI, P., "Study on 100,000 DWT Icebreaking Tanker", Proceedings of the 8th International Conference on Ports and Oceans under Arctic Conditions (POAC'85), Narssarsuaq, Greenland, 1985, Vol.III, pp.861-868.

NAEGLE, J.N., "Ice Resistance Motion Simulation for Ships Operating in the Continuous Mode of Icebreaking", Doctoral Thesis, University of Michigan, Ann Arbor MN, 1980. (microfilmed).

NOBLE, P., "Arctic Offshore Technology: An Overview", Marine Technology, SNAME, New York NY, October 1983, Vol.20 No.4, pp.323-331.

PARSONS, B.L., SNELLEN, J.B., HILL, B., "Physical Modelling and the Fracture Toughness of Sea Ice", Proceedings of the Fifth (1986) OMAE Symposium, ASME, New York NY, 1986, Vol.4, pp.358-364.

PEIRCE, T.H., PEIRCE, J.C., "M.V. ARCTIC - Spring 1986 Performance Trials Voyage Report", Transport Development Centre (TDC), Montreal, June 1986, TDC Report No. TP7745E. 38p.

PEIRCE, T.H., PEIRCE, J.C., GILLIES, T.K., "M.V. ARCTIC - Scientific Program 1979- 1985 Performance Review", TDC, Montreal, TDC Report No. TP6345E. 120p.

POPOV, E., "Introduction to Mechanics Of Solids", Prentice-Hall Inc., Englewood Cliffs NJ, 1968 (10th Ed.). 571p.

POZNYAK, T.T., IONOV, B.P., "The Division of Ice Resistance into Components", IceTech'81, SNAME, New York NY, 1981, pp.249-252.

RALSTON, T.D., "Plastic-Limit Analysis of Sheet Ice Loads on Conical Structures", (Pre-Print), IUTAM Symposium on the Physics and Mechanics Of Ice, Copenhagen, August 1979. (page no. N/A).

RALSTON, T.D., "Ice Force Design Considerations for Conical Offshore Structures", Proceedings of POAC'77, St. John's NF., 1977, pp.741-752.

REINCKE, T., "Analytical Approach for the Determination of Ice Forces using Plasticity Theory", (Pre-Print), IUTAM Symposium on the Physics and Mechanics of Ice, Copenhagen, August 1979. (page no. N/A).

SALVESON, N, TUCK, E.O., FALTINSEN, O., "Ship Motions and Sea Loads", Transactions, SNAME, New York NY, Vol.78, 1970, pp.250-287.

SCHONECHT, R., LUSCH, J., SCHELZEL, M., OBENHAUS, H., "Schiffe und Schifffahrt von Morgen (Ships and Shipping of Tomorrow)", 1978, (Translation) KAHLER, R.C., Cornell Maritime Press, Centreville MD, 1983, pp. 141-145.

SCHWARZ, J., "Advances in Icebreaker Technology in West Germany", Proceedings of IPTC'86, D.F. Dickens Associates, Vancouver, 1986, Vol.1, pp.201-219.

see also: Discussion, p.278, IPTC'86, Vol.1.

SCHWARZ, J., "Some Latest Developments In Icebreaker Technology", Proceedings of the 4th International OMAE Symposium, ASME, New York NY, 1985, pp.322-326.

SCHWARTZ, J., "New Developments in Ice Modelling Problems", Proceedings of POAC'77, St. John's NF., 1977, Vol.I, pp.45-61.

SHVAISHTAIN, Z.I., "Icebreakers for Making Ice-Free Channels", Problemy Arktiki i Antarktiki (Problems of the Arctic and Antarctic), Leningrad, pp. 133-136 (English Translation Available, 4p.).

SILVERSTONE, P.H., "Directory of the World's Capital Ships", Ian Allen Ltd., London, 1984. 500p.

STUBBS, J., MAKINEN, E., "Arctic Marine Technology: State of the Art Prospects for the 1990's", Proc. of IPTC'86, D.F. Dickens Associates, Vancouver, 1986, Vol.1, pp.220-243.

SUKSELAINEN, I.J., "Current Problems In Arctic Vessel Research", Proceedings of IPTC'86, D.F. Dickens Associates, Vancouver, 1986, Vol.1, pp.41-65.

TATINCLAUX, J.C., "Design and Testing of a River Ice Prow", IAHR Symposium on Ice 1986, Iowa City, 1986, Vol.II, pp.137-150.

TATINCLAUX, J.C., "Model Tests in Ice of Canadian Coast Guard R-Class Icebreaker" CRREL, Special Report No.84-6, Hanover NH, April 1984. 31p.

TIMCO, G.W., "EG/AD/S: A New Type of Model Ice for Refrigerated Towing Tanks", pre-print, submitted to Cold Regions Science and Technology, Elsevier Publishing Co., for publication. 50p. (Appeared April 12, Vol.12, No.2, pp.175-196 with revisions.)

TIMCO, G.W., "The Mechanical Properties of Saline-Doped and Carbamide (Urea)-Doped Model Ice", Cold Regions Science And Technology, Elsevier Publishing Co., Amsterdam, 1980, Vol.3, pp.45-56.

TRONIN, V.A., POLYAKOV, A.S., MALINOVSKY, V.A., "Investigation of Ice Navigation and Organization of Icebreaking Operations in River Basins", IAHR Symposium on Ice 1986, Iowa City, 1986, Vol. II, pp. 87-100.

TUSIMA, K., "Friction of a Steel Ball on a Single Crystal", Journal of Glaciology, International Glaciological Society, 1977, Vol. 19 No. 81, pp. 225-235.

URABE, N., IWASAKI, T., YOSHITAKE, A., "Fracture Toughness of Sea Ice", Cold Regions Science and Technology, Elsevier Publishing Co., Amsterdam, 1980, Vol. 3, p. 29-37.

VAUDREY, K.D., "Ice Engineering- Study of Related Properties of Floating Sea Ice Sheets and Summary of Elastic and Viscoelastic Analyses", Civil Engineering Laboratory, Naval Construction Battalion Center, Port Hueneme CA, December 1977, Report No. R860. 80p.

WILCKENS, H., FREITAS, A., "Thyssen-Waas Icebreaker Concept-Model Tests and Full Scale Trials", Cold Regions Science and Technology, Elsevier Science Publishers B.V., Amsterdam, 1983, Vol. 7, pp. 285-291.

WILLIAMS, F.M., SNELLEN, J.B., BELL, J.M., "The Effect of Surface Friction on Ship Model Resistance in Level Ice", IMD, NRCC, Report No. TR-AVR-02, St. John's, April 1987, 29p.

#### PERIODICALS, GOVERNMENT PUBLICATIONS, CORPORATE LITERATURE

ARCTIC NEWS RECORD, N. Wade (editor), Arctic News-Record Scanews, Bergen.

"New Icebreaking Bow makes Debut", Fall/Winter 1986, Vol. 5.3, pp. 17-18.

"Commercial Trials of Thyssen-Waas Bow", Spring (April) 1986, Vol. 5.1, p. 27

"Fighting Ice to Extend Beafort Season", 1984/85, Vol. 3.3, p. 7

ARCTIC SHIP TECHNOLOGY, prepared for TDC by Melville Shipping Ltd., TDC Report TP3094E, Vol. I, Ottawa, March 1986. 305p.

CANADIAN SHIPPING AND MARINE ENGINEERING, P. Brophy (ed.), "M.V. PATERSON", An Arthurs Publication, Mississauga, ONT, June 1985, pp. 34-35.

THE MOTORSHIP, K. Wilson (ed.), IPC industrial Press Ltd., London.

"'HAMLET ALICE' - First B. and W. Multiflex Ship", October 1977, Vol.58 No.687, pp.87-90.

"New-type Icebreaking Bow for Great Lakes Bulk Carriers", August 1977, Vol.58 No.685, p.69.

NORTHERN OFFSHORE, "The Semi-Submersible Icebreaking Tanker", 1976, No.2, p.71-72.

OFFSHORE ENGINEER (INCORPORATING NORTHERN OFFSHORE), D. Morgan (ed.), Thomas Telford Ltd., London.

"Good Results, Advanced Fleet bring Gulf to Arctic Forefront", December 1984, pp.24-30.

SAILING DIRECTIONS- ARCTIC CANADA, Department of Fisheries and Oceans, Scientific Information and Publications Branch, Ottawa, 3 volumes; Vol.I, 3rd Ed., 1982, 285p.; Vol.II, 3rd Ed., 1978, 300p.; Vol.III, 4th Ed., 1986, 250p..

SHIPBUILDING AND MARINE ENGINEERING INTERNATIONAL, "Canadian-built ice-breaking bulk-carrier 'ARCTIC'", October 1978, pp.478-485.

WORLD FISHING, "M.F.V. PENNSMART for Lake Group Ltd. Canada", R. Hancock (ed.), IPC Business Press Ltd., London, May 1982, Vol.31, pp.24-26.

ZANEN VERSTOEP B.V. Holland, "Dredging Projects in Canada's Arctic", corporate brochure, 1981.

#### UNPUBLISHED SOURCES

PATERSON, R.B., LAU, W.H., "Summary of the Ice Data from the Small Tank", Internal Report, Ocean Engineering Group, Memorial University of Newfoundland, 1986. 30p.

TABLE 1: DETAILS OF ALTERNATIVE S-BOW CONFIGURATIONS

Designation	Forefoot	Forecastle	Comments
FF1A	Inverted-Pontoon with two side runners	N/A	
FF1B	Inverted-Pontoon with three equal sized runners	N/A	
FF1C	Inverted-Pontoon, three runners, CL runner raised	N/A	
FF2	A long Snout-type forefoot, tunnel shoulders with runners	N/A	
SS1	FF2	Stem Profile Only	Flow Type
SS2	FF2	"	Spoon Profile Overhanging
SS3	FF2	"	Flow with Overhang
FB1	FF2	Extreme Overhang Spoon Profile	
FB1R	FF2 with runners reduced	"	
FB2	FF2 with no runners	Narrow Platform	
FB3	Short Snout form, tumble-home on sides, tunnel shoulders and runners	Wide Platform Blunt Stem	Developed as tests proceeded
FB3M	"	Ram-Flow, as FB3 extended, sharp, stem	
FB4	As FB3M, but with runners removed	"	
FB5	Snout forefoot with tumble-home, truncated airfoil shoulders		Selected for IMD Resistance Trials

TABLE 2: SUMMARY OF SMALL-SCALE TESTS BY BOW TYPE

TYPE	: No. Tests:	RATING									: Drilled
		X	F	FF	F	FG	G	GE	E		
FF1A	: 12	: 4	5	0	0	1	2	0	0	: 0	
FF1B	: 6	: 1	1	0	1	1	0	1	1	: 1	
FF1C	: 7	: 1	1	0	0	0	3	1	1	: 3	
FF2	: 11	: 3	2	1	1	0	0	2	2	: 0	
FFx	: 36	: 9	9	1	2	2	5	4	4	: 4	
CONE	: 2	: 0	0	0	0	0	2	0	0	: 2	
SSx/ FF2	: 22	: 1	9	3	1	4	3	0	1	: 6	
SUB-TOTAL	: 60	: 10	18	4	3	6	10	4	5	: 12	
FB1	: 3	: 0	0	0	0	0	0	1	2	: 1	
FB1R	: 7	: 2	1	0	0	1	0	0	3	: 5	
FB2	: 6	: 0	1	0	0	1	1	1	2	: 3	
FB3	: 7	: 2	1	0	0	0	2	1	1	: 3	
FB3M	: 9	: 2	3	0	3	1	0	0	0	: 6	
FB4	: 14	: 4	3	0	1	1	1	3	1	: 6	
FB5	: 17	: 1	5	0	7	1	3	2	0	: 0	
FBx	: 63	: 11	12	0	11	5	7	8	9	: 24	
TOTALS	: <u>123</u>	: 21	30	4	14	11	17	12	14	: 36	
X	: <u>100%</u>	: 17	24	3	11	9	14	10	11	: 29	
SUCCESSFUL	: <u>102</u>	: *	-	-	: 14	11	17	12	14	= <u>68</u>	
ISUCCESS	: <u>100%</u>	: *	29	4	: 14	11	17	12	14	= <u>87%</u>	



**TABLE 4: SUMMARY OF AVERAGE RESISTANCE DATA**  
**M326BMS and M326BP**

TEST TANK/ TRIAL DESIGNATION	$h_m$ (mm)	$v_m$ (m/s)	$R_m$ (N)	$R_m'$ (N)	$h_p$ (m)	$V_p$ (kts)	$R_p$ (kN)	$R_p'$ (kN)
<b>M326BMS - Melville Bow</b>								
-Arctec Canada	26.1	0.15	22.5	-	0.78	1.60	608	-
-HSVA	26.0	0.22	24.5	-	0.78	2.34	662	-
"	26.0	0.34	28.4	-	0.78	3.62	767	-
-Arctec Canada	27.6	0.47	38.4	-	0.83	5.00	1037	-
"	28.6	0.74	51.7	-	0.86	8.09	1306	-
<b>M326BMS</b>								
-IMD	40.0	0.15	47.1	-	1.20	1.61	1272	-
"	"	0.19	51.0	-	"	1.98	1401	-
"	"	0.28	64.7	-	"	2.97	1747	-
"	"	0.46	70	-	"	4.88	1890	-
"	"	0.65	84	-	"	6.92	2268	-
<b>M326BMS</b>								
Pre-Sawn	25.0	0.28	16	-	0.75	3.0	432	-
(Wartsila)	40.0	0.28	37	-	1.20	3.0	999	-
<b>M326BP - S-Bow</b>								
Test:2CL	23.3	0.19	68.9	68.9	0.70	1.51	1860	1860
*Iron QP	"	0.28	78.0	59.0*	"	3.01	2106	1609
"	"	0.47	101.8	-	"	5.00	2749	-
"	"	0.66	105.8	-	"	6.97	2857	-
<b>M326BP</b>								
Test:2QP	23.3	0.47	50.0	-	0.70	5.00	1350	-
(Pre-Sawn)	0.66	58.5	-	6.97	1578	-	-	-
<b>M326BP</b>								
Test:5.2CL	39.5	0.14	177.5	114.8	1.18	1.50	4793	3100
3CL	39.2	0.18	272.5	209.8	1.17	1.93	7358	5665
1CL	39.7	0.28	254.5	217.3	1.19	3.01	6872	5867
3CL	39.2	0.47	358.2	298.2	1.17	4.97	9671	8051
<b>M326BP</b>								
Test:1(3)QP	39.7	0.14	112.6 <sup>3</sup>	76.6	1.19	1.50	3039	2068
3QP	39.2	0.18	175.0	-	1.17	1.93	4725	-
1QP	39.7	0.28	179.2	-	1.19	3.01	4838	-
5QP	39.5	0.47	205.0	-	1.18	4.98	5535	-
5QP	39.5	0.65	296.0	-	1.18	6.95	7984	-

NOTE: 1) Effect of Heavy (30cm) Snow Cover on M326BMS:  
 $dR = +270$  kN (full scale)

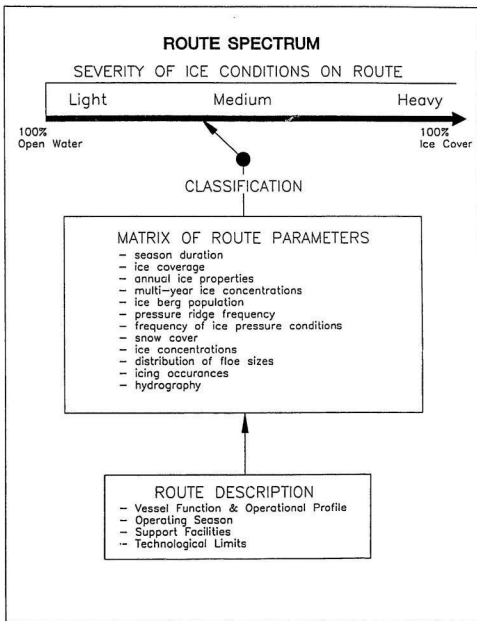
2) All 25mm M326BMS data from Baker (1985) - Test Tank indicated.

TABLE 5: SUMMARY OF THE NUMERICAL ANALYSIS

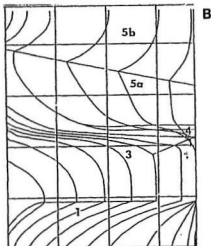
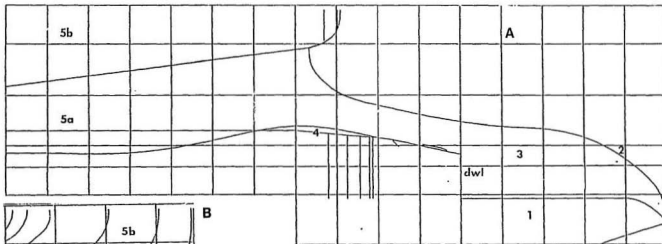
Input Data:  $\sigma_c=17$  kPa  $\sigma_c=55$  kPa  $\sigma_c=6$  kPa (31 kPa max.)  $\mu=0.1$   
 $h=25$  mm;  $l_c=0.235$  m;  $E=25$  MPa  
 $\lambda=30$   $h=40$  mm;  $l_c=0.413$  m;  $E=52$  MPa  
 Stem angle  $\alpha=17^\circ-43^\circ$ ; Forecastle Slope  $23^\circ-60^\circ$  Shoulders= $21,39^\circ$   
 Forecastle Entrance  $\beta=25-31^\circ$ ; Forecastle Station Spacing= $0.2$  m; Forecastle length= $0.724$  m  
 Depth of Crescents= $0.163$  m= $0.271$  m; Ice Piece Size= $0.176-0.31$  m

Resistance by Component: [Reference for model in brackets]

Component	$R_1$ (N):	h=25 mm			h = 40 mm			Notes
		Typical	Min.	Max.	Typical	Min.	Max.	
Deformation ahead on Snout	-	7	(36)	-	15	71	Brackets a total for cone	
Radial Cracking on Snout		11	32		17	48		
Circumferential Crack on Snout	5	2	12	15	4	26		
Bending at Shoulders	5	4	17	10	8	25		
Crushing at Shoulders	-	121	273	-	194	437	length=6 cm, wedge angle $5^\circ-45^\circ$ ; Plane Stress	
Ice Ride-Up - Snout	35	20	46	70	37	94		
	$R_1$ (N)	Overall	Per $St^N$	Per $St^N$	Overall	Per $St^N$	Per $St^N$	OA=Per $St^N$ X 3.5
I., Ride-Up Forecastle [10]	30	9	11	65	16	23		
Reaction Under Flare	Limit Stress	593	134	177	948	219	283	OA=Per $St^N$ X 7
	Collapse Load	99	22	106	253	57	206	
	Driving Force	31	8	19	164	16	45	
Failure	Crescent Tip	15	6	43	25	9	69	
	Failure	( $\sigma_c=31$ kPa) (24)	(67)	-	(38)	(107)		
Crushing at Mid body	Limit Stress	30	48	85	45	77	136	
	Buckling	-	9	53	-	27	155	



**FIGURE 1:** Schematic of the Route Spectrum based on ice conditions; for analysis of the operational profile of a proposed vessel.



## M326BP LINES S-BOW MODEL

FIGURE 2: The S-Bow lines, as produced for NC machining; the bow underside is not shown.

- A) Profile and shoulder details
- B) Half-body plan

### Components Identified:

- 1) Underside of forefoot (snout) - Melville Bow
- 2) Stem runner location
- 3) Forefoot - Snout
- 4) Shoulder (shearing edge region)
- 5a) Forecastle under flared forepeak
- 5b) Flared forepeak

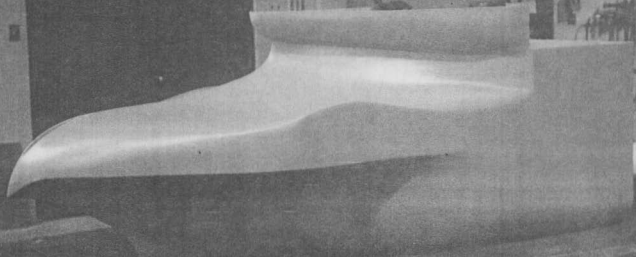
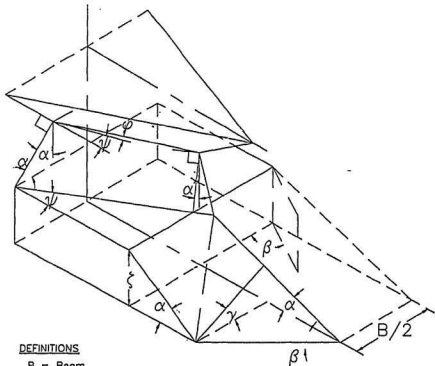


FIGURE 3: The S-Bow model segment used in the IMD resistance trials, prior to application of waterline marks. Note the Melville Bow faired into the underside. The test waterline was located approximately halfway up the stem runner.

## SCHEMATIC OF S-BOW

**DEFINITIONS**

- B = Beam
- z = Shoulder Height
- $\alpha$  = Stem or Slope Angle
- $\alpha'$  = Complement of Angle
- $\beta$  = Waterline Half-Entrance Angles
- $\beta'$  = Local Shoulder Half-Entrance Angle
- $\gamma$  = Local Frame Angle
- $\psi, \phi$  = Angles defining Forepeak Edge

FIGURE 4: Schematic of the S-Bow components showing angle definitions; used for the numerical analysis following the model trials.



FIGURE 5: The S-Bow icebreaking sequence in level, uniform ice; from the IMD model trials.

- a) Initial stem crack (indicated by arrow) - accompanied with deflection of the ice sheet in the model trials. (Left)
- b) Formation of circumferential crack at stem (indicated by arrow) - to form a "tee" with the initial stem crack - and the shearing at the shoulders. (Right)

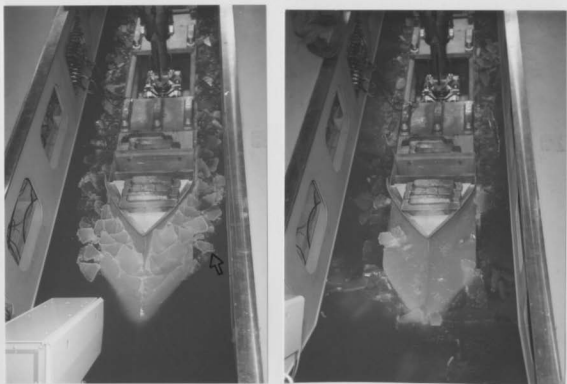


FIGURE 5 (Continued): The S-Bow icebreaking sequence.

- c) Elimination of the broken ice. Outer pieces are moved off near the shoulders, while the inner pieces are carried aft onto the forecastle before exit. Note the vertical row of ice pieces along the model hull. Note also the difference in the ice piece size with Figure 5a. (Left)

FIGURE 6: The S-Bow in pre-sawn ice - photo taken at the end of the channel at low speed. Note the absence of ice on the bow and adjacent ice compared with Figure 5c. Broken ice was displaced laterally under the ice sheet edge. (Right)

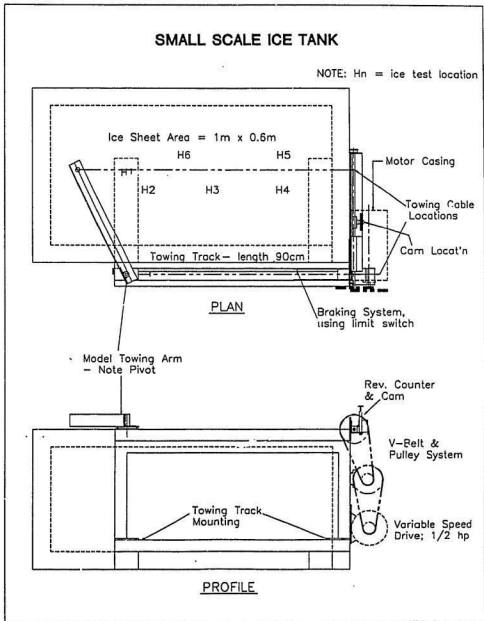
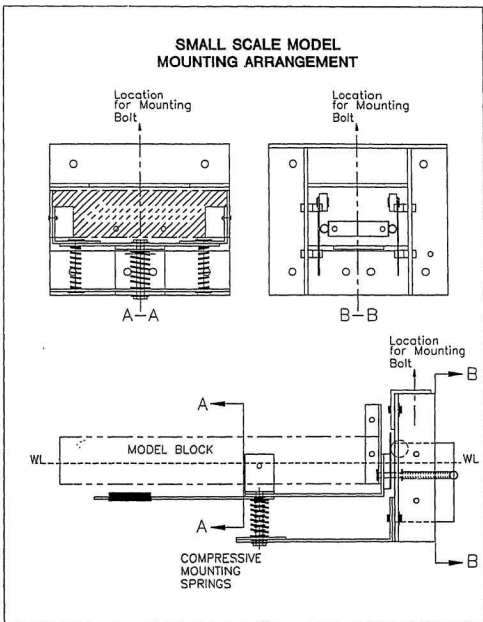


FIGURE 8: Small scale model mounting - showing spring system intended to simulate hull motion for the bow configuration tests.



**FIGURE 7:** Small-scale ice towing tank - used in bow configuration evaluation tests in the M.U.N. Engineering Cold Room. The monorail towing system is located at the right of the tank.



FIGURE 9: FF1 - the Pontoon-type forefoot. Photo shows version FF1C, which featured a raised centreline runner with the two side runners.



FIGURE 10: FF2 - the initial Snout-type forefoot - fitted with the version FB2 forecastle.



FIGURE 11: The overhanging forecastle used in the FB1 forebody with the FF2 forefoot.

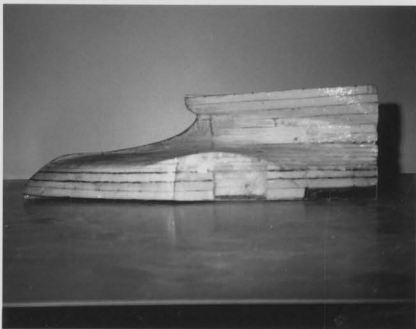


FIGURE 12: FB5 - the final bow configuration tested, of a series of models beginning with FB3. Note the shorter forefoot is more closely integrated with the forecastle than the FB2.

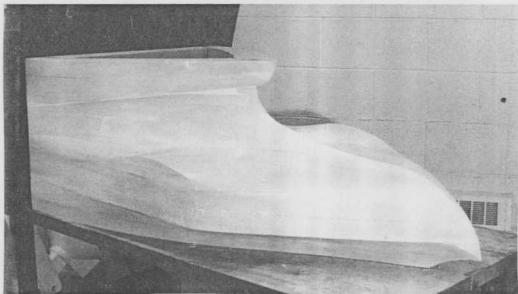


FIGURE 13: Construction of the 1:30 scale S-Bow segment used in the IMD trials. Refer to Figure 3 for a view of the completed bow segment.

- a) Plug consisting of laminated foam being milled by the IMD CAM system, from programmed lines plan (Figure 2). (Top)
- b) Finished view of foam S-Bow plug for production of the fibreglass shell, following milling and finishing but prior to joining the lower Melville Bow section. (Bottom)



FIGURE 14: Example of excessive ice deflection around the snout - during the IMD model trials. Note the distance the deflected region extends out from the snout, and the lack of secondary fracture.

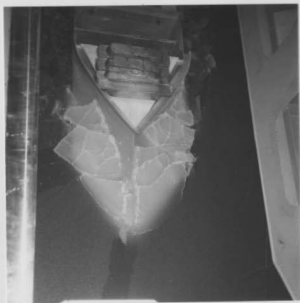


FIGURE 15: Example of the radial cracking and "calving" of the ice sheet that occurred between the model and the previously created central channel during quarter point channel.

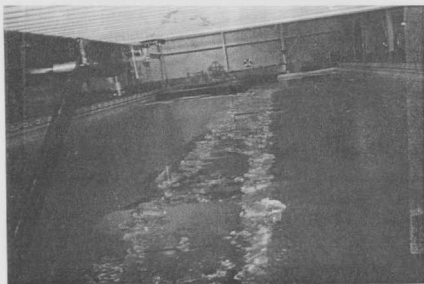
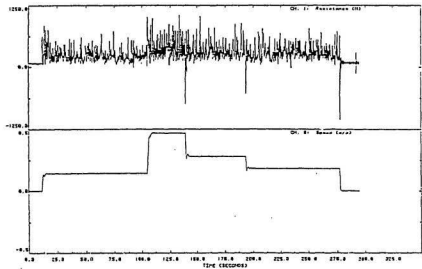


FIGURE 16: Condition of the channel broken by the S-Bow during the IMD trials.

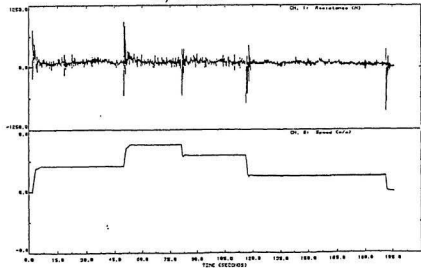
a) Channel in 40mm ice. (Top)

b) Channel in 25mm ice. (Bottom)

## SAMPLE RESISTANCE TIME HISTORIES From IMD Model Trials



a.) S-Bow



b.) Melville Bow

FIGURE 17: Comparison of resistance time histories obtained from IMD trials of the S-Bow (a - Top) and the Melville Bow (b - Bottom)

# RESISTANCE DATA - IMD MODEL TESTS

S-Bow and Melville Bow

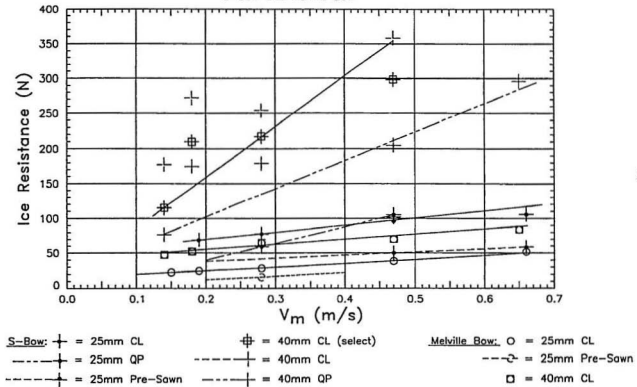


FIGURE 18: Plot of average model resistance for the S-Bow and the Melville Bow in 25mm and 40mm EG/AD/S ice.

## A. HISTORICAL BACKGROUND TO THE DEVELOPMENT OF THE UPWARD-ACTING BOW FORM

### A.1 HISTORY OF THE UPWARD-ACTING ICEBREAKING BOW

Inclined surfaces have long been used on river obstacles and lighthouse piers for icebreaking (Schwarz and Kloppenburg, (discussion), 1976). The first example of an ice-going vessel with an upward-acting bow was the Upper Canadian paddle driven, wooden steam packet "CHIEF JUSTICE ROBINSON", constructed in 1842, at least two decades before the first European icebreaker. It operated for over a decade on an extended season on Lake Ontario (Barry, 1973). More recently, a number of Canadian Great Lakes freighters have been fitted with an inclined stem to assist in late season operations (The Motorship, 1977). A related application was an attempt to combine a ram with a small bulb in an offshore trawler for work in pack ice (World Fishing, 1982).

Attempts to develop a fully capable upward-acting ice-breaking bow (as opposed to an ice-clearing bow) have centred on the ice plow. In 1951-52 the Arctic and Antarctic Institute of the Soviet Union investigated the use of an ice plow to produce an ice-free channel which would facilitate more efficient escort of shipping. Field trials conducted in 1953 with the 450 kW tug "IVAN VAZOV" were disappointing. The tug was underpowered and there were problems in clearing the broken ice away from the hull which would eventually

stall progress. As with subsequent designs, the edges of the channel were observed to collapse under the weight of the broken ice (Shvaistein,1971). Soviet activity in this field seems to have ceased after these trials.

Development of the ice plow in Canada centred on the Alex-Bow, patented by S.E. Alexander; the unique feature was the addition of a centre-line splitter blade which aided in the initial fracture of the ice sheet (Alexander,1970). Model tests were conducted in paraffin wax in the mid-1960's; a pilot project using the Alex-Bow as an bow appendage on a 990 kW tug was tested in March 1967 on Lake Ontario (Shvaistein,1970). These tests encouraged PanArctic Oil Ltd to sponsor the testing of an icebreaking tug-barge combination for re-supply of their Western Arctic operations. The barge "L.A. LEARMONTH" was fitted with an Alex-Bow and was pushed by a tug which also towed another barge. The system was employed in the re-supply of Melville Island operations in August 1968. Interest was expressed in the use of the Alex-Bow with the S.T. "MANHATTAN" at this time (Gray and Maybourn,1981). However during re-supply operations in August 1969 the tug-barge combination was caught in heavy dynamic ice conditions in Barrow Strait, and the "LEARMONTH" and an accompanying barge were lost.

The circumstances of the incident are described by Davies (1969). The loss primarily resulted from structural failure due to ice pressure, complemented by a lack of rigidity of the towing system. Neither barge was ice-strengthened except for the bow area; the barges would have to be built to CASPPR Class 2 standards to operate in the area today. The ice conditions were severe enough that the escorting icebreaker C.C.G.S. "LABRADOR" was beset. Prior to the incident, the Alex-Bow had difficulty following the icebreaker because the broken ice from the "LABRADOR" would lodge on the bow and not deflect, eventually accumulating to stall the tow. There is no evidence that the Alex-Bow directly contributed to the loss, in particular by causing the barge to run under the ice sheet; the "LEARMONTH" sank stern first. Nevertheless the belief persists that the Alex-Bow was responsible for the loss (Gray and Maybourn, 1981).

Development of the Alex-Bow continued after 1969 primarily for use with unconventional hull forms. Interest focused on what are treated as operational advantages in this text (German and Dadachanji, 1975; German, 1971). However more recent innovations seem to have overtaken the Alex-Bow.

There has been peripheral U.S. involvement with upward-acting icebreakers. The Alex-Bow was tested along with a

downward-acting M.I.T./White Bow in large-scale (1:6) model trials for the icebreaking tanker "MANHATTAN" conducted in Sogreah, France in 1968. Concern over the ridge transitting capability was reported as the main reason for rejecting the Alex-Bow (Gray and Maybourn,1981; Mookhoek et al.,1981). The Alex-Bow was later unsuccessfully tested as an attachment for river icebreaking (J.E. Carter, conversation, 1985). A few unorthodox upward-acting icebreaki.g systems have been investigated for river icebreaking in the United States; several systems which fracture the ice sheet by gas-blasting have been successfully tested (Mellor,1984; Coburn and Ehrlich,1973).

Following the "MANHATTAN" trials an icebreaking tanker featuring a narrow beam and an upward-acting icebreaking bow was proposed by Kallipke (1972) in West Germany. A similar design appeared in a 1978 East German textbook (Schoneckt et al., 1978). This seems to be the most recent reference to upward-acting icebreaking, except for the ice-clearing designs described above.

#### A.1.2 RELATED OPEN WATER BOW FORMS

As indicated in Section 2.1 in the text, two types of open water bow form bear some relation to the S-Bow. The first type is the snout bow employed on some nineteenth century

warships to improve sea keeping and to avoid blast damage when carrying heavy armament forward. The snout bow was developed from the ram bow, which could be found on all major warships designed in the mid- and late- nineteenth century. Some old battleships fitted with a ram bow were employed as emergency icebreakers during and after the First World War (discussion, Kloppenburg and Schwartz, 1976).

Another development of the ram bow is the modern bulbous bow (Comstock, 1965). Many modern medium-sized cargo vessels are fitted with a large bulbous bow to improve open water efficiency. The mechanism that makes a bulb effective for this class of vessel, which operate at relatively low Froude numbers, is not well understood. Originally the bow bulb was employed with higher speed vessels to suppress the Kelvin bow wave system; at lower Froude numbers a bulb is believed to be effective in reducing the "wave-breaking resistance" associated with the localized bow wave (Harvald, 1981; Eckert and Sharma, 1973). No negative effect on seakeeping has been reported (Eckert, 1973). The potential of the bow bulb was considered when developing the S-bow form.

## B. SPECIFICATIONS OF THE M.V. "ARCTIC: MODEL M326B/M326BMS

### B.1 PARTICULARS AND HYDROSTATICS

The motor vessel (M.V.) "ARCTIC" began service in 1978 as a CASPPR Class 2 Bulk Carrier of 28000 DWT. From 1984-1986 it was converted to an oil/bulk ore carrier and upgraded to a conditional CASPPR Class 4 (Baker and Thompson, 1985/86). The "ARCTIC" was refitted with a new bow of improved ice-breaking capability, referred to as the "Melville Bow" (Luce and Sneyd, 1986; Baker and Thompson, 1985/86; Baker, 1985). The original propulsion system (11 MW shaft power, 160 tonnes bollard pull) was retained. The upgraded "ARCTIC" was used as a test case for the IMD resistance trials. A body plan of the Melville bow is shown in Figure B.1; the original bow was somewhat shorter, with higher characteristic angles.

The hydrostatic particulars for the upgraded M.V. "ARCTIC" and the 1:30 scale model designated M326BMS are given in Table B.1, and the form coefficients are given in Table B.2. Some of the S-Bow motion calculations were based on the old form because it better represented the S-Bow dimensions.

### B.2 MODEL DETAILS

The model of the M.V. "ARCTIC" used in the comparative resistance trials was constructed at a scale of 1:30 for a

friction resistance program, reported by Williams et al. (1987). The model has been referred to as M326B in most published sources (Baker, 1985; Molyneux, 1983), but the designation used in the SMP file, M326BMS, was adopted for the IMD tests. The SMP file contained the data required for milling the model plug, which is then used to create the fibreglass hull shell. The data are stored as a series of offsets for a given station, with the hull typically divided into 20 stations; further substations and profiles are entered to describe regions of more complex geometry.

The model was ballasted (Table B.1) to the design waterline with the assistance of pre-set trim hooks located at the perpendiculars, on each side of the hull. The ballast was located to give a realistic motion response. An inclining test was used to determine the metacentric height (GM), and the radii of gyration (k) were determined from the pitch and roll period (r) using a formula from Bhattacharya (1978):

$$r = 2\pi k[(1+a)/(g(GM))]^{1/2} \quad (B-2.1)$$

where a=0.2 for roll, 0.9 for pitch

This data was obtained for the friction resistance trials (Williams et al., 1987) but were also used for this program.

### B.3 MODEL SURFACE PREPARATION

The M326BMS model was constructed as one of a series for an experimental friction resistance program. The model used for the S-Bow comparative resistance trials was painted with the coating referred to as Surface 1 in Williams et al. (1987). The friction data for the surfaces was obtained from tests using a "Friction Jig", set up at the side of the ice tank. A sample board, painted coincidentally with the model, was pushed past a fixed block of EG/AD/S ice cut from the ice sheet and loaded with a range of known weights. Only one speed was tested. The friction coefficient was calculated from a readout produced from a load cell on the "jig" using the standard formula. The surface roughnesses and friction coefficients for M326BMS with Surface 1 are given below, as reported in Williams et al. (1987).

Surface 1 Roughnesses: Bow =  $1.291 \pm 0.189 \mu\text{m}$   
 Mid-Body =  $1.276 \pm 0.340 \mu\text{m}$   
 Plate =  $1.206 \pm 0.191 \mu\text{m}$   
 Stern =  $1.304 \pm 0.193 \mu\text{m}$   
 Stern Plate =  $1.290 \pm 0.207 \mu\text{m}$

Surface 1 Friction Coefficient: Bow, Mid-Body  $\mu = 0.060 \pm 0.007$   
 Stern  $\mu = 0.099 \pm 0.009$

## B.4 TRIM MOMENT ESTIMATE

Prior to form development, the trim moment available for ice fracture had to be investigated. The old M.V. "ARCTIC" hull was used because it was closer to the expected upward-acting bow length. From Table B.1:

$$MCT1m = \theta_{sw}(I_L)/L_{pp} = \Delta(BM_L)/L_{pp} \quad (B-6.1)$$

$$= (38259t)(274.34m)/(196.59m) = \underline{5339} \text{ t*m/m trim}$$

A 1m trim would produce a vertical load of  $P_v$  at the FP of:

$$P_v = MCT1m / (0.5L_{pp} - LCF_H) \quad (B-6.2)$$

$$= 5339t*m / (0.5(196.59m) - 0.18m) = \underline{544} \text{ t.}$$

A crude estimate of ice load was made from cantilever beam failure, using a high value for  $\sigma_t$  (Timco, 1980), and an assumed forefoot length equal to ice piece size, and an ice thickness with safety factor:

$$P_t = \sigma_t B h^2 / 6gl \quad (B-6.3)$$

$$= (800 \text{ kPa})(23m)(1.5m)^2 / [6(9.81m/s^2)(4m)]$$

$$= \underline{176 \text{ tonnes}}$$

and a weight of broken ice based on bow length:

$$P_w = \rho_i L B h \quad (B-6.4)$$

$$= (0.92 \text{ t/m}^3)(20m)(23m)(1.5m) = \underline{644 \text{ tonnes}}$$

It was generalized that the induced trim would be about the thickness of the ice sheet; the angle induced by a trim of 1.5m would be:

$$\phi = \arcsin(h / (0.5L_{pp} - LCF_H)) = 1.5m / ((0.5(196.59m) - 0.18m) - 0.015 \text{ rad} < 1^\circ$$

TABLE B.1: HYDROSTATIC PARTICULARS OF THE M.V."ARCTIC" AND 1:30 SCALE MODEL M326BMS

DESIGNATION:		"ARCTIC"		M326BMS
LENGTH <sup>1</sup> (PERPENDICULARS)	$L_{pp}, m$	206.16	(196.6) <sup>1</sup>	6.872
LENGTH (WATERLINE)	$L_{wl}, m$	210.33	(200.8)	7.011
BEAM (AT WATERLINE)	$B, m$	22.86		0.762
DESIGN DRAUGHT	$T, m$	10.97		0.366
DEPTH	$D, m$	15.00		0.500
LOCATION OF MIDSHIPS (Fwd of AP)	$L_M, m$	103.08		3.436
CENTRES OF BUOYANCY: (Fwd of Midships) (above baseline) <sup>2</sup>	$LCB, m$ $KB, m$	-0.41 5.84	(3.52) (5.80)	-0.014 0.195
DISPLACED VOLUME	$V, m^3$	37667	(37293)	1.395
DISPLACEMENT	$\Delta, tonnes$	38642	(38259)	1.393 <sup>(3)</sup>
CENTRE OF FLOTATION (Fwd of Midships)	$LCF, m$	-0.58	(0.18)	-0.019
WATERPLANE AREA	$A_{wp}, m^2$	4122	(3940)	4.580
TRANSVERSE METACENTRIC RADIUS	$BM_t, m$	4.23	(4.09)	0.141
LONGITUDINAL METACENTRIC RADIUS	$BM_l, m$	310.6	(274)	10.353
LONGITUDINAL CENTRE OF GRAVITY (Fwd of AP)	$LCG, m$	102.6		3.422
VERTICAL CENTRE OF GRAVITY (above baseline)	$KG, m$	8.49		0.283
METACENTRIC HEIGHT (transverse)	$GM, m$	1.58		0.053
RADII OF GYRATION (Transverse) (Longitudinal)	$R_t, m$ $R_l, m$	8.01 49.14		0.267 1.638

TABLE B.1 NOTES:

- 1) Bracketed numbers refer to M.V. "ARCTIC" with the old Class 2 bow (no stability data given).
- 2) The "ARCTIC" normally operates at zero trim; the baseline is coincident with the moulded keel elevation.
- 3) The model displacement was calculated using freshwater.
- 4) Hydrostatics based on the bare hull, no appendages.

Model Towing Details:

- 1) Location of the towing gimbal for M326BMS (also M326BP):  
Top Surface: 0.168m above the baseline (BL)  
CG of Template: 3.422m fwd of AP  
(30cm cut out for clearance).  
Top surface for Yaw restraint gimbal: 0.252m above BL
  - 2) Location of ballasting shelves in M326BMS:
    - 1 platform low as possible in each model segment.
    - 1 platform max. fwd at 0.56m above BL.
    - 1 platform max. aft at 0.46m above BL.
    - platforms fwd and aft of gimbal, 0.5m above BL.
- (ballast locations in stern and midbody not changed for M326BP)
-

TABLE B.2: FORM COEFFICIENTS FOR M.V. "ARCTIC"- MELVILLE BOW

COEFFICIENTS BASED ON: LENGTH BETWEEN PERPENDICULARS BEAM, DRAUGHT AT MIDSHIPS	
L/B	9.019
L/T	18.789
B/T	2.083
AFT BODY $L_{HL}/L$	0.520
FOREBODY $L_{HL}/L$	0.500
BLOCK, $C_B$	0.728
$C_B$ , AFT BODY	0.725
$C_B$ , FOREBODY	0.731
MIDSHIPS, $C_M$	0.991
PRISMATIC, $C_P$	0.735
%LCB/L	-0.197 }
%LCB(AFT BODY)/L	-19.369 } Fwd of Midships
%LCB(FOREBODY)/L	18.819 }
WATERPLANE, $C_W$	0.875
$C_W$ OF AFT BODY	0.878
$C_W$ OF FOREBODY	0.871
%LCF/L	-0.282 }
%LCF(AFT BODY)/L	-22.418 } Fwd of Midships
%LCF(FOREBODY)/L	22.031 }
$BM_t/B$	0.185
$BM_1/L$	1.507

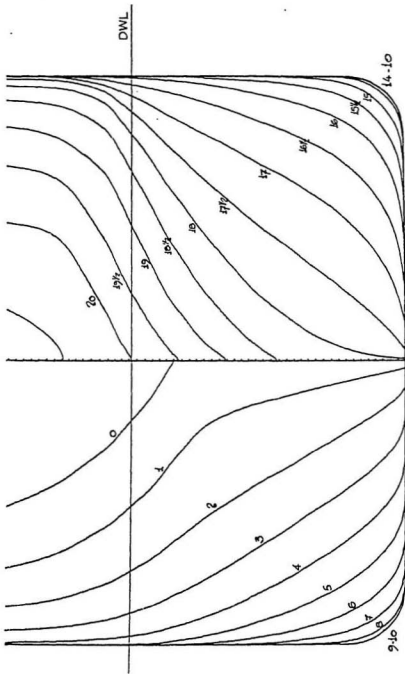


FIGURE B.1: Body Plan of the Melville Bow on the M.V. "ARCTIC".

## C. ICE CHARACTERIZATION TESTS FOR THE SMALL-SCALE ICE TANK

### C.1 ICE GROWTH PROCEDURES

The standard urea ice was replaced by a mix consisting of urea, detergent, and sugar. This mix (UR/D/S ice?) was selected because it reduced initial flexural strength significantly. See Table C.1 for mix calculations.

Repetition of ice growing procedures was emphasized with the intent that the ice properties measured in a particular ice sheet would be reproduced in other ice sheets, minimizing calibration tests for each sheet. The ice was grown at an average temperature of  $-25^{\circ}\text{C}$ . The cold room took approximately 30 minutes to reach this temperature. During this time the old ice was removed from the tank with the assistance of an aluminum mesh screen, and was placed in storage buckets for melting and re-use. When thermocouples indicated air temperature had reached  $-20^{\circ}\text{C}$ , the ice was "seeded". A final skim to remove ice was never totally successful, but was most successful when the water was least disturbed. The melt from previous tests was added. The ice was seeded using a hand-held, compressed air-operated insecticide "mist-er", which sprayed a fine mist of warm tap water. Spraying took about 30 seconds.

Growing time during the calibration tests varied from 3 hours to 2 hours, as ice thickness was found to stabilize after an initial period of rapid growth. At  $-25^{\circ}\text{C}$  an ice sheet with an average thickness of about 1.5 cm was produced over the growing time. The ice was then "tempered" at an average temperature of  $-2^{\circ}\text{C}$  ( $-28^{\circ}\text{F}$ ) for up to 2 hours; this gave a good balance between tempering time and an unacceptably wet ice surface.

## C.2 PRESENTATION OF DATA

The data obtained up to February 17, 1986 are presented in Figures C.1-C.3.

### C.2.a) Flexural Strength Data: (Figures C.1,C.2)

$$\text{Formula: } \sigma = 6FL/bh^2 \quad (\text{C-2.1})$$

Notes: i) (Figure C.1) Urea Concentration = + indicates standard 0.9% urea ice. Else data are for UR/D/S ice.

ii) (Figure C.2) Data obtained from beams failed adjacent to beams tested for modulus E. All with UR/D/S ice.

### C.2.b) Cantilever Beam Deflection Data: (Figure C.3)

$$\text{Formula: } E_r = 2/3 \sigma_{rk} l^2 / \delta (1 + ls/L) h \quad (\text{C-2.2})$$

Notes: i) All tests in UR/D/S ice.

ii) Flex test performed on beam adjacent to deflected beam (see C.2.a).

- iii) In later tests, growing time reduced from 3 hours to 2 1/2 hours.

C.2.c) Shear Tests:

$$\text{Formulae: } \tau = F/A = F/Bh \quad (\text{C-2.3})$$

Notes: i) All tests in UR/D/S ice, 3 hours growing time.

- ii) The shear tests were conducted using a "guillotine" device similar to that described by Timco (1980). Unfortunately it proved difficult to obtain pure shear failure with the device, and consequently the test data was highly scattered. A clear trend with tempering could not be identified.

C.3 STRUCTURE

Several horizontal and vertical thin sections were prepared from samples taken from different locations in the ice tank. A selection of photographs are shown in Figures C.4. The three zone structure characteristics of urea ice is evident in photographs. The first zone consisting of fine randomly oriented crystals produced by seeding is barely visible in the vertical section. The second zone is a transition layer of random polycrystalline structure. These two upper layers are believed to control the mechanical properties. The lower zone is a mechanically weak layer having a columnar structure characteristic of dendritic growth.

The structure of UR/D/S ice was similar to sea ice, with a columnar structure and brine-like cells; however, the upper polycrystalline layer was proportionally much thicker than the upper layer in sea ice. This may be attributed to the growing conditions and also may be a scale effect associated with growing a relatively thin ice sheet, i.e. the transition zone did not scale down. The resulting ice was somewhere between conventional urea ice and WARC fine grained ice. An additional difference is that in the columnar zone UR/D/S ice tended to grow two-dimensionally as platelets, rather than as truly three-dimensional columns.

The average grain size was obtained from the thin sections using an average from a 1 cm<sup>2</sup> grid. The average grain size increases from 0.17 cm<sup>2</sup> near the top surface to 0.31 cm<sup>2</sup> near the bottom. The upper layer makes up an average of 21% of the total ice thickness. Grain size data for each sample are given in Table C.2.

#### C.4 ADDENDUM: Tests after February 1986

Following the characterization tests, the tank was prepared for model testing, and then the test programme for the icebreaking bow began. In the course of these tests, some additional observations were made:

- a) Increased water levels, to accommodate the model, increased the ice growth rate. It was possible to reduce the growing time to 1.5 hours to attain the desired ice thickness. Uniformity of ice sheet thickness decreased with increased water level.
- b) The size of the tank affects the ice sheet when water is displaced, such as when the model is mounted. This effect will occur in all ice tanks, but is much more serious in a small tank. The water will either distort the ice sheet slightly because of the constraint on the sides of the ice sheet, or will permeate upward onto the ice surface. In either case the ice sheet becomes more ductile.
- c) Maintaining a standard set of ice properties proved impossible with the available equipment; the ice sheet was insufficiently isolated from outside ambient conditions and was affected by mechanical and water quality problems. The characterization tests proved useful in identifying the scaling limits of the ice sheet, but each towing trial had to be assessed individually based on videotaped observation

TABLE C.1 : UR/D/S ICE MIX CALCULATIONS

By weight% :  $W_i = N (\rho_w V)$

For Unit Volume =  $1m^3$  :  $\rho_w = 1000 \text{ kg/m}^3$

Urea:  $N_u = 1.90\%$  ;  $W_u' = 19.0\text{kg}$

Sugar:  $N_s = 0.03\%$  ;  $W_s' = 0.3\text{kg}$

Detergent:  $N_d = 0.05\%$  ;  $W_d' = 0.5\text{kg}$

Tank Dimensions: l= 115cm ; b= 60cm ; d= 41cm

Tank Volume: V = 0.2829  $m^3$

Mix Calculation: Urea :

$W_u = 5.3751\text{kg}$

Sugar:  $W_s = 0.08487\text{kg} = 84.87\text{g}$

Detergent:  $W_d = 0.14145\text{kg} = 141.45\text{g}$

TABLE C.2 : GRAIN SIZE (d) FROM THIN SECTIONS

	Elevation (cm)		top	Grain Size d (cm)	
	mid-section	base		mid-section	base
0.50	1.90	0.188	0.246	-	
0.45	1.70	0.186	0.230	0.376	
0.70	1.80	0.160	0.191	0.266	
0.30	1.40	0.146	0.238	0.333	
0.47	1.80	0.151	0.191	0.274	
0.40	1.60	0.194	0.235	0.302	

# SMALL TANK- ICE QUALITY TESTS

Flexural Strength vs Tempering Time

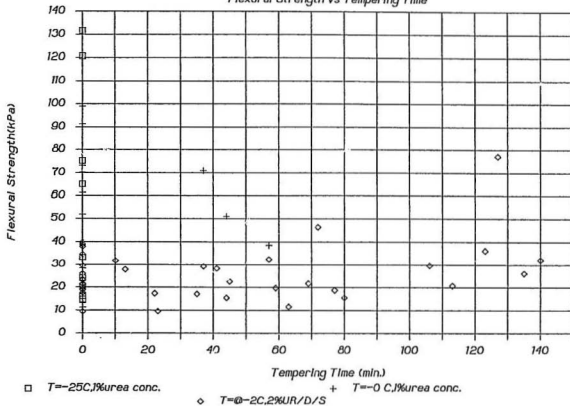


FIGURE C.1:

Flexural strength tempering data for UR/D/S ice - obtained from the small scale M.U.N. ice tank from cantilever bending tests.



## SMALL ICE TANK - ICE QUALITY TESTS

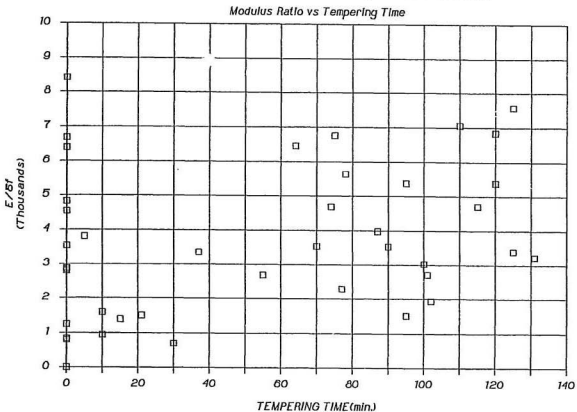


FIGURE C.3: Modulus data plotted against tempering time for UR/D/S ice - obtained from the small scale M.U.N. ice tank using a cantilever deflection test.

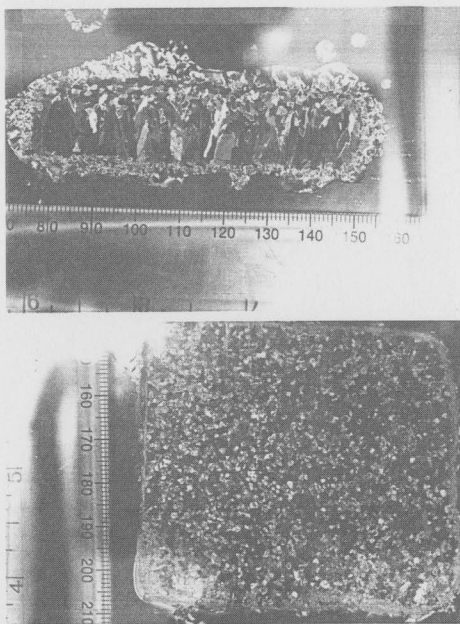


FIGURE C.4: Thin Sections of the UR/D/S model ice grown in the Small-Scale M.U.N. Ice Tank.

- a) Profile section of UR/D/S ice. Maximum thickness is about 16mm. Note the transition from a fine grained top layer into columnar platelets.
- b) Horizontal section of the seeded top layer of UR/D/S ice. Note the randomly oriented fine-grained structure.

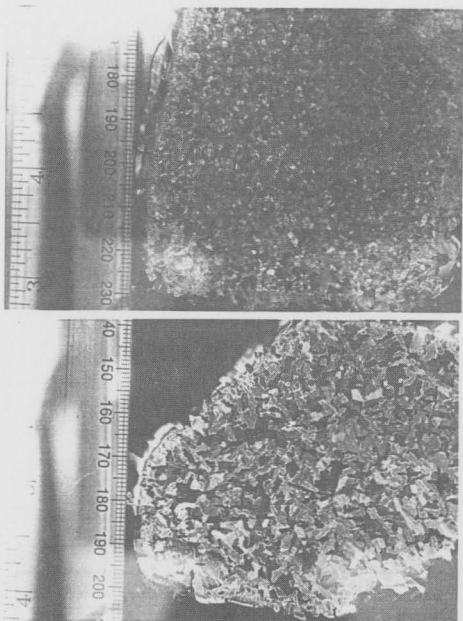


FIGURE C.4 (Continued): Thin Sections of UR/D/S ice.

- c) Horizontal section of the transition zone in UR/D/S ice. The structure remains quite random, but the grains are larger, indicating preferential growth.
- d) Horizontal section near the bottom of the UR/D/S ice sample. Note the two-dimensional shape of the grains, typical of platelet growth, as opposed to a truly three-dimensional columnar structure. Note also the size of the grains.

## D. DESIGN OF THE SMALL-SCALE MODEL MOUNTING

### D.1 INTRODUCTION

The icebreaking model consisted of a bow segment mounted on an aluminum frame with a set of springs intended to simulate the restoring buoyant force produced by the hull. The springs were scaled using a seakeeping analogue of the hull motion induced by the ice sheet. Added mass associated with icebreaker motion was calculated using a computer simulation, HANSEL, based on Salveson et al. (1970); damping is generally negligible in icebreaking analyses (Milano, 1982; Naegle, 1980). The ice characterization tests (Appendix C) indicated that a distortion factor of about two would be required to accommodate the scaling limits of the UR/D/S ice with the geometric scale ( $\lambda = 100$ ). Note that the mounting had to be designed prior to any form design, necessitating a number of assumptions regarding hydrostatics and ice loading.

### D.2 CALCULATION OF SPRING CONSTANTS FOR THE MODEL MOUNTING

#### D.2.1) Ice Model - from Milano (1980)

a) Class 4 conditions - with safety factor = 0.8

Ice thickness:  $h = 1.5 \text{ m} = 5 \text{ ft.}$

b) Radius of loading ( $r$ ) for applicable ice cantilever  
 $r = 1.3 h = 1.98 \text{ m} = 6.5 \text{ ft.}$

c) Ice Piece Size  $X'$ - From radius of loading to point of failure,  $X'$ , a characteristic ice piece size approximates the icebreaking cycle distance

Regression Equation for X': (in ft.)

$$X' = 0.8612 h - 0.238U + 8.978 \quad (D-2.1)$$

For  $h = 5$  ft. and  $U = 5.067$  ft./s = 3 knots

Speed Independent  $X'(0) = 13.284$  ft. = 4.049 m

Depth of Wedge  $X'(U) = 12.078$  ft. = 3.681 m =  $X'$

Model Ice piece size: ~ 4cm

D.2.2) Wave Analogue - An input wave to simulate icebreaker hull motion for strip theory program, (HANSEL, based on Salveson, Tuck, Ogilvie <1970>).

General Form of Displacement:  $\eta_i = A_i \cos(\omega.t)$  (D-2.2)

where: a)  $t$  = time;  $A_i$  = amplitude of motion, approximately  $h$ , based on hydrostatics of M.V. "ARCTIC", and a trim estimate (Appendix B.6). Subscripts:

$i = 3$  = heave ;  $i = 5$  = pitch

b) The form of  $\eta_i$  assumes a linear, harmonic wave. For strip theory to apply, the condition  $U \gg \partial \eta_i / \partial t$  must be satisfied to isolate the input wave from any radiated waves. As the vessel is travelling through ice, any radiation effects would be negligible.

D.2.3) Scaling Requirements for Springs - For a geometric scale factor  $\lambda = 100$ , linear displacement  $x$ , and force  $F$ :

$$F_p/F_m = k_p(x_p)/k_m(x_m) = (k_p/k_m)\lambda = \lambda^3 \quad (D-2.3)$$

therefore:  $k_p = \lambda^3 k_m$  - Linear Spring Constant

For angular displacement  $h$  and Moment  $M$ :

$$M_p/M_m = J_p(h_p)/J_m(h_m) = \pi g I_p^3 L_p / (\pi g L_m^3 L_m) = \lambda^4 \quad (D-2.4)$$

therefore:  $J_p = \lambda^4 J_m$  - Angular Spring Constant

Substituting:  $\lambda = 100$  ;

$$k_m = 10^{-4} k_p ; J_m = 10^{-8} J_p$$

D.2.4) Computer Analysis of Spring Constants -using HANSEL

Inputs: a) Wave length, L, based on the pitching action of the Class 2 M.V. "ARCTIC" hull about its LCF, and the cycle distance X'. This approximation is quite acceptable because of the near fore-aft symmetry of the M.V. "ARCTIC".

$$\text{Wavelength } \lambda = X' + L_{WL} = 203.7 \text{ m} = 668 \text{ ft.} \quad (\text{D-2.5})$$

b) The program was run with three Froude numbers corresponding to velocities of 1 to 3 knots.

General Equation of Motion: for  $i, j = 3$  (heave), 5 (pitch)

$$F_{e_i}(x_j) = (M_{i,j} + A_{i,j})\ddot{\eta}_i + (B_{i,j})\dot{\eta}_i + (C_{i,j})\eta_i \quad (\text{D-2.6})$$

Interpreting Results:

- a) The analogue relates to the heave and pitch motion induced by the ice. The program was used to produce the added mass and damping coefficients for the M.V. "ARCTIC".
- b) The encounter frequency,  $\omega_e$ , is calculated to identify the added mass coefficients applicable to the analogue. The frequency is referred to as an encounter frequency in that there is no vessel oscillation without forward motion.

$$\text{Frequency: } \omega_e = \sqrt{2\pi g/\lambda} \quad (\text{D-2.7})$$

$$\text{Non-dimensionalizing } \omega_{e,ND} = \omega_e \sqrt{L_{WL}/g} = 2.484 \quad (\text{D-2.8})$$

c) The added mass coefficients are given for  $\omega_{e,ND} = 2.555$ , the lowest frequency calculated:

$$\text{Heave: } CA_{33} = 0.802$$

$$\text{Pitch: } CA_{55} = 4.329 * 10^{-1}$$

$$\text{Cross Coupling: } CA_{35} = CA_{53} = 1.5561 * 10^{-4}$$

Note that the cross-coupled coefficient is much smaller than the other two coefficients. This was a result of the fore-aft symmetry of the M.V. "ARCTIC". (LCF = 0.18m ahead of midships). Cross-coupled terms can reasonably be neglected, which simplified the spring analogue.

- d) The added mass coefficients were calculated using the following data for the M.V. "ARCTIC"; (noting HANSEL uses Imperial (U.S.) units).

Mass:  $M = 1176.79$  tons  $s^2/ft$ . Length:  $L_{WL} = 656$  ft.  
 Area of Waterplane:  $A_{WP} = 4 \times 10^4$  sq.ft.  
 Metacentric Radius:  $BM_L = 900$  ft.  
 Radius of Gyration:  $r_s = 0.3L$  (from HANSEL program)  
 Longitudinal Centre of Flotation:  $LCF = 0.6$  ft.  
 (from midships)

The added masses were calculated as:

$$\text{Heave: } A_{3,3} - CA_{3,3} \times M = \underline{950 \text{ tons} \cdot s^2/ft}$$

$$\text{Pitch: } A_{5,5} - CA_{5,5} \times M \times L^2 = \underline{2.2 \cdot 10^7 \text{ tons} \cdot s^2 \cdot ft^2/ft.}$$

The hydrostatic terms were calculated as:

$$\text{Heave: } C_{3,3} - A_{WP} = \underline{1200 \text{ tons/ft.}}$$

$$\text{Pitch: } C_{5,5} - I_{WP} = MgBM_L = \underline{3.4 \cdot 10^7 \text{ ton} \cdot ft}$$

- e) The equations of motion can be simplified because of the cruiser stern of the M.V. "ARCTIC". The restoring force provided by the spring analogue is written alongside:

$$\text{Heave: } F_3 = [(M + A_{3,3})\omega_0^2 + C_{3,3}]h_3 = [k_3]h_3 \quad (D-2.9a)$$

$$\text{Pitch: } F_5 = [(I_3 + A_{5,5})\omega_0^2 + C_{5,5}]h_5 = [J_5]h_5 \quad (D-2.9b)$$

$$\text{where: } I_3 = M(r_s^2)$$

Damping terms were neglected as they were negligible for the frequencies being considered. The spring constants were calculated as:

$$\text{Heave: } k_3 = (M + A_{3,3})\omega_0^2 + C_{3,3} = 1850 \text{ tons/ft.} \quad (D-2.10)$$

$$k_3 = \underline{6000 \text{ tonnes/m.}}$$

$$\text{Pitch: } J_5 = (Mr_s^2 + A_{5,5})\omega_0^2 + C_{5,5} \quad (D-2.11)$$

$$= 5.3 \times 10^7 \text{ tons} \cdot ft/\text{rad.}$$

$$J_5 = \underline{1.6 \cdot 10^7 \text{ tonnes} \cdot m/\text{rad}}$$

D.2.5) Scaling of Results - Noting the scaling laws developed earlier, and that  $\lambda = 100$ :

Heave:  $k_{3m} = 600 \text{ kg/m} = \underline{6 \text{ kg/cm}}$ .

In scaling pitch,  $J_3$ , it was noted that for a motion amplitude equal to  $h=1.5 \text{ m}$ , the pitch angle was very small:

Pitch angle:  $\phi = \arcsin [h/(L/2)]$  (D-2.12)  
 $= 0.9^\circ = 0.015 \text{ radians}$

Thus it was possible to neglect pitch angle, and just treat the displacement due to the pitching motion. It was assumed the springs were set  $0.1L$  back from the bow forward perpendicular.

For  $h_m = 1.5 \text{ cm}$ , pitch angle  $\phi = 0.015 \text{ radians}$ :

Pitch Moment:  $M_{3m} = 10^{-8} (J_{3p}) \phi = \underline{2.4 \text{ kg}^*\text{m}}$

Pitch Restoring Force:  $F_{3m} = M_{3m} / (0.5L_m - 0.1L_m)$  (D-2.13)  
 $= \underline{3.00 \text{ kg}}$

Pitch Spring Constant:  $k_{3m} = F_{3m} / h_m = 250.0 \text{ kg/m}$  (D-2.14)  
 $= \underline{2.5 \text{ kg/cm}}$

D.2.6) Selection of Springs for Model -

Superposition of the heave and pitch components in the spring analogue indicated that the heave component  $k_3$  is about three times the pitch component  $k_3$ ; the icebreaking motion will more readily induce a restoring force due to pitch, and therefore:

$k'_m = k_{3m} = \underline{2.5 \text{ kg/cm}}$

The final size of the springs would have a distortion factor,  $S$ , based on the scaling limitation of the model, discussed in the main body.

Model Spring Constant:  $k_m = S \cdot k'_m$  (D-2.15)

The model mounting arrangements are shown in Figure 8 in the main text. The horizontal springs provided restraint for the model against the roller bearings, but did not affect the vertical motion.

## E. SMALL ICE TANK TEST PROGRAM DATA

## E.1 EVALUATION OF THE TRIALS

The object of the small ice tank test program was to develop the S-Bow configuration. The bow evaluation was based on qualitative observations and consequently the data recorded for each trial consisted of the test conditions, rather than performance data. The quality of each trial was rated from the videotape record, based on the quality of the fracture action and the size of the broken ice pieces produced, where:

- 4= excellent
- 3= good
- 2= fair to good
- 1= fair

The ratings are recorded as "RATE" in Table E.1. Ratings did not relate to the performance of the bow configuration (see Table 1 in text) being tested.

About half of the trials were rated fair to excellent, and the observations from these trials were used to evaluate the alternative bow configurations. Those trials with the suffix "D" indicate a pre-drilled sheet. Reasons for rejecting a trial included: mechanical failure, loss of speed record, and poor ice quality. The following are some notes to accompany Table E.1.

- a) The location of the ice thickness measurements (H1- H6) are shown in Figure 7 in the text. H1 was the root of the test cantilever beam. Thicknesses H2- H6 were taken around the broken channel to get an ice sheet profile; precise location varied with the condition of the sheet, contributing to variation in ice thicknesses recorded.
- b) Where the flexural strength was too low to register on the push-pull gauge, a default value of 8kPa was assigned, based on the previous ice sheet calibration tests.
- c) The model speed ( $v_n$ ) was approximated as the tangential velocity of the towing axle. Full scale velocity is recorded as "V" in knots. "SET" indicates the percentage of full power set on the motor control box to obtain the target speed.

The most significant feature of the trial data is the lack of correlation between the ice strength data and the quality of the trial. This was probably a result of the time duration between the flexural test and the trial run, local ice sheet inconsistencies, and the lack of an effective fracture toughness test.

## E.2 NOTES ON SMALL-SCALE TRIALS

These notes are related to Table 1 in the main text.

- 1) The leading causes of trial failures were: cable fail-

ure (10.6%); ice deterioration (3.3%); while other system problems affected about 3% of the trials. 7 trials were affected by a non-critical malfunction. A successful trial could still be rated as of poor quality.

- 2) About 30% of the trials were performed in a pre-drilled ice sheet. This technique involved drilling a pattern of small holes in the ice sheet using a wooden template, to act as stress points. The holes were located to give a predicted ice piece size of 4cm, as calculated from a semi-empirical equation (Milano,1980).
- 3) The cold room had no humidity control, such that humid weather affected the quality of the afternoon ice sheet.
- 4) Covering the tank produced a more uniform ice sheet but it drastically reduced the growth rate.

TABLE E.1: DATA FOR SMALL-SCALE ICE TANK TRIALS

DATE/ SHEET <D=drilled>	SET:	H1	H2	H3 (mm)	H4	H5	H6	$\sigma_{fn}$ (kPa)	$v_n$ (m/s)	V (kts)	RATE <*=nominal>
<b>FF1A</b>											
02/4-1	82	2.41	2.80	2.26	1.93	2.04	2.21	18.2	-----	-	-
03/4-1	82	-----	-----	-----	-----	-----	-----	-----	-----	-	-
04/4-1	82	1.99	1.99	1.5	1.00	-----	-----	-----	-----	-	-
04/4-2	82	2.00	1.85	1.60	1.45	1.35	1.69	8.0	.147	2.85	2
07/4-1	82	-----	-----	-----	-----	-----	-----	-----	-----	-	-
08/4-1	82	1.68	1.50	1.80	1.46	1.24	1.58	60.7	.145	2.82	1
08/4-2	82	1.49	1.86	1.75	1.40	1.37	1.75	34.5	-	3*	-
09/4-1	82	-----	-----	-----	-----	-----	-----	-----	-----	-	-
09/4-2	54	2.03	1.98	1.65	1.57	1.58	1.73	48.0	-	2*	-
10/4-1	54	1.78	1.76	1.48	1.49	1.53	1.51	18.2	-	2*	-
10/4-2	35	1.84	-	-	1.26	1.30	-	40.5	-	1*	-
11/4-1	35	1.77	1.65	1.48	1.36	1.36	1.67	21.6	.038	0.74	2
<b>FF1B</b>											
14/4-1	82	1.61	1.73	1.39	1.16	1.16	1.32	47.7	-	3*	-
15/4-1	82	1.69	1.38	1.52	1.35	1.15	1.39	37.5	.055	1.07	2
15/4-2	82	1.62	1.60	1.31	1.31	1.38	1.78	28.0	.119	2.31	4
16/4-1	35	1.76	1.67	1.39	1.33	1.27	1.84	29.1	.041	0.80	1
16/4-2	35	1.70	1.24	1.27	1.22	1.21	1.44	8.0	N/A	1*	-
17/4-1D	82	1.73	1.69	1.46	1.42	1.36	1.72	41.1	.129	2.51	3
<b>CONE</b>											
17/4-2D	82	1.63	-	-	-	-	-	40.9	N/A	3*	-
18/4-1D	82	-	1.88	1.82	1.40	1.32	1.62	-----	-----	-	-
<b>FF1C</b>											
21/4-1	82	1.61	1.74	1.38	1.36	1.50	1.56	50.3	N/A	3*	(3)
21/4-2D	82	1.48	1.54	1.32	1.22	1.26	1.43	28.2	N/A	3*	(3)
22/4-1	54	1.85	1.71	1.53	1.48	1.49	1.82	30.4	N/A	2*	(3)
22/4-2D	54	-	0.90	0.96	1.00	1.02	1.23	8.0	.070	1.38	3
23/4-1	35	1.62	1.65	1.57	1.49	1.47	1.55	30.0	N/A	1*	-
23/4-2D	35	1.46	-----	-----	-----	-----	-----	-----	-----	-	-
24/4-1D	35	1.72	1.79	1.67	1.53	1.48	1.78	43.1	.045	0.88	4
<b>FF2</b>											
30/4-1	82	1.91	2.03	2.05	1.46	1.40	1.52	21.9	.162	3.15	3
30/4-2	82	1.52	1.95	1.50	1.53	1.50	1.64	38.2	.167	3.24	4
01/5-1	82	1.86	2.02	1.76	1.66	1.46	1.87	33.8	.173	3.36	4
01/5-2	82	1.72	-----	-----	-----	-----	-----	22.9	-----	-	-
02/5-1	82	1.80	1.84	1.40	1.43	1.40	1.61	39.1	-	3*	-
02/5-2	82	1.36	1.24	1.20	1.12	1.10	1.37	11.1	.166	3.22	3
05/5-1	54	1.61	2.05	1.84	1.50	1.41	1.74	25.2	.109	2.12	2
05/5-2	54	1.52	-----	-----	-----	-----	-----	-----	-----	-	-
06/5-1	54	1.62	1.80	1.66	1.31	1.46	1.68	29.4	-	2*	-
06/5-2	54	1.64	1.79	1.53	1.38	1.32	1.60	16.3	-	2*	-
07/5-1	35	1.53	1.74	1.60	1.30	1.20	1.68	53.9	-	1*	-

TABLE E.1 (Continued): DATA FOR SMALL-SCALE ICE TANK TRIALS

DATE/: SHEET <D=drilled>	SET:	H1	H2	H3 (mm)	H4	H5	H6	$\sigma_{fa}$ (kPa)	$v_n$ (m/s)	V (kts)	:RATE
											<*=nominal>
<u>SS1/FF2</u>											
09/5-1	82	2.06						19.3			-
12/5-1D	82	1.80	2.12	1.76	1.43	1.46	1.80	16.4	.168	3.26	2
12/5-2	82	1.76	1.96	1.70	1.53	1.49	1.85	11.6	-	3*	-
13/5-1	54	1.71	2.08	1.59	1.41	1.36	1.66	28.5	-	2*	-
13/5-2D	54	1.74	1.68	1.50	1.43	1.34	1.63	8.0	.109	2.12	2
14/5-1D	35	1.79	1.79	1.45	1.20	1.28	1.57	24.2	.066	1.28	3
14/5-2	35	1.50	1.53	1.58	1.51	1.42	1.55	7.2	-	1*	-
<u>SS2/FF2</u>											
15/5-1D	82	1.76	1.84	1.60	1.48	1.38	1.46	34.0	.160	3.10	4
15/5-2	82	1.75	1.86	1.68	1.37	1.33	1.64	6.4	-	3*	-
16/5-1	54	1.84	2.00	1.74	1.50	1.44	1.55	35.2	-	2*	-
16/5-2D	54	1.56	1.72	1.52	1.38	1.40	1.72	28.0	.147	2.85	2
19/5-1	35	1.45						18.2			-
20/5-1	35	1.76	1.85	1.55	1.46	1.41	1.74	8.0	-	1*	-
20/5-2	35	1.61	1.72	1.59	1.41	1.37	1.58	8.0	-	1*	-
<u>SS3/FF2</u>											
21/5-1	82	1.91	1.90	1.76	1.57	1.57	1.74	32.3	-	3*	-
21/5-2	82	1.64									-
22/5-1	82	1.80	1.71	1.70	1.42	1.39	1.73	15.4			-
22/5-2	82	1.61	1.52	1.43	1.37	1.34	1.55	8.0	N/A	3*	-
23/5-1D	54	1.56	1.76	1.48	1.45	1.36	1.57	8.0	.167	3.24	2
28/5-1D	54	1.78	1.94	1.56	1.43	1.36	1.58	8.0	.121	2.35	1
28/5-2D	35	1.25	1.40	1.32	1.02	1.05	1.20	22.2			-
29/5-1D	35	1.51	1.80	1.43	1.20	1.24	1.50	46.2	.069	1.34	2
<u>FB1</u>											
03/6-1	82	1.71	1.72	1.55	1.48	1.44	1.58	8.0	.167	3.24	4
04/6-1	82	1.72	1.98	1.62	1.54	1.54	1.61	35.5	.175	3.39	4
04/6-2D	82	1.63	1.88	1.61	1.42	1.36	1.60	30.2	.171	3.32	3
<u>FB1R</u>											
05/6-1D	82	1.72	1.66	1.59	1.39	1.38	1.82	10.9	.175	3.39	4
05/6-2	82	1.30									-
06/6-1D	82	1.61	1.96	1.52	1.20	1.24	1.61	8.6	.177	3.43	3
09/6-1	82	1.50	1.88	1.44	1.30	1.10	1.46	8.0	.167	3.24	4
09/6-2	54	1.55	2.00	1.51	1.34	1.31	1.56	11.7	-	2*	-
10/6-1D	35	2.08	2.26	1.76	1.59	1.62	1.94	67.9			-
10/6-2D	54	1.50	1.60	1.56	1.20	1.24	1.64	12.0	.091	1.77	4
<u>FB2</u>											
13/6-1	82	1.60	1.91	1.62	1.42	1.36	1.79	8.0	.153	2.80	4
13/6-2D	82	1.74	1.80	1.70	1.46	1.48	1.75	22.7	-	3*	-
16/6-1D	35	1.68	2.00	1.64	1.50	1.46	1.74	21.3	.052	1.01	3
17/6-1D	54	1.62	1.76	1.70	1.40	1.35	1.53	5.4	.102	1.98	2
18/6-1	54	1.72	1.94	1.67	1.32	1.37	1.64	8.0	.092	1.79	4
19/6-1	35	1.62	1.90	1.62	1.33	1.30	1.76	4.5	.070	1.36	2

TABLE E.1 (Continued): DATA FOR SMALL-SCALE ICE TANK TRIALS

DATE/: SHEET <D=drilled>	SET:	H1	H2	H3 (mm)	H4	H5	H6	$\sigma_{fs}$ (kPa)	$V_n$ (m/s)	V <*=nominal>	:RATE
<b>FB3</b>											
01/7-1	82	1.65	1.86	1.76	1.30	1.26	1.62	37.0	-	3*	-
02/7-1	82	-	-	-	-	-	-	-	-	-	-
02/7-2	82	1.74	1.88	1.74	1.43	1.40	1.80	25.4	.139	2.70	4
03/7-1D	82	1.72	-	-	-	-	-	30.6	-	-	-
03/7-2D	82	1.40	1.36	1.31	1.20	1.25	1.50	8.0	.151	2.93	2
04/7-1	82	1.71	1.80	1.50	1.28	1.35	1.56	11.1	.143	2.78	3
04/7-2D	82	1.46	1.52	1.45	1.23	1.17	1.42	6.4	.141	2.74	2
<b>FB3M</b>											
08/7-1	82	1.44	1.62	1.36	1.24	1.12	1.30	8.9	.151	2.92	1
08/7-2D	82	1.25	-	-	-	-	-	8.0	-	-	-
09/7-1	82	1.69	1.95	1.79	1.43	1.43	1.75	11.0	-	3*	-
09/7-2D	82	1.17	1.34	1.24	1.13	1.18	1.37	8.0	-	3*	-
09/7-3	82	1.62	1.78	1.56	1.32	1.34	1.56	16.1	-	3*	-
10/7-1D	35	1.70	-	-	-	-	-	-	-	-	-
10/7-2D	35	1.36	1.32	1.40	1.34	1.34	1.56	8.0	.050	0.97	1
10/7-3	35	1.64	1.79	1.62	1.32	1.36	1.65	20.6	.040	0.78	1
11/7-1D	54	1.72	1.93	1.67	1.33	1.40	1.60	13.9	.071	1.37	2
<b>FB4</b>											
15/7-1	82	1.84	-	-	-	-	-	13.6	-	-	-
16/7-1	82	1.90	1.96	1.74	1.52	1.46	1.82	33.4	-	3*	-
16/7-2D	82	1.73	1.95	1.82	1.56	1.48	1.74	23.6	-	3*	-
21/7-1D	82	1.81	1.86	1.55	1.32	1.39	1.76	28.3	.160	3.10	1
21/7-2	82	1.67	-	-	-	-	-	8.0	-	-	-
21/7-3	82	1.54	1.60	1.38	1.17	1.23	1.50	6.4	.177	3.44	2
22/7-1	82	1.67	1.80	1.50	1.26	1.34	1.63	15.7	.145	2.82	4
22/7-2D	54	1.62	-	-	-	-	-	-	-	-	-
22/7-3D	54	1.73	-	-	-	-	-	8.0	-	-	-
23/7-1	54	1.68	1.67	1.53	1.34	1.44	1.66	46.2	.114	2.21	3
23/7-2	54	1.45	1.53	1.36	1.24	1.24	1.44	10.5	.089	1.72	2
23/7-3	35	1.70	1.85	1.66	1.36	1.42	1.86	18.6	.057	1.11	3
24/7-1D	35	1.80	1.87	1.68	1.47	1.46	1.91	10.4	-	1*	-
24/7-2D	54	1.69	1.75	1.63	1.30	1.38	1.76	10.4	.090	1.75	3
<b>FB5</b>											
27/7-1	82	1.70	1.85	1.56	1.37	1.46	1.79	13.8	.136	2.65	1
27/7-2	82	1.80	1.90	1.76	1.45	1.32	1.53	11.5	-	3*	-
28/7-1	82	1.76	2.08	1.77	1.47	1.51	1.85	33.0	.123	2.38	2
28/7-2	54	1.68	1.68	1.86	1.28	1.34	1.62	11.1	.097	1.88	1
29/7-1	54	1.83	2.09	1.72	1.52	1.52	1.71	21.0	.111	2.16	3
29/7-2	35	1.48	1.55	1.54	1.31	1.30	1.43	7.7	.042	0.82	3
29/7-3	35	1.76	1.84	1.68	1.43	1.36	1.67	50.4	.044	0.85	1
23/9-1	82	1.77	2.05	1.58	1.30	1.42	1.55	8.9	.164	3.18	2
24/9-1	82	1.55	1.85	1.65	1.34	1.39	1.68	20.4	-	3*	-
25/9-1	82	1.59	-	-	-	-	-	50.9	-	-	-
26/9-1	82	1.57	1.57	1.36	1.28	1.29	1.60	12.7	.145	2.82	3

TABLE E.1 (Continued): DATA FOR SMALL-SCALE ICE TANK TRIALS

DATE/: SHEET <D=drilled>	SET:	H1	H2	H3 (mm)	H4	H5	H6	: $\sigma_{fn}$ (kPa)	$v_n$ (m/s)	V (kts)	:RATE	
											<*=nominal>	
<u>FB5 (continued)</u>												
26/9-2	82	1.51	1.68	1.64	1.36	1.30	1.52	11.7	.145	2.82	2	
29/9-1	54	1.59	1.75	1.58	1.30	1.24	1.88	7.9	.091	1.77	2	
30/9-1	54	1.39	-----					8.0	-----			-
30/9-2	54	1.70	1.71	1.64	1.32	1.36	1.67	13.1	.091	1.77	3	
01/10-1	35	1.55	1.61	1.42	1.20	1.25	1.51	8.0	.070	1.36	2	
01/10-2	35	1.33	1.37	1.20	1.13	0.99	1.33	8.0	.049	0.95	3	

F. SPECIFICATIONS OF THE M.V. "ARCTIC" FITTED WITH THE S-BOW:  
MODEL 326BP

F.1 PARTICULARS AND HYDROSTATICS

The M.V. "ARCTIC" was selected as the test case for the S-Bow because it featured a large trim moment (Appendix B.4), has been widely tested in both the laboratory and the field, and a three-segment 1:30 scale model was available at IMD. The existing data base meant comparative performance data were available, allowing the allocation of more tank time to S-Bow trials. The model specifications were stored as an SMP file (Appendix B.2), which simplified the construction of an S-Bow model. The S-Bow lines were faired into the Melville Bow at the 20.0cm waterline (6.0m full scale), forward of a section 523.0cm (156.9m full scale) from the aft perpendicular. The S-Bow underside was not treated in this program. The model construction history is described in Section 4.4.2 of the text. The hydrostatics for the M.V. "ARCTIC" fitted with the S-Bow, designated M326BP, are presented in Table F.1; the form coefficients are given in Table F.2.

F.2 COMPARISON OF M326BMS and M326BP:

Model specifications were compared to locate the towing equipment and check the ballast for the M326BP towing trials. The decrease in hull length was offset by the change

in LCG, so it was unnecessary to change the position of the towing post in the model. Two other points of comparison described in the text are detailed below. Subscript "s" indicates S-Bow, M326BP; subscript "m" indicates Melville Bow, M326BMS.

- a) Decrease in Bow Length: From station 205.92" = 523cm forward of the aft perpendicular.

$$1 - ((656.46\text{cm} - 523.04\text{cm}) / (707.49\text{cm} - 523.04\text{cm})) = .277$$

$$= \underline{27.67\%} \text{ reduction in bow length}$$

- b) Block Coefficients:  $C_{B_s} / C_{B_m} = 0.769 / 0.728 = 1.056$   
 Aft Body:  $C_{BAs} : C_{BAm} = 0.710 / 0.725 = 0.979$   
 Fore Body:  $C_{BFs} : C_{BFm} = 0.829 / 0.731 = 1.134$

### F.3 TRIM CALCULATIONS

Objective: To vary trim from 0 to 1cm (model scale) at the shoulders, 0.3m (1ft.) full scale. The intent was to vary the bow geometry, particularly the exposure of the shoulders, to identify an optimum orientation. The hull was trimmed by the stern in Test 1, and then by the bow in Test 3.

Moment to Change Trim 1cm: see equation B-6.1, Appendix B;

$$MCT1\text{cm} = \underline{21.5 \text{ kg}\cdot\text{m}/\text{cm}}$$

Amount of Trim Required: where

$$\begin{array}{lll} \text{(Shoulder location} & L_{BP} = 6.498\text{m} & \\ \text{from AP)} & L_{sh} = 5.814\text{m} & \text{(Station 4.5)} \\ & LCF = 3.415\text{m} & \end{array}$$

Trim at FP:  $t_{fp}$  ; if trim at shoulders =  $t_s$

$$t_{fp} = t_s (L_{BP} - LCF) / (L_{sh} - LCF) = t_s (1.285) \quad \text{<F-3.1>}$$

For  $t_s = 0.5\text{cm}$  ;  $t_{fp} = 0.65\text{cm}$   
 $t_s = 1.0\text{cm}$  ;  $t_{fp} = 1.31\text{cm}$   
 $t_s = 2.5\text{cm}$  ;  $t_{fp} = 3.21\text{cm}$

Trimming Moments Required:  $MCT(0.65cm) = 14 \text{ kg*m}$   
 $MCT(1.31cm) = 28 \text{ kg*m}$   
 $MCT(3.21cm) = 69 \text{ kg*m}$

and where the shifting distance for a weight W is obtained by dividing the weight into the moment to change trim.

#### F.4 M326BP BOW SEGMENT FRICTION DATA

The sample board painted simultaneously with the bow segment was tested twice, under varying normal loads.

The friction coefficients were:

Test 1:  $\mu = 0.098 \pm 0.005$

Test 2:  $\mu = 0.123 \pm 0.008$

Overall:  $\mu = 0.110 \pm 0.014$

The friction coefficients for the other hull segments are given in Appendix B.3. All friction coefficients were obtained using the friction described in Williams et al. (1987). The target value of  $\mu = 0.1$  was used in the numerical analysis (Appendix H).

TABLE F.1: HYDROSTATIC PARTICULARS OF MODEL M326BP

SCALE:		FULL	1:30
LENGTH (PERPENDICULARS)	$L_{PP}, m$	194.94	6.498
LENGTH (WATERLINE)	$L_{WL}, m$	199.14	6.638
BEAM (AT WATERLINE)	$B, m$	22.86	0.762
DESIGN DRAUGHT	$T, m$	10.97	0.366
DEPTH	$D, m$	15.00	0.500
LOCATION OF MIDSHIPS (Fwd of AP)	$L_M, m$	98.39	3.249
CENTRES OF BUOYANCY: (Fwd of Midships)	$LCB, m$	5.16	0.170
(above baseline)	$KB, m$	5.93	0.196
WETTED SURFACE AREA	$S, m^2$	7304	7.964
DISPLACED VOLUME	$V, m^3$	37611	1.393
DISPLACEMENT	$\Delta, tonnes$	38589 <s.w>	1.391 <f.w.>
CENTRE OF FLOTATION (Fwd of Midships)	$LCF, m$	5.02	0.166
WATERPLANE AREA	$A_{wp}, m^2$	4168	4.545
TRANSVERSE METACENTRIC RADIUS	$BM_t, m$	4.28	0.141
LONGITUDINAL METACENTRIC RADIUS	$BM_l, m$	303.35	10.017
LONGITUDINAL CENTRE OF GRAVITY	$LCG, m$	102.57	3.419

## TABLE F.1 NOTES:

- 1) Hydrostatics based on the bare hull, no appendages.
- 2) As indicated by the comparison of data in Appendix F.2, it was possible to use the same ballasting and towing

arrangements as M326BMS; both KG and the radii of gyration were assumed similar. See Appendix B, Table B.1 notes.

TABLE F.2: FORM COEFFICIENTS FOR M.V. "ARCTIC" WITH S-BOW

COEFFICIENTS BASED ON: LENGTH BETWEEN PERPENDICULARS  
BEAM, DRAUGHT AT MIDSHIPS

L/B	8.527	
L/T	17.769	
B/T	2.084	
AFT BODY $L_{WL}/L$	0.522	
FOREBODY $L_{WL}/L$	0.500	
BLOCK, $C_B$	0.769	
$C_B$ , AFT BODY	0.710	
$C_B$ , FOREBODY	0.829	
MIDSHIPS, $C_M$	0.991	
PRISMATIC, $C_P$	0.777	
%LCB/L	2.624	} Fwd of Midships
%LCB(AFT BODY)/L	-19.071	
%LCB(FOREBODY)/L	21.191	
WATERPLANE, $C_W$	0.918	
$C_W$ OF AFT BODY	0.863	
$C_W$ OF FOREBODY	0.973	
%LCF/L	2.552	} Fwd of Midships
%LCF(AFT BODY)/L	-22.082	
%LCF(FOREBODY)/L	24.406	
$BM_t/B$	0.185	
$BM_1/L$	1.542	

## G. SUMMARY OF THE IMD RESISTANCE TRIALS

## G.1 INDIVIDUAL TRIAL SUMMARIES - MODEL RESISTANCE DATA

The resistance data from each trial are summarized in the tables below, along with test ice conditions and notes from the trials. R1 and R2 refer to resistance data from channels 1 and 2 respectively; all data have been zeroed. R<sub>s</sub> refers to selective resistance data described in Section 4.4 of the text. QP indicates a test performed on the quarter point. The resistance corresponding to model speed 0/0 is the zero-speed resistance measured at the start and end of each run. The hull motion data are given in Appendix G.2. The nomenclature for the ice properties is as follows:

E = ice sheet modulus measured by disc deflection method (Baker, 1985).

$\sigma_c$  = flexural strength from cantilever beam test (Timco, 1980) taken upward or downward.

$l_c$  = critical length of ice sheet, related to deflection and fracture behaviour.

$\sigma_c$  = uniaxial compressive strength of ice sheet, from beam apparatus (Timco, 1980).

$K_{Ic}$  = stress intensity factor given by the notched beam test (Parsons et al., 1986).

h = ice thickness

## G.1.1 S-BOW TEST 1

Test Designation: 1 Waas : M326BP-1  
Date : 9/ 12 / 1986

Objective: To check bow geometry by trimming by the stern

Ice Properties:  $E = 44.67 \pm 1.76$  MPa ;  $E/\sigma_c = 1490$  ;

$l_c = 0.3992 \pm 0.004$  m ;  $\sigma_c = 56.5 \pm 8.5$  kPa ;

$K_{Ic} = 4.95 \pm 1.25$  kPa+m<sup>-1/2</sup> ;

Downward:  $\sigma_c = 28.7$  kPa ;  $\sigma_c/K_{Ic} = 5.8$  m<sup>-1/2</sup>

Upward:  $\sigma_c = 14.0$  kPa ;  $\sigma_c/K_{Ic} = 3.0$  m<sup>-1/2</sup>

Ice Thickness:  $h = 39.65 \pm 0.64$  mm average

TABLE G.1.1 RESISTANCE DATA - TEST 1

v(m/s)	R1 (N)	R2 (N)	Rs (N)	Notes
0.283	255.3	253.7	217.3	0 trim
0/0	73.2/158.9	71.0/157.4	-	start/stop; %coverage= 0/100
0.283	294.6	293.0	-	0.5cm by stern
0/0	196.4/71.8	195.0/70.2	-	%coverage= 20/90
0.283	274.0	273.0	-	1.0cm by stern
0/0	28.3/106.6	27.1/47.8	-	%coverage= 20/80
QP Trials				
0.283	179.8	178.5	-	0 trim
0.142	134.2	132.9	76.6	-
0/0	28.6/49.3	27.5/47.8	-	%coverage= 50/95
0.142	152.5	150.9	-	1.0cm trim
0/0	22.6/72.3	21.0/70.7	-	%coverage= 90/70

G.1.2 S-BOW TEST 2

Test Designation: 2 Waas : M326BP-2  
Date : 10/ 12 / 1986

Objective: Resistance tests in 25mm (0.75m) ice at 0 trim  
Pre-sawn test on Quarter point, except 3 knots.

Ice Properties:  $E = 13.47 \pm 0.77$  MPa ;  $E/\sigma_t = 653$  ;  
 $l_c = 0.1992 \pm 0.003$ m ;  $\sigma_o = 60 \pm 10$  kPa ;  
 $K_{Ic} = 3.55 \pm 0.6$  kPa\*m<sup>-1/2</sup>

Downward:  $\sigma_t = 18.0$  kPa ;  $\sigma_t/K_{Ic} = 5.1$  m<sup>-1/2</sup>

Upward:  $\sigma_t = 11.0$  kPa ;  $\sigma_t/K_{Ic} = 3.1$  m<sup>-1/2</sup>

Ice Thickness:  $h = 23.31 \pm 0.64$ mm average

TABLE G.1.2 RESISTANCE DATA - TEST 2

v (m/s)	R1 (N)	R2 (N)	Notes
0.191	69.7	68.1	0 trim all speeds
0.283	78.8	77.2	-
0.470	102.7	100.8	-
0.655	106.5	105.0	-
0/0	9.1/58.9	6.3/57.3	%coverage= 0/70
QP Trial: Unseen -----			
0.283	62.6	59.6	0 trim; unseen
QP Trials: Pre-Sawn -----			
0.469	51.4	48.6	0 trim all speeds
0.655	59.9	57.0	-
0/0	55.4/17.4	54.8/7.3	%coverage= 65/70

NOTE: selective resistance analysis produced minor variation in resistances.

G.1.3 S-BOW TEST 3

Test Designation: 3 Waas : M326BP-3  
Date : 11/ 12 / 1986

Objective: Attempted to improve shearing action by trimming by the bow, lowering shoulder height; CL tests run with 2cm trim by bow; QP tests run with 1cm trim.

Ice Properties:  $E = 53.75 \pm 4.40$  MPa ;  $E/\sigma_t = 1250$  ;

$l_c = 0.4026 \pm 0.008$  m ;  $\sigma_c = 53.5 \pm 16.0$  kPa ;

$K_{Ic} = 4.55 \pm 0.65$  kPa\*m<sup>-1/2</sup>

Downward:  $\sigma_t = 31.4$  kPa ;  $\sigma_t/K_{Ic} = 6.9$  m<sup>-1/2</sup>

Upward:  $\sigma_t = 18.5$  kPa ;  $\sigma_t/K_{Ic} = 4.1$  m<sup>-1/2</sup>

Ice Thickness:  $h = 39.16 \pm 0.55$  mm average

TABLE G.1.3: RESISTANCE DATA - TEST 3-

v(m/s)	R1 (N)	R2 (N)	Rs (N)	Notes
0.141	217.5	216.5	160.7	2cm trim for all speeds
0.181	273.3	271.6	209.8	-
0.280	287.6	285.5	269.9	-
0.467	358.9	357.4	298.2	-
0/0	68.8/72.3	68.4/70.9	-	%coverage= 60/100
QP Trial	-----			
0.141	113.4	111.7	N/A	1cm trim for all speeds
0.181	175.8	174.2	N/A	-
0.284	191.8	190.1	N/A	-
0.467	220.6	218.5	N/A	-
0/0	49.6/124.0	47.4/122.5	-	%coverage= 60/100

G.1.4 S-BOW TEST 4

Test Designation: 4 Waas : M326BP-4  
Date : 12/ 12 / 1986

Objective: Perform resistance tests at two different flexural strengths in 25mm ice; lcm trim by bow. QP run performed with spacers in central channel more closely spaced (2m interval) to reduce "calving".

Ice Properties:  $E = 25 \pm 2$  MPa ;  $E/\sigma_c = 745$  ;  
 $l_c = 0.235 \pm 0.005$  m ;  
 $\sigma_c = 64.5 \pm 12.0$  kPa (after Run 1)

Run 1:  $K_{Ic} = 6.65$  kPa\*m<sup>-1/2</sup>  
Downward:  $\sigma_f = 41.5$  kPa ;  $\sigma_f/K_{Ic} = 6.2$  m<sup>-1/2</sup>  
Upward:  $\sigma_f = 21.5$  kPa ;  $\sigma_f/K_{Ic} = 3.2$  m<sup>-1/2</sup>  
Ice Thickness: h = 23.8mm average

Run 2:  $K_{Ic} = 5.20$  kPa\*m<sup>-1/2</sup> ;  $\sigma_f/K_{Ic} = 6.35$  m<sup>-1/2</sup>  
( & QP ) Downward:  $\sigma_f = 24.2$  kPa ;  $\sigma_f/K_{Ic} = 4.6$  m<sup>-1/2</sup>  
Upward:  $\sigma_f = 13.2$  kPa ;  $\sigma_f/K_{Ic} = 3.5$  m<sup>-1/2</sup>  
Ice Thickness: h = 24.51±0.44mm average

TABLE G.1.4: RESISTANCE DATA - TEST 4

v(m/s)	R1 (N)	R2 (N)	Rs (N)	Notes
0.139	77.0	76.9	69.1	high $\sigma_f$
0.279	106.0	106.0	-	-
0/0	91.5/35.1	91.5/35.7	-	%coverage= 60/100
-----				
0.139	83.5	84.4	82.8	low $\sigma_f$
0.278	101.5	102.5	-	-
0/0	18.0/32.6	19.7/33.9	-	%coverage= 85/95
-----				
QP Trial	-----			
0.466	117.8	119.0	104.8	2m spacers; less calving
0.652	125.8	126.2	126.0	-
0/0	30.5/47.2	31.3/48.3	-	%coverage= 60/80

NOTES on Test 4: 1) the resistance levels are higher than in Test 2, in spite of an apparent improved shearing action with the trim.

2) the variation in flexural strength produced little variation in resistance.

### G.1.5 S-BOW TEST 5

Test Designation: 5 Waas : M326BP-5

Date : 16/ 12 / 1986

Objective: Perform resistance tests at two different flexural strengths in 40mm ice; 1cm trim by bow. QP run with spacers at 2m intervals.

#### Ice Properties:

Run 1:  $E = 86 \pm 2$  MPa ;  $E/\sigma_f = 1480$  ;  $l_c = 0.458 \pm 0.003$  m ;  
 $K_{Ic} = 7.05$  kPa\*m<sup>-1/2</sup> ;  $\sigma_c = 117$  kPa ;  
 Downward:  $\sigma_f = 62.75$  kPa ;  $\sigma_f/K_{Ic} = 8.9$   
 Upward:  $\sigma_f = 34.50$  kPa ;  $\sigma_f/K_{Ic} = 4.9$   
 Ice Thickness:  $h = 37.5$ mm average

Run 2:  $E = 52 \pm 4$  MPa ;  $E/\sigma_f = 1350$  ;  $l_c = 0.413 \pm 0.008$  m ;  
 (& QP)  $K_{Ic} = 5.40$  kPa\*m<sup>-1/2</sup> ;  $\sigma_c = 53.5$  kPa ;  
 Downward:  $\sigma_f = 36.5$  kPa ;  $\sigma_f/K_{Ic} = 6.8$   
 Upward:  $\sigma_f = 19.0$  kPa ;  $\sigma_f/K_{Ic} = 3.52$   
 Ice Thickness:  $h = 39.48 \pm 0.56$ mm average

TABLE G.1.5: RESISTANCE DATA - TEST 5

v(m/s)	R1 (N)	R2 (N)	Rs (N)	Notes
0.141	266.4	265.1	N/A	high $\sigma_f$
0.281	310.8	309.9	N/A	-
0/0	270/217.2	269.2/216.1	-	%coverage= 60/95
0.141	179.0	176.1	114.8	low $\sigma_f$
0.282	287.9	284.8	229.0	-
0/0	-15.1/33.0	-17.8/30.4	-	%coverage= 0/95
QP Trial				
0.468	206.4	203.6	N/A	2m spacers; ineffective
0.653	297.1	294.3	N/A	-
0/0	-13.3/115.4	-15.0/112.6	-	%coverage= 75/80

- NOTES (Test 5): 1) Resistances higher than Test 1
- 2) Resistance actually increased in the ice sheet with reduced flexural and compressive strengths.
- 

#### G.1.6 IMD Test Data for the Melville Bow

The resistance data for the Melville Bow that provided the basis for comparison for the 40mm trials were obtained experimentally at IMD, to account for the effect of EG/AD/S ice and local variation. These trials were performed as part of a series of friction tests (Williams et al., 1987), and was provided with the permission of Melville Shipping Limited. The test specifically designated for comparison had to be deleted because of instrument problems; consequently the data were obtained from a later test. The test data, with published resistance data for the 25mm sheet obtained from Baker (1985), are listed in Table 4 in the main text.

#### G.2 MOTION DATA ANALYSIS

The dynamometer recorded hull motion on three separate channels as port, starboard, and forward displacements respectively. Two aspects of the hull motion were of interest. One was the amount of trim induced by the ice sheet at the forward perpendicular; the estimated trim was predicted to be about the thickness of the ice sheet, but the videotapes suggested it was actually much less. An IMD computer

program was used to convert the displacement data to pitch and roll angles directly from the time histories. Displacement at the forward perpendicular (FP) was estimated as the sum of the average heave and the induced trim by the pitch angle. The heave record remained relatively steady for each trial. The data from selected tests are presented as Table G.2; note that displacement downward is shown as a positive value. The maximum roll amplitudes were of interest because some severe rolling events were observed, associated with fracture of large, heavily deformed ice segments during Tests 3 and 5.

TABLE G.2: MODEL MOTION DATA FOR TYPICAL TESTS

Test No.	$v_a$ (m/s)	h (mm)	Heave (mm)	Pitch(deg.)		Displ.FP(mm)		Roll(deg.)	
				Avg.	Max.	Avg.	Max.	Avg.	Max.
target	-	40.0	-	0.86	1.0	36.0	42.0	-	-
1.1CL	0.28	39.7	5.55	0.11	0.32	10.2	19.0	0.17	2.12
1.2CL	0.28	"	6.35	0.18	0.40	13.9	23.1	1.25	2.87
1.3CL	0.28	"	5.85	0.11	0.37	10.5	21.0	0.92	2.61
1.1QP	0.28	"	5.17	0.25	0.49	15.7	25.7	1.00	3.00
1.1QP	0.14	"	5.16	0.21	0.40	14.4	22.4	0.62	2.07
2CL	0.19	23.3	2.97	0.08	0.17	6.3	10.1	-	0.56
2CL	0.28	"	5.66	0.08	0.16	9.0	12.4	-	0.43
2CL	0.47	"	3.98	0.11	0.16	8.6	10.7	-	0.37
2CL	0.65	"	6.08	0.10	0.16	10.3	12.8	-	0.21
4.1CL	0.14	24.7	3.26	0.19	0.29	11.3	15.4	-	0.89
4.1CL	0.28	"	3.66	0.22	0.31	12.9	16.7	-	1.05
5.2CL	0.14	39.7	5.48	0.20	0.50	13.9	26.4	-	5.79
5.2CL	0.28	"	7.13	0.22	0.50	16.3	28.0	-	5.21

The data were selected to correspond to trial points used to plot the average resistance plot in the main text (Figure 18); other points are included to exhibit extreme values.

The major feature of the table is the disparity between the predicted and actual values of displacement at the forward perpendicular. The overprediction of bow trim is clearly demonstrated by the data.

#### H. NUMERICAL ANALYSIS OF S-BOW RESISTANCE

A numerical analysis of the breaking action of the S-Bow was performed to provide quantitative verification of the hypothesis that the high resistances recorded during the IMD model tests were related to design problems observed during the trials. It was unrealistic to expect to accurately calculate total resistance with existing methods. The intent was to identify resistance levels associated with individual events and to make some relative assessment of their influence.

A simplified geometry was adopted for the bow components, as shown in Figure 4 of the text. Individual events in the breaking sequence were then analyzed using several simple models published in the open literature. The reader is referred to the original source for the theoretical development of each model. Where possible, several models were used to analyze a particular event, to reflect variations in failure mode and the uncertainty regarding the rheology of model ice failure. Variation of resistance with speed was assumed to be a function of the frequency of events; none of the models featured an explicit speed dependent term. The effect of a particular event was assessed based on a convergence of the resistances calculated by different models (where possible), comparison with the experimental data, and

comparison with the fracture component calculated numerically. The fracture component was used as a basis for comparison because the numerical models were the most highly developed.

The results of the numerical analysis verified the design problems identified visually (poor contact at the shoulders; excessive ice deflection around the snout; entrapment/crushing of ice under the forepeak; wedging of ice between the hull and channel) had a significant influence on the total ice resistance. The analysis suggested that a major reduction in level ice resistance could be achieved through the refinement of the bow design.

The numerical analysis also indicated that the resistance associated with the lifting of broken ice was not compensated by the elimination of hydrodynamically-induced effects. The trend in the data suggested that fracture component was primarily dependent on stem/slope angle and ice strength. Field data from beam tests (Mellor, 1980) indicates that the flexural strength of ice did not vary significantly with load direction. This implies the fracture component would be neutral in a comparison of upward- and downward-acting icebreakers. The variation in model ice flexural strength with load direction, and the variation in

temperature and salinity with ice thickness might suggest a need for further research on the importance of load direction.

Apart from the stem angle, the type of form had little effect on calculated resistance levels. The dominant factor affecting the lifting/sliding resistance component was the contact area. These comments relate to the physics of upward-acting icebreakers and place limitations on their application, as discussed in Section 5.2 of the text.

A brief description of the analysis of each resistance event is presented below, with a list of the different sources used, and typical resistance levels calculated for each event. The results are summarised as Table 5 in the text.

#### H.1 REGION OF ICE DEFLECTION AROUND SNOOT

A deflected region was observed around the snout, approximating a cone, was observed while the model was stopped; a large resistance was also recorded at zero speed. This feature was treated as a plastic zone because of the loading times involved, using Ralston's (1979) plastic-limit analysis for an upward-breaking cone. The conical region was approximated from the stem height, to give a slope of  $17^\circ$ .

Ralston uses both a Tresca and Johansson yield criteria, but the two analyses gave similar results. The failure sequence is broken into the following subcomponents: circumferential cracking, side cracking, "foundation" (buoyancy) reaction, deformation region, ride-up of broken ice (lifting component), and frictional dissipation. This subdivision differs from Frederking and Timco's (1985) treatment of an inclined plane, as did the relative magnitudes of different components. However, the results compared well with the experimental data (Appendix G); for the 25mm ice sheet, resistance was estimated at 35 N; for 40mm ice, a resistance of 70 N was calculated. It was observed that the largest individual resistance component was the ice ride-up component (the lifting component described above). It should be noted that this component was specific to when the model was stopped.

## H.2 ICE FRACTURE RESISTANCE

The ice fracture resistance was treated as several components which would not reach peak levels simultaneously (see Frederking and Timco, 1985). The resistance associated with fracture was related to the action of the central skeg and the shearing action of the shoulders. The numerical models calculate a peak failure load, the failure geometry having been defined by the cracking pattern.

### H.2.1 Radial Cracking at Snout-

H.2.1a) Method - The analysis of the resistance associated with radial cracking component followed the same basic method. A vertical line load ( $P_v$ ) exerted by the ice sheet was resolved into a horizontal resistance by considering the width of the structure ( $B$ ), in this case the ship's beam, and using a resolution factor:

$$\epsilon = \frac{(\tan\alpha + \mu)}{(1 - \mu\tan\alpha)} = \frac{(\sin\alpha + \mu\cos\alpha)}{(\cos\alpha - \mu\sin\alpha)} \quad (\text{H-2.1})$$

; noting that a friction factor is included.

Therefore the resistance due to radial cracking will be:

$$R_{12} = \epsilon \times P_v \times B \quad (\text{H-2.2})$$

Localized crushing at the stem was not considered unless treated in the calculation of  $P_v$ .

H.2.1b) Calculation of the Vertical Load  $P_v$  - The fracture pattern resulting from the actual snout and shoulder geometry was too complex to analyze with the simple models available. Consequently a variety of models were applied to provide an envelope for radial crack induced resistance. The stem (slope) angle was varied from  $17^\circ$  to  $43^\circ$  to represent local form variations and the effect of trim on resistance. The models were based on different geometries and involved a variety of rheological assumptions. Some details are summarised below:

TABLE H.2.1 - RADIAL CRACKING RESISTANCE MODELS

Model	Geometry	Rheological Model
Frederking & Timco (1985)	Inclined Plane	Semi-Empirical, from Linear Elastic (Nevel)
Meyerhof (from Milano, 1982)	Wedge Failure	Plastic
Coon & Mohaehgh (from Milano, 1982)	Wedge Failure	Elastic-Plastic
Allyn (1982)	Inclined Plane	Linear Elastic, Multi-axial derivation
Bercha (1982)	Inclined Plane	Multi-modal Linear Elastic (compression neglected)
Ralston (1977)	Inverted Cone	Initial Crack, Elastic-Plastic Theory

The wedge models were evaluated over a range of interior angles from 30° to 75° to reflect variation in the ice fracture geometry.

In spite of the differences in geometry and rheology, the data generated were well grouped and consistent. The results given by Ralston's (1977) initial crack model gave an upper bound on resistance; the effect of stem angle can be seen in the table below:

TABLE H.2.2 - RADIAL CRACKING RESISTANCE FROM RALSTON (1977)						
h(mm)	B(m)	R <sub>v</sub> *B (N)	Resistance (N) by Stem Angle			
			α: 43.7	28.8	34.6	17.2
25	0.76	27.0	31.6	18.6	23.0	11.4
40	0.76	41.2	48.3	28.5	35.1	17.3

In general it can be concluded that the stem angle (or trim angle) influenced resistance, but the effect of form (cone or inclined plane) was minor. None of the models discussed how load direction might affect the fracture resistance.

#### H.2.2) Ice Fracture- Circumferential Cracking Component

The circumferential cracking resistance component was associated with the formation of the crack which separated an ice segment from the ice sheet. The cracking geometry observed during the IMD tests suggested that this component may have been accentuated by the trim behaviour of the model, and possibly the fracture properties of model ice.

H.2.2a) Method-Two methods were used for the analysis. Frederking and Timco (1985) calculated the resistance due to circumferential cracking for an inclined plane for an ice wedge defined by the angle formed by the radial crack and the structure's side. Three values were chosen for the angle because the radial crack orientation was observed to vary in different trials; this may have been a result of inconsistent fracture toughness. A similar range of bow geometries was investigated as for radial cracking. The other analysis used the circumferential cracking component of Ralston's (1979) plastic limit analysis of an upward-acting cone. A steeper cone angle

was included to represent a crack location farther up on the snout.

H.2.2b) Results - The resistance calculated for circumferential cracking-related resistance varied significantly with crack geometry, and the type of indenter (inclined plane or cone). The smallest values were calculated for an inclined plane with a  $17^\circ$  slope; typically 3 N for 25mm ice, 6 N for 40mm ice; the steepest cone angle gave the maximum; 12 N in 25mm ice, 26 N in 40mm ice. Given that the different models were intended to represent different cracking patterns, the variation in results indicates the influence of fracture properties (crack orientation) on fracture resistance. In general, the resistance associated with circumferential cracking was about 30-40% of radial cracking resistance; as indicated by the breaking sequence, these resistances would not be coincident.

### H.2.3 Analysis at Shoulders- Bending Modes

This resistance component was associated with "secondary" fracture of the crescent segments produced by the initial fracture sequence. The specific event analyzed was flexure at the crescent segment tips, with the ice geometry identified from still photographs. The method used to analyze bending failure at the shoulder were similar to those applied to the radial cracking analysis.

For a specified geometry based on the local shoulder dimensions, a resolution factor  $\epsilon$  was used to convert a vertical load into a resistance component. The standard failure situation was investigated using formulae from Frederking and Timco (1985) and from Bercha (1982), which gave typical resistances of 5 N in 25mm ice and 8 N in 40mm ice. There was some variation with slope. These values are relatively small in comparison with the other fracture resistance components, but the interference of adjacent ice on the shoulder may be underestimated.

Ralston's (1977) formula for a hinge crack failure was used to investigate an unclean breaking action associated with poor shear action, typical of later tests. In this case resistances were almost double those calculated for the standard failure situation.

### H.3 CRUSHING AT THE SHOULDERS

Crushing at the shoulders was not apparent during the trials by visual observation, but merited investigation because of the poorly defined shearing edges at the shoulders. Some flexing of the ice sheet could be seen on videotape. It was evident that this was a more complex loading situation than might be represented by a simple limit-stress case. Reincke's (1979) plastic limit analysis of in-plane ice forces seemed to better represent the ice flexing con-

dition. The analysis is based on the division of the region around a wedge indenter into zones of plastic deformation, each with an associated energy dissipation. The indenter was sized to match the shoulder; the equivalent indenter had a spread angle of about  $40^\circ$  and a base width of 0.06m.

Indenter pressure ( $\sigma_c'$ ) was calculated from a set of yield functions based on orthogonal stresses, with plane stress, free slip conditions applying. The use of orthogonal stresses was not well suited to the laboratory ice data, and required some improvisation to derive a tensile stress for EG/AD/S ice. The IMD ice data was scaled according to the ratios and data provided by Reincke.

The analysis gave large resistance values, with some variation with deformation zone angle. A typical resistance for 25mm ice was 150 N for a zone angle of  $30^\circ$ ; resistance was about 240 N for similar conditions in 40mm ice.

The calculated resistances, particularly in 25mm ice, were excessive when compared with the average resistances recorded experimentally; however they did not exceed recorded peak values. This might suggest that crushing at the shoulder region, acting on a small surface area for a brief instance (and not easily observed), could have caused large peak loads, and consequently increased average resistance.

#### H.4 RESISTANCE DUE TO ICE MOVEMENT OVER THE BOW

##### H.4.1 Sliding Resistance over the Forefoot Region -

The calculation of the ice fracture resistance did not include a sliding resistance component, and therefore would apply regardless of loading direction. The sliding resistance associated with the lifting and movement of ice segments would be affected by the relative difference in density resulting from lifting rather than submergence of the ice.

The sliding resistance over the forefoot was analyzed for two forms, the cone and the inclined plane. The cone form was analyzed using the appropriate components from Ralston's (1979) plastic limit analysis; the ride-up, deformation, and "foundation" reaction, each corrected for friction. Two slope angles were used to reflect changes in trim and bow geometry. The inclined plane analysis was taken from Frederking and Timco (1985) which included a resistance component associated with rotating the broken ice segments, acting out of phase with the sliding and edge load resistance.

The coincident forces acting on an inclined plane with a slope of  $30^\circ$  were 37 N in 25mm ice and 72 N for 40mm ice; for the cone the resistances were 72 N in 25mm ice and 60 N in 40mm ice. The primary difference between

the two analyses was the surface area of the forms. The results suggest an advantage of the snout form over the inverted-pontoon form, and generally would suggest that minimizing contact area should be a priority.

Of particular importance were the relatively large magnitudes of resistance, which approximated the resistance associated with ice fracture. Because the lifting component is a function of the density difference involved in lifting rather than submerging ice, and because broken ice management is believed to account for about 50% of total average resistance, the results suggest a significant inherent resistance penalty associated with an upward-acting bow. The recommendations of Section 5.2 in the text reflect this observation.

#### H.4.2 Ice Movement on the Forecastle -

The forecastle was modelled as a wedge with inclined sides of varying slope  $\alpha$ , as shown in Figure 4 of the text. The force associated with ice movement up the forecastle slope was calculated strip-wise, by station spacing, and then resolved into a resistance component. This technique accounted for geometric variations and gave some insight into local resistance levels, as ice rarely covered the forecastle completely.

The sliding force was calculated from the sliding resistance component given in Frederking and Timco (1985); ice edge loading or rotation was not applicable. The station spacing was 0.1975m, with averaged slope angles varying from 30° to 67°. It was found that local resistance for each station varied little with slope angle: resistance per station in 25mm ice was typically about 10 N, and about 19 N in 40mm ice. Contact area would seem to be the dominant factor. Total resistance due to sliding over the forecastle was about 37 N for 25mm ice and 73 N for 40mm ice. As with the forefoot, the magnitudes of resistance are significant, but complete coverage of the forecastle was only observed with major ice deformation and large broken ice pieces (Tests 3,5).

#### H.5 ICE LOADING - CRUSHING UNDER THE FOREPEAK

Ice sheet contact under the flared forepeak was the most visible design problem observed during the S-Bow trials. When forecastle ice coverage was extensive, crushing and buckling under the forepeak flare was frequent and regular. In more highly fractured ice sheets, contact under the flare was more localized, often associated with the cusp entrapment problem described in Section 4.4.1 of the text. It was recognized that these conditions produced different failure sequences, and consequently the reaction force under the forepeak was analyzed using three different models.

H.5.1 Limit Stress Condition - The extreme case occurred when the ice sheet was driven against the forepeak flare, reaching its compressive strength before failure. This would apply to when large ice pieces and high deformations were observed.

The flared forepeak was treated as an orthogonal segment on the forecastle, as shown in Figure 4 of the text. A force based on the compressive strength of EG/AD/S ice was calculated per station width, as with the sliding force (Section H.4.2). This force was then resolved into a resistance component based on the forepeak flare orientation.

The analysis yielded high resistances, but full contact was assumed; for a compressive strength of 55 kPa, resistance was 400 N in 25mm ice and 670 N in 40mm ice. As in the case of shoulder crushing (Section H.3), the results were interpreted to be an indication of the gravity of this mode of failure; the resistances corresponded with instantaneous peak loads recorded experimentally.

H.5.2 Limit-Force Analysis - This condition applied where the broken ice under the flare collapsed at some level below the crushing strength, as in the case of a highly fractured ice load. The situation was treated using a

number of models developed for rubble pile collapse, as presented by Bercha et al. (1982, 1979) and Allyn (1982) applied per station width as in the limit stress case.

These models generally involved a multi-modal analysis, where a failure stress was calculated from either buckling or crushing at the rubble edge, and then converted to a unit load. This load was then resolved into a resistance component based on the forecastle slope and forepeak flare orientation.

Bercha (1982) also includes a model based on soil mechanics theory which considers a confinement condition, such as might have occurred between the ice edge and the forepeak flare. The results agreed reasonably well with the other models.

The resistances calculated from limit-force methods were considerably lower than those calculated by limit stress, but the magnitudes were still significant, approximating the ice fracture resistance component. Contact distance along the forepeak and the assumed compressive strength produced some variation in the resistances calculated. Forecastle slope had a negligible effect. If a compressive strength of 55 kPa was assumed, local resistances were about 15 N per station in 25mm ice

and 25 N in 40mm ice; total resistance was about 60 N in 25mm ice, 100 N in 40mm ice. If a larger compressive strength of 110 kPa was assumed, buckling failure was indicated to dominate. Resistances were approximately doubled.

The soil mechanics model (Bercha, 1982) also tended to give a value in this higher range. The uncertainty about compressive strength relates to the wide scatter of experimental data obtained from uniaxial tests.

H.5.3 Crescent Failure Analysis - A sequence was observed where the force exerted by the ice trapped under the forepeak caused the tip of the crescent beam segment to fail, releasing the ice trapped in the "hollow" of the crescent (Section 4.4.1 of the text). The tip of the crescent was modelled as cantilever which failed parallel to the plane of the ice sheet. A line load on the ice was estimated from a linear elastic formula for tensile strength of a uniformly loaded cantilever (Popov, 1958). The tensile strength estimated for shoulder crushing (Section H.3) was used. The calculated line load was then resolved into a loading under the forepeak as in the limit-force case and also including the orientation of the crescent. The dimensions of the crescent segment proved to be the dominant variable.

For a crescent radius of 0.2m, a contact length of 0.1m, and a low EG/AD/S tensile strength (7 kPa), the resistances calculated were: 10 N in 25mm ice and 16 N in 40mm ice. At a very high tensile strength (31 kPa) and similar crescent geometry, resistance was 43 N in 25mm ice and 68 N in 40mm ice.

#### H.5.5 Summary of the Forepeak/Ice Interaction Analysis -

Three cases were analyzed to reflect the different failure modes observed during the trials. The highest force levels were calculated from the limit-stress case, which was based on the uniaxial crushing strength of the model ice. This analysis represented an extreme case where a nearly intact ice sheet was in contact with the forepeak flare. This situation may reflect a scaling limitation rather than a design problem, but it would account for some high instantaneous resistances. The other two cases, based on rubble pile failure and crescent tip failure yielded lower resistances, but did approximate the magnitudes of the ice fracture component.

#### H.6 RESISTANCE FROM ICE CONTACT WITH THE PARALLEL MID-BODY

During the IMD trials broken ice was observed in the channel between the hull and the edge of the ice sheet;

it was reported as a significant source of ice resistance in trials performed with the M.V. "ARCTIC" fitted with the CASPPR Class 2 bow (Baker, 1985).

A simple model was used to calculate the resistance, where an entrapped piece of ice was assumed to transmit a normal force between the hull and the ice sheet. The normal force per unit length  $N'$  was calculated for the compressive strength and for the buckling strength of the ice from Bercha (1982) and Allyn (1982) using the ice sheet thickness; a sample length ( $l$ ) of broken ice gave resistance per ice contact. Ice piece lengths were selected from still photographs or calculated as a fraction of the critical length (Frederking and Timco, 1985). Resistance per ice piece was then calculated as the friction force resulting from the transmitted normal force, based on a Coulomb friction coefficient of 0.1 :

$$R_{p_{ice}} = \mu N = \mu [\sigma_{(c,b)} h] l \quad (H-6.1)$$

The resistances calculated for ice contact with the parallel mid-body varied with the calculation method. Allyn's (1982) method calculated a resistance of 10 N in 25mm ice, and 45 N in 40mm ice. These resistances were less than half those calculated by the other two methods. The results of this analysis would be conservative because factors such as degree of contact and load distribution were

neglected. This component would not seem to be as important as some of the other resistance components.

#### H.7 ADDITIONAL RESISTANCE-CAUSING FACTORS

The numerical analysis investigated resistance events observed during the model trials, but there are additional factors that are not modelled accurately. These factors tend to affect a downward-acting bow specifically, such that when they are neglected may skew the comparison between the two bow types. The question of variation in flexural strength with load direction has been alluded to above. Additional concerns relate to the following mechanisms.

H.7.1 Ice Friction - All analyses treated ice friction according to the basic Coulomb friction model, whereas experimental evidence suggests that ice friction depends on more complex mechanisms, and water lubrication may be a factor. Consequently it is not clear whether initial contact with the softer, warmer underside of the ice sheet, associated with upward-acting icebreakers, is an advantage.

H.7.2 Hydrodynamic Effects - Observations of full scale continuous level icebreaking operations with conventional (downward-acting) icebreakers report a set of hydrodynamic effects associated with the rotation of broken

ice floes, referred to as ventilation effects by Enkvist (1972). This resistance would appear to be a velocity dependent or inertial component (Naegle, 1980; Enkvist, 1972). This phenomena is not observed, at least to the same degree, at model scale. This component would be eliminated by an upward-acting bow, but is not recorded in comparative trials at model scale.

H.7.3 Effect of Snow Cover - The effect of snow cover has been commented frequently (Peirce, 1986; Enkvist and Mustamaki, 1986; Milano, 1975; Enkvist, 1972; Macdonald, 1969). It is frequently cited as a major source of friction acting on the hull, and probably has an associated energy loss due to compaction. More recent bow forms featuring low stem angles and a large "foot print" are most affected. Snow cover is not simulated in the ice tank, and analytical models are rudimentary (Tatinclaux, 1984; Carter, 1983). It is probably the most significant resistance component (of the three described in this section) that would be eliminated by the upward-action of the S-Bow.

## I. PERFORMANCE ANALYSIS: TWO OPERATIONAL PROFILE CASE STUDIES.

### I.1 ICE BREAKING TANKER FEATURING NARROW BEAM

During the 1970's several conceptual studies for ice-breaking tankers based on a narrow beamed, triangular hull section were proposed (Schonecht et al., 1978; German and Dadachanji, 1975; Kallipke, 1972; German, 1971). This hull form was intended to reduce ice resistance, as beam was recognized as having a significant effect on ice resistance. It was frequently commented that such forms were more easily faired into an upward-breaking bow.

This type of hull form was evaluated with the S-Bow, as the narrow beam may have compensated for the resistance penalty identified for an upward-acting bow. Because the open water performance of these hull forms is predicted to be relatively poor (German and Dadachanji, 1975), the application of this hull type would be restricted to heavy ice-breaking applications. Consequently the performance of a narrow beamed form fitted with the S-Bow had to demonstrate a significant reduction in resistance to justify the additional capital cost associated with the unorthodox hull form.

A simple investigation was performed into the merits of a narrow beamed hull form fitted with the S-Bow. Motozuna et al. (1985) published resistance data based on model tests for a 100 kDWT icebreaking tanker with a 44m beam. The IMD resistance data for the S-Bow model, obtained for the 23m beam of the "ARCTIC" were plotted against the tanker data, as shown in Figure I.1. The effect of the additional waterline length required to obtain 100DWT was neglected. Even though the resistance penalty was reduced, the resistance of the S-Bow did not indicate any advantage over the more conventional icebreaking tanker hull form. Beam reduction was incapable of compensating for the resistance penalty associated with the S-Bow, although resistance magnitudes would be reduced for a given hull displacement.

## I.2 OPEN WATER PERFORMANCE ANALYSIS: OPERATIONAL PROFILE CASE STUDY

### I.2.1 Details of the Case Study

- 1) M.V. "ARCTIC" serving the two northern mines (Nanisivik and Polaris) over the 15 year lifetime of the mines (Pharand, 1984). Estimate performance when fitted with the S-Bow compared with the Melville Bow, to determine required open water performance for the S-Bow.
- 2) Southern terminal at Montreal (vs. Antwerp); length of open water leg (south of 60° N) = 1920 n.mi. (3530km).

- 3) Same cycle of trading as reported for 1979-1981 (Peirce et al., 1985); treat cycle  $\times 5 = 15$  years; northern route conditions taken from Dick (1983) for each voyage leg.
- 4) Tables of resistances (see below) apply over the full 15 year cycle, i.e. ice conditions, maintenance constant.
- 5) Off-season employment not considered but would be a factor in the final design decision; employment on an open water route would favour open water performance while an extension of operations in ice-covered waters would favour superior icebreaking capability.

#### I.2.2 Route Description

The route description is based on the trading cycle as described above. The ice conditions are classified as open water (OW), open pack (OP), medium pack (MP), thin cover (TC), heavy ice cover (HC). The distances (in nautical miles) are classified according to the year they represent from the trading cycle reported by Peirce et al. (1985) multiplied by 5 to get a 15 year history. The individual distances (x) will be divided by the total route distance (S) to get the ratio SF.

TABLE I.1: ROUTE DESCRIPTION

ROUTE	;	DISTANCES (n.mi)				RATIO
CONDITION;	(1979 x 5);	(1980 x 5);	(1981 X 5);	TOTAL (i);	SF	
OW	;	142550	119325	196150	458025	0.918
OP	;	2450	225	11650	14325	0.029
MP	;	4450	7200	6150	17800	0.036
TC	;	0	2425	4100	6525	0.013
HC	;	1000	0	1500	2500	0.005
TOTALS	;	150450	129175	219550	499175	1.000

### I.2.3 Summary of Performance Data

The performance on the route was analyzed based on the speed used by the M.V. "ARCTIC" in each type of environmental condition identified by Dick (1983), as reported by Peirce (1986). The speed for each condition was used to identify a corresponding resistance, based on published data (Baker, 1985; Molyneux, 1983) or the IMD data. The effective power  $P_e$  is also presented, noting that the developed power is about 10 MW for the "ARCTIC".

As is indicated by the power data, the major limitation of this method is that resistance (and therefore power) is seriously overpredicted by simply scaling the model resistance data. For the purposes of the case study, it was assumed that each bow was equally affected by the scaling problem, such that the comparison would be valid. This assumption may be questionable (Section 4.4.1 of the text).

A range of resistance values were used for the S-Bow to account for the range exhibited in the ice resistance (selective data vs. overall). A sea state factor of 1.3 was applied to the open water data (Bhattacharya, 1978); this is included as OWs. All other factors were assumed equal.

TABLE I.2: PERFORMANCE DATA FOR CASE STUDY

MODE CONDITION	V (knots)	Melville Bow $R_1$ (kN)	$P_o$ (kW)	S-Bow $R_1$ (kN)	$P_o$ (kW)	RATIO SF
OW	: 15	; 615	4744	; -	-	; 0.918
OWs	: 15	; 800	6178	; -	-	; 0.918
OP	: 7	; 146	526	; 146*	526	; 0.029
MP	: 3	; 432	667	; 1312	2026	; 0.036
TC	: 3	; 729	1126	; 1609	2484	; 0.013
				; 2106	3252	
HC	: 1.5	; 1272	982	; 3100	2394	; 0.005
				; 4793	3546	
<CASPPR>	: 3	; 1531	2364	; 5867	9060	; 0.005

- Notes: a) open pack assumes essentially an open water condition, with speed reduced for hazard avoidance. It was assumed that the resistance at 7 knots would not vary significantly between the Melville Bow and the S-Bow.
- b) medium pack is based on 0.75m (0.25mm) pre-sawn tests. The Melville Bow value had to be based on the old Class 2 bow, as no pre-sawn data were available for the new bow at that speed. The S-Bow data are also taken noting that the bow underside was not developed.
- c) the disparity in resistances for the S-Bow in thin and heavy cover is due to the difference between the selective and overall resistances (section 4.4.1).

- d) Note that although the  $P_e$  requirement in ice cover is relatively small, this is an overload condition, and therefore propulsive efficiency is quite small relative to the open water case. The data indicates that significantly more power would be required for the S-Bow to operate in the given ice conditions, to provide adequate thrust.
- e) the heavy ice cover was treated at 1.5 knots based on Peirce (1986); the CASPPR heavy cover performance was treated because 3 knots is generally the required regulation speed.
- f) ridge transit data was not available for Table I.2. Peirce (1986) reported that the frequency of ridging is not high and would only pertain to the first and last voyages of the season.

#### I.2.4 Calculation of the Required Open Water Performance

The energy consumption rate ECR is calculated for each mode of operation as:

$$ECR_j = R_j * SF_j \quad \text{<kN*n.mi./n.mi.>} \quad (I.1)$$

;where j = the operating condition.

It was assumed that actual fuel consumption is directly proportional to resistance. The required S-Bow open water performance will then be:

$$R_{ow} \sim ([ECR_{ow} + ECR_1]_{HB} - [ECR_1]_{SB})(S/x_{ow}) \quad (I.2)$$

The ECR data for each mode of operation are presented in Table I.3 below. The open pack performance (7 knots, open water resistance) was assumed similar. The incremental improvement required of the S-Bow open water performance was then expressed as a percentage of the Melville Bow open water performance.

TABLE I.3: ENERGY CONSUMPTION RATES (ECR)

MODE:	;	Melville Bow ECR	;	S-Bow ECR
				minimum      maximum
<u>Open Water Transit</u>				
OWs	;	734.400	;	ECR <sub>ow</sub>
OP	;	4.234	;	4.234
<u>Ice Transit</u>				
MP	;	15.552	;	47.232      47.232
TC	;	9.477	;	20.917      27.378
HC	;	6.360	;	15.500      22.965
CASPPR	;	7.655	;	29.335
TOTAL (ICE);		31.389	;	83.649      97.575
CASPPR(ICE);		32.684	;	97.484

### I.2.5 Results

CASE 1. Minimum Values:  $R_{owS} = 571.6 \text{ kN}$  ;

Increment = 0.07 = 7.05% reduction

CASE 2. Maximum Values:  $R_{owS} = 559.9 \text{ kN}$  ;

Increment = 0.09 = 8.95% reduction

CASE 3. CASPPR Values:  $R_{owS} = 560.0 \text{ kN}$  ;

Increment = 0.09 = 8.94% reduction

- Conclusions: 1) A study of slow speed bulbous bow performance (Eckert and Sharma, 1973) indicates that the required increments are within reasonable capability of a bulbous bow. A bulb is intended to suppress the breaking wave at the bow (wave breaking resistance), and improve flow around the hull at low Froude numbers.
- 2) The magnitudes of the resistances in unbroken ice cover exceed the thrust capability of the propulsion system of the M.V. "ARCTIC", (bollard pull = 1570 kN). Noting the problems with scaling model resistance data, the resistances are still so large that even if the propulsion system was upgraded to full CASPPR Class 4 standards (16 MW) the required thrust probably could not be provided; a single screw system could not provide adequate thrust because of the dimensions (draught) of the stern.
- 3) Any compensation provided by improved open water performance would be negated by the cost of the added propulsion system required for ice transit. The failure to satisfy absolute performance criteria dominates the comparative analysis and provides a requirement for further research.
- 4) If an improvement in level ice resistance was achieved, the required incremental improvement in open water performance would be further reduced, enhancing the potential of the bulb concept.

NARROW BEAM ANALYSIS - 100KDWT TANKER  
 Beam Ratio = 1.91 (Plotted Full Scale)

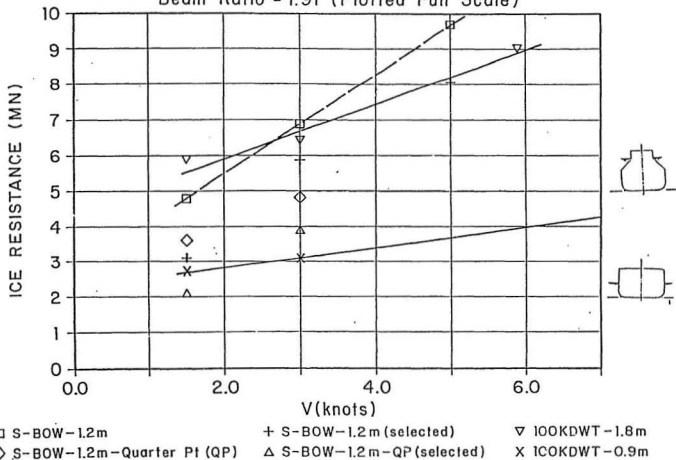


FIGURE I.1: Resistance Data for Narrow Beam Case Study.







